Clustering and source localisation of interictal epileptiform discharges in scalp EEG and design of an interface for the clinic

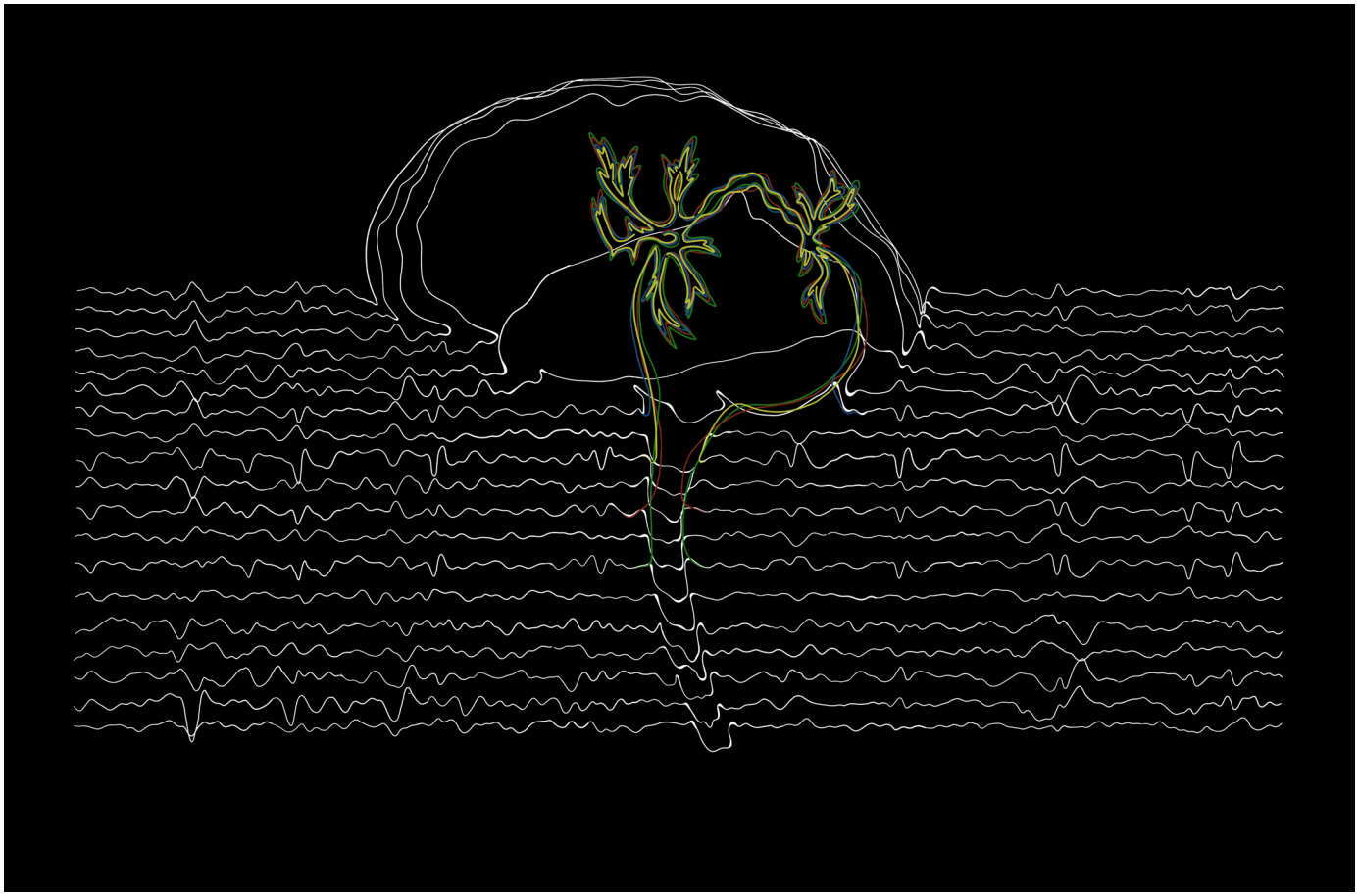

E.M. van Steenis

C. Lourenço, MSc
ir. E.E.G. Hekman
prof.dr.ir. M.J.A.M. van Putten
prof.dr.ir. H.F.J.M. Koopman

A thesis presented for the title of
MSc Biomedical Engineering & MSc Industrial Design Engineering

---

Departement of Clinical Neurophysiology
University of Twente
the Netherlands

18-08-21
s1706799
BE-838

Abstract

Objective: To aid the neurologist with the epilepsy diagnosis and classification, with a user interface for an algorithm that clusters and localises the sources of Interictal Epileptiform Discharges (IEDs), based on the output of a deep learning model.
Methods: This work presents two algorithms that localise and cluster IEDs, from epochs likely containing IEDs. An adaptation of the VGG Neural Network, from the work of Lourenço et al. (2020), labelled the input epochs [1]. For development and testing purposes, MST Enschede provided 31 anonymized EEG signals, consisting of Rolandic (N=14), other focal (N=8) and multi-focal (N=9) epilepsy patients. A clinical neurophysiologist evaluated the clusters, classifying them as correct, incorrect or inconclusive. Dipole modelling determined the dipoles for the first spike peak of all clusters and their corresponding Goodness of Fit (GoF) values.
Semi-functional prototypes of two concepts were created, based on knowledge about the current EEG analysis system and the end users. Usability testing with end users led to insights into the preferred aesthetic and interaction. The final design incorporates the results.
Results: The method that localises IEDs by their slope yielded the best clusters. This algorithm found at least one correct cluster for each patient. The algorithm found more correct clusters for multi-focal patients (3.6 $\pm$ 1.8 (mean $\pm$ sd)) than for focal patients (2.0 $\pm$ 1.6, for Rolandic and 2.5 $\pm$ 1.2 for other focal patients). Source localisation found dipoles located in the centrotemporal area for Rolandic patients, which corresponds to the location of the Rolandic area. Correct clusters showed higher GoF values (84.0% $\pm$ 17.4) than incorrect clusters (64.7% $\pm$ 17.2).
The final design presents information that neurologists will often utilise in the epilepsy diagnosis. Usability testing confirmed that the images are familiar to the end users and the interaction is intuitive. The design links the analyses to the raw EEG signal. A semi-functional prototype shows possible interaction with the interface.
Conclusion: The algorithm succeeds in localisation and clustering of IEDs and subsequent source analysis. The dipoles from clusters revealed that a high GoF value is associated with correct clusters. The interface design adheres to the preferences of the end users, as determined with usability testing. This interface design improves ease of use and clinical acceptance.
Significance: The algorithm presented in this work may decrease EEG analysis time in the clinic. Furthermore, the automated detection and clustering may reveal IEDs that were missed during manual analysis. Moreover, the sources of electrical activity in the brain can verify or extend the epilepsy diagnosis. Finally, the interface design and the response to usability testing show the potential of the algorithm in the clinic.

Contents

List of Figures

List of Tables

List of abbreviations

EEG:	Electroencephalogram
IED:	Interictal Epileptiform Discharge
AED:	Anti-Epileptic Drug
GoF:	Goodness of Fit
MST:	Medisch Spectrum Twente
MRI:	Magnetic Resonance Imaging
MEG:	Magnetoencephalography
NREM:	Non-Rapid Eye Movement
REM:	Rapid Eye Movement
SWA:	Slow Wave Activity
SIFT:	Scale-Invariant Feature Transform

1 Introduction

Epilepsy is a prevalent neurological disorder, with 1% of the population affected worldwide [2]. Diagnosis of epilepsy can be based on interictal electroencephalogram (EEG) signals, as the presence of Interictal Epileptiform Discharges (IEDs) may indicate an underlying epileptic disorder [3–5]. Therefore, IED detection is an important responsibility of neurologists. If the detected IEDs vary over time, clustering can identify all IED locations and shapes. Localising the sources in the brain of those IEDs can yield additional information, to aid the neurologist in setting a diagnosis and classification.

1.1 State of the Art

Currently, manual IED detection by neurologists, based on visual analysis, is the gold standard [6, 7]. This is a time-consuming process and errors are easily made. Therefore, misdiagnosis rates are still too high, up to 30% [8–10]. Additionally, clustering of IEDs is not practised in the clinic. Various authors explored automated IED detection [9,11–13]. The performance of those algorithms has not exceeded that of visual analysis [6, 9, 14, 15]. A popular method for automated IED detection is usage of Neural Networks [1, 9, 16–18]. This automates detection of the approximate location of the IED, but not the exact location. Furthermore, the results often contain false positives [1, 9, 16, 17, 19].
The high number of false positives is a recurring problem in both spike detection and clustering [14, 15]. Various detection and clustering methods, such as mimetic methods, template matching, wavelet analysis, k-means and hierarchical clustering, have their own advantages, but share the same problem [9, 20–23]. Some commercial spike detection, clustering and source localisation algorithms exist, such as Persyst P13 (Persyst, San Diego, CA, USA) and Epilog (Epilog, Ghent, Belgium). These systems prove that commercial clustering shows potential. However, van Mierlo et al. (2017) recommend usage in addition to visual analysis and they limit the results to a maximum of two clusters [24]. Furthermore, Halford et al. (2018) reported that the Persyst P13 yields a higher false positive rate than visual analysis (between 0.2 and 4 false positives per minute, depending on the sensitivity threshold) [10, 25]. In conclusion, while some detection and clustering techniques are available, reliable results and translation to the clinic are lacking.
After IED detection and clustering, source localisation models can reveal their sources. Source modelling localises sources in the brain, based on the electric potentials of an EEG signal and the geometry and conductivity of tissues in the head [2]. By localising the neuronal groups generating the electrical activity, source localisation yields insight into brain activity, cognitive processes and possible pathological functioning [26–28]. The advantages of source localisation based on surface EEG are its non-invasive nature, the usage of readily available tools and the addition of spatial resolution to the temporal EEG signal. Various authors discussed source localisation of EEG signals [29–35]. However, these studies are mainly experimental and conducted on small-scale datasets. Currently, source localisation in a clinical setting (for example for pre-operative evaluation) requires an extensive and specific set-up with a certain goal determined beforehand. Likewise, larger studies on source localisation have been performed. These studies often investigate patients with the same epilepsy type and require many electrodes (or intracerebral depth electrodes) and a patient-specific head model [24,27,36–38]. Overall, there is a lack of generic implementations of source localisation models that are suitable for routine epilepsy care in the clinic [35, 39, 40].
Another issue with automated clustering and subsequent source localisation is clinical acceptance. In practice, clinicians rarely use automated detection, which is in part due to a lack of faith in the performance of those algorithms [15, 41, 42]. Therefore, the presentation of the method and the results are important components for translation to the clinic. An interface design will improve

ease of use for clinicians. Furthermore, a legible and transparent design may also increase clinical acceptance.

1.2 Target group

The target group for this project is clinical neurophysiologists and neurologists, who are tasked with extensive EEG analyses. Automated detection and clustering would decrease the analysis time. Furthermore, it yields new information, such as averaged IEDs, clusters and sources in the brain. This aids the neurologists in providing the best care to their patients.
The project is mainly targeted at the information collection and signal analysis in routine epilepsy care. In Appendix B the current information cycle in the hospital is shown.

1.3 Research Goals

The primary goal is to create an algorithm to automatically localise and cluster IEDs from EEG signals. A second goal is to implement a generic source localisation algorithm, which provide complementary information about the IEDs. This combination will reduce EEG analysis time in the clinic. Furthermore, it provides more information for the neurologists, leading to a more informed epilepsy diagnosis.
To maximise the clinical value of the algorithm, a proposal for an interface will be delivered. Semi-functional prototypes of concepts will be used to evaluate the usage of the interface by neurologists. This feedback will result in a final design.

2 Theory

2.1 Electroencephalogram

Electroencephalography (EEG) is a measurement technique that records electrical brain activity from the cortex. The signal is a summation of excitatory and inhibitory postsynaptic potentials of cortical pyramidal neurons [43, 44]. The clinic often uses scalp EEG recordings because of the clinical information they provide. Furthermore, the clinic prefers EEG over alternatives (such as MEG and fMRI) due to their non-invasive nature, affordability and high temporal resolution [7, 45, 46].

2.2 Epilepsy

Epilepsy is an umbrella term for certain neurological disorders defined by, among other symptoms, recurrent seizures [47]. Excessive, abnormal and hypersynchronous neuronal activity underlays these epileptic seizures [48]. The seizures can either be focal, when only (a part of) one hemisphere is involved, or generalised, when both hemispheres are involved. Additionally, other features and manifestations of the symptoms (such as patient demographics, brain areas involved, usual course etc.) determine the specific epilepsy syndrome [5, 49, 50].
The epilepsy type (generalised or focal) and the specific epilepsy syndrome are pivotal in setting a diagnosis and classification. Furthermore, they can influence prognosis and treatment options, such as prescription of Anti-Epileptic Drugs (AEDs) or surgery.

2.3 IEDs

While the epilepsy diagnosis would ideally be based on ictal EEG (measured during a seizure), this is impractical in reality due to the low availability. However, epileptic patients often display Interictal Epileptic Discharges (IEDs) during interictal EEG (measured when the patient is not seizing). Non-epileptic EEG signals rarely display these IEDs, which makes them a substitute diagnostic tool for epilepsy [3, 4, 51]. To improve accuracy and decrease analysis time, Neural Networks can detect IEDs [1]. The output of the network is the probability for each EEG epoch (of 2 seconds in this work) to contain an IED. Presently, this informs the clinician of the presence and frequency of IEDs, thus aiding him in the diagnosis of epilepsy. However, further analysis can extract additional information from the IEDs, based on the spike morphology and topography [52, 53].

2.4 Detection & clustering

Several methods can detect and cluster IEDs. Some of the methods used in this thesis are discussed below. The first method can be used for IED detection, the second for both IED detection and clustering and the third is a clustering method.

2.4.1 Topographic prominence

Literature proposes several criteria to define IEDs. All these criteria describe an abrupt change in polarity, presenting as a sharp peak or valley [3, 54, 55]. Finding these peaks helps localise the IED, as the first peak is close to the IED onset.
Topographic prominence is the vertical distance between the peak and its lowest contour line, This indicates the distinctiveness of the peak relative to the baseline, as shown in Figure 1 [56, 57]. This measure is useful for EEG signals as it is not affected by inter-variability of amplitudes between patients.

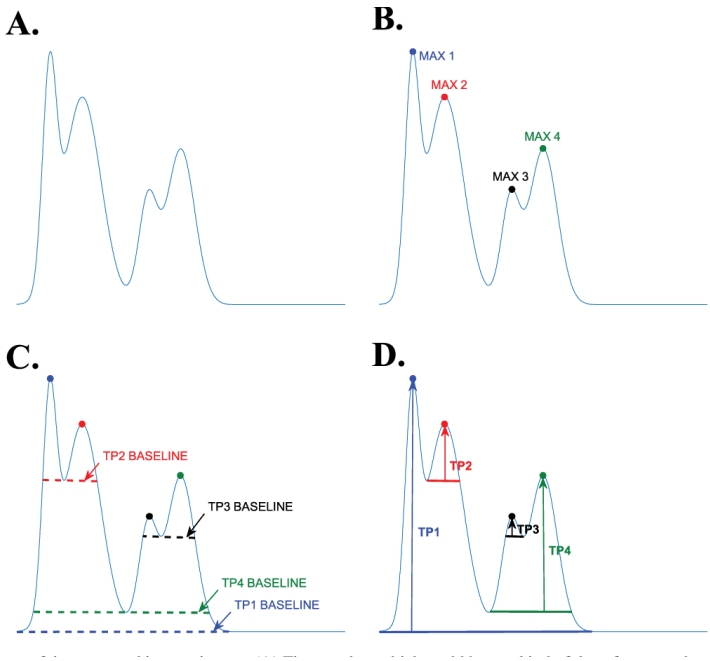

Figure 1: The raw data (A). The maxima of this raw data (B). The lowest contour lines are indicated with dashed lines (C). The topographic prominences are shown as the relative height of each maximum above the baseline (D). From Choi et al. (2017) [58].

2.4.2 Cross-correlation

Cross-correlation is a measure of similarity between two time series. The result is a correlation-coefficient, ranging between -1 (exact opposites) and 1 (maximally similar) for each displacement between the two signals [59].
Cross-correlation between IEDs should be high, because of the similarity between IED shapes [60]. Contrarily, cross-correlation between background activity will almost always be low.
The input are two 1-dimensional signals. The correlation coefficient depends on the chosen channel and time samples. For too many time samples, the effect of background activity will be larger and the correlation-coefficient thus lower. On the other hand, too little time samples could exclude part of the IED shape [61].

2.4.3 Agglomerative hierarchical clustering

Hierarchical clustering is a method that groups similar objects in a dataset into clusters. Agglomerative hierarchical clustering is a subgroup, defined by the 'bottom-up' approach of cluster forming. It starts with all individual data points as its own cluster (N clusters) and merges the points together with the lowest distance between them (N-1 clusters, N-2 clusters, etc.), until the preferred amount of clusters is left [62–64]. A distance matrix contains the distances between all data-points. This measure of dissimilarity between data-points determines which points will be clustered together. A commonly chosen distance measure is the Eucledian distance between data points. In the case of a multi-channel EEG signal, that could be the Euclidean distances between the Frobenius norm of data points [65, 66]. Another option is to use the inverse of the correlation-coefficients between epochs.
Wards method is a variation of Hierarchical clustering, which minimises the sum of squared differences within the clusters [65–67].

2.5 Source localisation

The epileptogenic region (or seizure-onset zone) is an important factor in determining epilepsy type and syndrome. IEDs can reveal this region, as the irritative zone often relates to the location of the epileptogenic region [3, 51–53, 68]. Source localisation methods localise the brain areas where IEDs originate and propagate. These methods consist of a forward and an inverse solution. The EEG forward problem explains how cortical pyramidal neurons create ionic current sources which are measured at the scalp by electrodes, resulting in an EEG signal. Mathematically, this is represented as

$$m = GD + n \tag{1}$$

with m the measured data (the EEG signal), G the lead field matrix, D the matrix of dipole moments and n the noise or perturbation matrix [2, 28, 69, 70].
The forward problem is used to calculate the lead-field matrix G. This matrix describes the current flow for each electrode, for all dipole moments. The result is a matrix where each element contains the current flow for the i^{th} electrode, due to the j^{th} dipole or voxel.

The inverse problem starts with a simulated source inside the brain which leads to a simulated EEG signal. Source localisation methods determine the optimal location, orientation and strength of simulated sources, leading to a simulated EEG as close to the original EEG signal as possible. Thus the inverse problem estimates the dipole moments matrix $\hat{D}$. The inverse problem is expressed as

$$\hat{D} = G^{-g}m \tag{2}$$

$$\min \left\| m - G\hat{D} \right\| \tag{3}$$

with G^{-g} the generalised inverse of lead-field matrix G [2, 28, 69].

Since the inverse problem is non-unique, there are several solutions. There are multiple methods that solve the inverse problem and can localise the sources. The difference between these methods is mainly in the a priori assumptions and constraints, either mathematical, neurophysiological or biophysiological [2, 29, 69, 70].
A selection of them, consisting of methods often used in IED source localisation, are elaborated below. The first method, dipole modelling, is an equivalent dipole model. This refers to its approach, which is to simulate one or a few dipoles with certain locations, orientations and strength. The three remaining models are distributed source models. In distributed source methods, the number of dipoles and their positions are not estimated beforehand. Instead, they use a pre-defined grid of sources, imposed on the 3D brain volume. Therefore, only the strength and orientation of these sources is estimated.

2.5.1 Dipole modelling

The original approach to source localisation was dipole modelling. This model assumes that only one or a few dipoles are needed to solve the inverse problem. This implies that it is possible to explain the scalp potential field with a few active areas. The model simulates the signal based on the dipole parameters; position, orientation and strength. With the constraint of limited sources imposed, the difference between actual and model data is minimised with least-squares optimisation. The pitfall of dipole modelling is that the model can over- or underestimate the number of dipoles, leading to inaccurate results. Dipole modelling is best suited to localise the irritative zone in focal epilepsy [29, 70].
The result of this model is a dipole with a certain location, orientation and strength with regards

to the brain model. This indicates the position, orientation and strength of the group of neurons responsible for the measured electrical activity. Furthermore, dipole modelling returns a Goodness of Fit (GoF) value, which is a measure for the accuracy of the dipole. This value ranges between 0 and 100%, where 0% means that the electrical activity estimated by the dipole is not alike the input EEG and 100% indicates that the dipole can perfectly predict the input EEG.

2.5.2 MNE

Hämäläinen and Imoniemi (1994) first proposed the Minimum Norm Estimate (MNE) as a solution to the inverse problem with a distributed source method. The imposed constraint is that the current distribution over all source points in the grid has minimum energy [2, 28, 69]. Then the model minimises the least-squares error. The resulting dipole moments can be expressed as

$$L(D) = ||D||^2 \tag{4}$$

$$\hat{D}_{MNE} = (G^T G + \alpha I)^{-1} G^T m \tag{5}$$

with α the regularisation parameter and I the identity matrix [28, 69].

Usage of MNE may require additional assumptions, such as restriction of the area for the search of sources. Furthermore, MNE has a bias towards superficial sources, as those are located closer to the electrodes. The model can overcome this biased with weighting parameters, leading to weighted Minimum Norm Estimates (wMNE). One of these wMNE models is LORETA.

2.5.3 (s)LORETA

Low Resolution Electromagnetic Tomography (LORETA) compensates for deeper sources. For that purpose, the model minimises the norm of the second-order spatial derivative of the current source distribution [29, 69], expressed as

$$L(D) = ||\delta B.D||^2 \tag{6}$$

$$\hat{D}_{LOR} = (G^T G + \alpha B \delta^T \delta B)^{-1} G^T m \tag{7}$$

with $B = \Omega \wedge I_3$, to perform column normalisation of G [69].

LORETA assumes simultaneous and synchronous activity between neighbouring voxels. The current density at each voxel is maximally similar to the average current density of the voxels near it. This assumption can be defended on a biophysiological level. The result is smoothly distributed sources, with better reconstruction of deeper sources. [2, 29, 69]
LORETA is less suited for focal source estimation, because the smoothing also leads to a higher sensitivity and thus a lower spatial resolution [2, 69].
Standardised LORETA (sLORETA) uses a standardised current density. The standardisation is based on the variance consisting of source variance and noise variance. This entails that sLORETA considers the biological variance in the EEG signal, combined with the variance of noise in the measurements. The model normalises the MNE current density map with both variances at each voxel [2, 69].

2.5.4 dSPM

Dynamical Statistical Parameter Mapping (dSPM) also standardises the current density map. The model uses statistics to determine regions that display much activation. It analyses each voxel with a statistical test. Under the null hypothesis, the voxel values are distributed according to a known probability density function. The current density map is estimated with MNE. dSPM normalises this estimate based on noise sensitivity at each voxel, which yields statistical parametric maps (SPMs). dSPM is thus similar to sLORETA, as both return a normalised current density, corrected for background activity. However, dSPM only uses the noise covariance for standardisation, while sLORETA uses both noise covariance and source covariance [71]. The standardisation based on noise variance makes the dSPM solution more stable under noisy conditions than the original MNE solution [37].

2.6 Interface design

Presentation of and interaction with the algorithm are as important as the algorithm itself. Computer-human interaction can pose a challenge. Furthermore, design for healthcare is an essential field, where an inadequate design or an inoperable interface can have large implications [72–74]. Incorporation of design principles in the early development phase of a project may prevent later, higher costs and other problems [75].
In this project, User Interface Design is defined as the assembly of three principles: information architecture, interaction design and visual design. These principle are discussed below and will be used to guide the design phase.

2.6.1 Information architecture

With a product focused on providing information, it is vital to present information in an efficient and understandable way. Perhaps the most dangerous pitfall is information overload. Minimising the available information, based on its importance to the user, can prevent this. It can also be avoided by structuring, organising and labeling the information. The more information you intend to provide the user with, the more you should provide guidance on how to access and use said information.
Information gathering consists of three main players: users, content and context. The users of the interface have their own goals, strengths and weaknesses. It is important to get a grip on what they want to accomplish with the product and how they can best be aided. The content is the information that users try to find within the system. The context refers to the environment in which the interface will be used. In this case, the hospital provides context. Their goals, strategy, procedures, infrastructure and culture have an impact on the usage of the design.
The goal of the interface design is to get all aspects (user, context and content) together and guide the user through the interface based on their needs and preferences [76, 77].

2.6.2 Interaction design

A good design still needs to be functional. In general, this means that the design must be easy to learn, effective to use and lead to a positive user experience. Therefore, it is important to be aware of the interaction between the users and the design. One way to incorporate interaction design is to maximise effectiveness, efficiency, safety, utility, learnability and memorability. Effectiveness indicates whether the product allows users to accomplish their goals. Efficiency indicates whether the product, when used correctly, can lead to high productivity. Safety identifies possibly errors and helps users avoid and recover from them. Utility indicates whether the interface provides the functionality for the users to reach their goal. Learnability indicates the ease of learning to

use the system. Memorability indicates how easy it is to remember how the interface functions, once learned [78, 79].
Besides accounting for users in the design process, it is also important to involve them directly [80].

2.6.3 Visual design

Theory is important in design, but eventually theory will have to translate into a visual result. Multiple visual design principles, such as color usage, shapes, hierarchy, balance and space can be followed to reach a wholesome design [81, 82].

2.6.4 Interface design heuristics

The ten usability heuristics by Jakob Nielsen are general principles for user interface design, which are relevant for all interface designs [83]. These principles give general recommendations on what interface design should contain. As an example, the first principle refers to visibility of system status, which dictates that the users should at all times be aware of the current situation, by means of feedback from the system.
All ten principles can be found in Appendix C. Most of the principles also return in the theory above, but it is still useful to test any interface design to these principles.

2.6.5 Usability testing

A design that focuses on user-interaction benefits from usability testing. In usability testing, users evaluate a product by interacting with it. This provides useful information about eventual usage of the design in the clinic. Usability testing identifies problems within the design, to reveal opportunities within the design and to learn about the behavior and preferences of the end users [84–87]. This reveals weaknesses and strengths of the design, laying the foundation for improvements [87].

3 Methods

3.1 Data

3.1.1 EEG Data

Medisch Spectrum Twente (MST) in the Netherlands provided the EEG signals, measured from patients with epilepsy. They were recorded with the standard 10/20 electrode system, yielding 18 (DB montage) or 19 (G19 montage) channels. Patients were selected from the database of MST, based on the search terms 'Rolandic', 'focal' and 'multifocal'. Patients with suspected generalised epilepsy were excluded. Patients where the VGG returned a low number of epochs or mainly artefacts were also excluded. In total, 31 patients were used. These patients were suspected of having Rolandic epilepsy (N=14), other focal epilepsy types (N=8) or multi-focal epilepsy (N=9). The distribution of the dataset is shown in Figure 2. A complete overview of the used dataset can be found in Appendix D.

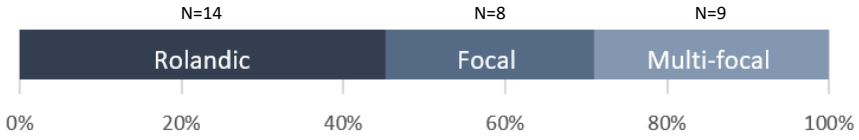

Figure 2: Distribution of included epilepsy types, with 45% Rolandic (N=14), 26% other focal (N=8) and 29% multi-focal (N=9) patients.

3.1.2 Pre-processing

Each signal was divided into epochs of 2 seconds. To reduce artefacts and noise, the entire signal was filtered with a band-pass filter between 0.5 and 30 Hz. The data was down-sampled to 125 Hz, to reduce processing time [29]. Four signals (patients 5, 18, 19 & 20) were referenced with the Double Banana (longitudinal) montage, due to technical issues during measurement. The rest of the signals were referenced with the G19 average reference montage, required for source localisation. Pre-processing was implemented in Matlab R2020a (The MathWorks Inc., Natick, MA).
The pre-processed signals were run through an adaptation of the VGG Convolutional Neural Network, from the work of Catarina Lourenço [1]. This yields a probability for each epoch, indicating its likelihood to contain an IED. The result is a 3-dimensional matrix of shape $R^{E\times T\times C}$, with E the number of epochs, T the number of time samples in an epoch and C the number of the channels. If many epochs were found by the VGG (>5.000 epochs, excluding epochs with artefacts), a smaller part of the signal was used (the first 10.000 or 5.000 epochs, depending on the number of epochs found by the VGG and the number of artefacts). The used and total number of epochs, the number of epochs from the VGG and the number of these epochs containing artefacts are included in Appendix D.

3.2 Algorithms

Epochs with a probability of at least 99% to contain an IED were included as input. All 2 second epochs without a detected IED were excluded from further analysis. Artefacts were removed from the included epochs by rejecting epochs with a peak-to-peak value above 15 µV (or 12 µV, 16 µV or none, depending on the artefact ratio).
Several data analysis steps are required to produce accurate average IEDs. These basic steps are

first localisation of IEDs, shifting of IEDs, false positive removal and clustering. Two algorithms were created, which differ in their approach of steps and the order and number of steps. The two methods are described in detail below. The threshold values for the methods were empirically determined. A simplified representation of the algorithms can be found in Figure 3. More in-depth architectures of the algorithms (still a simplification for method 1 and a more thorough architecture for method 2), including threshold values, can be found in Appendix E. The algorithms were implemented in Python 3.8. Alternatives for the removal of false positives and clustering, which were discarded for various reasons, can be found in Appendix F.

3.2.1 Method 1

Initial IED localisation
First, the IEDs must be located within the epochs from the VGG. Method 1 localises the IEDs by finding the extreme for each epoch. New epochs are created of 0.2 seconds before and 0.8 seconds after these peaks.
To frame the entire IED shape, a shift based on peaks before 0.2 seconds is performed twice. For each epoch, high peak prominences (>8.4 µV and >15 µV respectively) are sought between 0 and 0.184 seconds (0-23 samples), within the channel with maximum amplitude before 0.2 seconds. Found peaks are shifted to 0.2 seconds.

False positive removal
The VGG epochs still contain false positives [1]. Furthermore, IED localisation may have failed. Therefore, there could be false positives among the IEDs. To remove these false positives, cross-correlation is calculated for signals of 75 samples (0.12-0.64 s) between all epochs for all channels with many extremes (in >10% of all epochs). The epochs with low cross-correlation (<0.75) with many other epochs (>98% and >79% after first removal) are excluded. The epoch with the least lag with other epochs is used as template, to align all epochs.

Clustering
Epochs are first clustered based on IED channels. For each epoch, the three channels with the highest peaks are taken. Cross-correlation is calculated for those channels (35 samples around the found peak) with all other epochs. The channels that show high cross-correlations (>0.88) with the most other epochs are used for first clustering, where epochs with the same channel are clustered together. When a cluster contains at least four epochs and not all epochs show similar correlation coefficients, the cluster is split in two. The cross-correlation coefficients between epochs are used as a similarity matrix. The inverse of the cross-correlation matrix is the distance matrix, which is the input to Wards method of hierarchical clustering.
Within one cluster, false positives are again removed with cross-correlation. Here, cross-correlation is calculated for signals of 55 samples (0.12-0.48 s) between all epochs for the IED channel. If no clustering is performed, the channel with the most peaks is used. If this channels has little high cross-correlations to other epochs (<16% for >26% of epochs), the channel with the second number of largest peaks is chosen. The epochs with low cross-correlation (<0.85, <0.72 and <0.87 respectively) with many other epochs (>85%, >45% and >92% respectively) are excluded. The lags from the cross-correlation are again used to align epochs within one cluster. A prominence shift is performed for the entire cluster if the first peak of the cluster average is not located at 0.2 seconds.

False positive retrieval
In earlier steps, false positives may have been wrongly excluded. To increase the number of epochs within a cluster, 55 samples (0.08-0.52 s) of the average of that cluster is cross-correlated

with the same time instances of the false positives. If a false positive has high cross-correlation (>0.83) with the cluster average, this epoch is added to the cluster. The epoch is realigned based on the corresponding lag if needed.
A last false positive removal is performed within each cluster. Epochs with low cross-correlation (<0.85) with the average epoch of its cluster or a low amplitude (<0.5x the average cluster amplitude) are removed.

3.2.2 Method 2

Initial IED localisation
The seconds methods uses a different IED localisation approach. Aside from high amplitudes, IEDs often display steep slopes. Therefore, this method searches for the steepest slope within the epochs. Then, new epochs are created of 0.2 seconds before and 0.8 seconds after the extremity nearest the steepest slope. The channel with the steepest slope is used for the remainder of steps. A prominence shift is performed twice, searching for peaks before 0.2 seconds (0.06-0.18 s) in the IED channel. This shift frames the IED correctly within its epoch. If the prominence of a found peak is high (>25 µV), this peak is shifted to 0.2 seconds.

Clustering & false positive removal
Epochs with the same IED channel are clustered together. Within one cluster, cross-correlation is used to find the first false positives. Epochs with low cross-correlation (<0.75 and <0.87 after first removal) with many other epochs (>29-56% of epochs and >55-75% of epochs respectively, depending on the cluster size) are excluded. Within the cluster, the lags from the cross-correlation are used to align its epochs. Clusters with less than 10 epochs are removed if many of its epochs (>70%) have low prominence (<30 µV or <85 µV, depending on the artefact removal threshold) around 0.2 seconds (between 0.12-0.336 s).
If many epochs in a cluster (>80%) have high cross-correlations (>0.85) with the average of another cluster, the two clusters are merged. This is often necessary since the effect of epileptiform activity may be seen in multiple channels simultaneously. The lags are used to align the epochs from the two clusters. A prominence shift may be necessary to align the first peak of a cluster at 0.2 seconds.

False positive retrieval
For each cluster, 30 samples (0.12-0.36 s) of its averaged epoch are cross-correlated with the same time instances of the false positives. If a false positive has high cross-correlation (>0.91 or >0.95, depending on cluster size) with the cluster average and a peak around 0.2 seconds (prominence >35 µV or >45 µV, depending on cluster size), this epoch is added to the cluster. The epoch is realigned based on the corresponding lag if needed. A last cross-correlation between the average of a cluster and the individual epochs (>0.86 or >0.88 or >0.91, depending on the cluster size) is used to exclude remaining false positives.

3.2.3 Performance validation

An expert (Michel van Putten) evaluated the cluster averages. This expert determined whether a cluster contained epileptiform activity, for the results of both methods.
The cluster averages were used to decrease evaluation time. Furthermore, it improves the signal-to-noise ratio and thus IED quality.

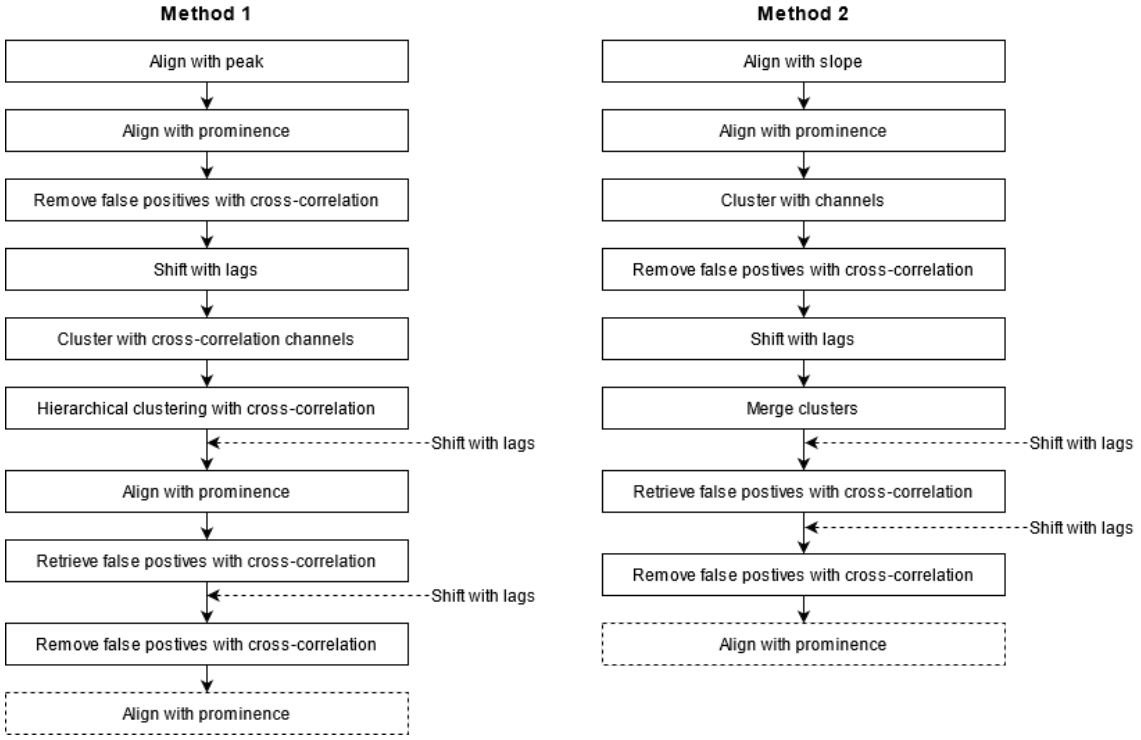

Figure 3: Simplified IED acquisition flow for method 1 (left) and method 2 (right). The sequential steps are shown from top to bottom. Both methods start with IED localisation, by the highest peak for method 1 (top left) and by steepest slope for method 2 (top right). They implement different approaches for clustering and false positive removal.

3.2.4 Influence of VGG sensitivity

The analyses were performed for a VGG sensitivity of 99%. This indicates that epochs with a probability of 99% and higher to contain an IED were used as input. However, this may not be the optimal value. Therefore, the results were also evaluated for sensitivities of 96, 94, 92, 90 and 85%. The resulting clusters were compared to the earlier classification by the expert. This analysis was run on Rolandic and other focal patients, to ease the comparison, since a limited number of clusters is expected.

3.3 Source localisation

For the source localisation, the MNE Python package (verion 0.21.0) was used. The implementation of this package is described and the different applications are mentioned below.

3.3.1 Implementation of the MNE model

Creating the forward model requires the electrode positions, a standard head model and the source space. The electrode positions were set according to the standard 10/20 international electrode system. Their coordinates were loaded from the MNE database. For the geometry of tissues in the head, a standard model from the MNE database (fsaverage) was used. The conductivities were set to the default 0.3 S/m for the brain and scalp and 0.006 S/m for the skull.
For the equivalent current dipole model, only time-varying dipole fitting of a single dipole at a single time instance is supported [88]. The time instances must be given. The equivalent current

dipole model is used here, since the data is of (multi-)focal patients.
The BEM model, the source space and the sensor locations must be defined in the same coordinate system. This is accomplished with co-registration, which relates the MRI coordinate system to the head coordinate system [88]. This step was also loaded from the database, and again based on a standard MRI.
Creating the inverse model requires the forward model, the evoked response of a cluster and the noise covariance matrix of the data. The source orientations were left unconstrained. Knowledge about noise in the data is needed for standardisation in some models and beneficial to distinguish significant brain activation in all models. An accurate noise covariance matrix can improve source localisation results [89]. The noise covariance was estimated from epochs where no IEDs were detected (VGG sensitivity <=50%).
The result of the equivalent current dipole model, is a dipole with a certain position, orientation, strength and GoF value.

3.3.2 Verification

One method to verify both the IED detection and the source localisation results, is to check the results for epilepsy types with known spike morphologies and stable dipole positions and orientations. Therefore, dipoles were calculated for the first peak of the average IEDs of Rolandic patients (whose dipoles are known to be stable). Using averages will yield better signal-to-noise ratios which improves the accuracy of the source localisation [66, 90, 91]. The location and orientation of the resulting dipoles were compared to those reported in literature.

3.3.3 Dipoles characteristics

To find possible differences between clusters with epileptiform and non-epileptiform activity, the characteristics of the dipoles between correct and incorrect clusters (as classified by the expert) were compared. The dipole strengths and the GoF values were used.

3.3.4 IED stability

To investigate whether the number of detected IEDs and their dipoles vary over time, the clusters and dipoles were calculated for each 2 hours of the home-recording EEGs of focal patients (patients 5, 7, 10, 18, 13, 21& 22). The results were analysed for patients where the algorithm detected at least 10 IEDs for at least 70% of the total 2 hours segments. Furthermore, the segments with detected IEDs must be sequential. In the end, this analysis was performed on three patients (patients 7, 10 & 13).

3.4 Interface design approach

The three principles for usability design by Gould and Lewis (1985) were used to guide the design process [92]. The first principle represents the first design phase and focuses on identification of the users and goals. This includes analyses and the theory of the three user interface design principles (information architecture, interaction design and visual design). The second phase focuses on usability testing with prototypes of the concepts. The third principle is iterative design, which implements results from the previous phases to improve the design. The components of the first two principles are described below.

3.4.1 Analyses

Several analyses were performed. First, a stakeholder analysis was made to identify the different stakeholders in the project and recognise their problems, goals and tools. The stakeholder analysis can be found in Appendix G. Moreover, a brand analysis investigated the nature of the brand currently used in the MST hospital, to ensure that the final design will fit this brand. This brand analysis can be found in Appendix H.
These analyses yielded that most important stakeholders are the neurologist, the patient, the hospital and Neurocenter. The neurologists have a goal to set an epilepsy diagnosis and determine treatment options. Their main tool is EEG measurements, which can be analysed with services from Neurocenter. Neurocenter is a brand with simplistic and professional designs. Their designs stand out because of the limited number of functionalities (and thus legible designs) and a consistent color palette (blues with orange accents).

3.4.2 Information architecture

Neurologists are adept at gathering information from EEG signals. Which means that less explicit explanations are needed and that the design should be transparent and adaptable, to combine the skills of the neurologists with the strengths of the algorithm.
The most obvious content is the average IED shape for each cluster and its sources. This must be visible on first access.
Because of the expertise of neurologists, they should be able to judge the clusters and the excluded artefacts and false positives. Different aspects of the exclusion parameters and clustering can be adjusted. Not only will this improve the result, but it likely has a positive effect on clinical acceptance.
A central point is the average IED signal on which the rest of the analyses are based. The user should be aware of the IED shape that is the basis for the following analyses. Therefore, a clue to inform the user of the selected IED cluster will always be visible, preferably in a subtle way.
The interface will be used in the hospital. Therefore, it will be used in a professional setting, where data gathering and analysis are common practise. The bright lights inside the hospital will have to be accounted for. Hospital designs often use white and blue colors and legible fonts.
Neurocenter analyses can be displayed on a small screen or on full screen. For the smaller screen area, not all the information may fit. Some information can be excluded, or the results can be displayed per cluster.

3.4.3 Interaction design

All elements needed to determine and interpret the average IED and its corresponding sources must be present and easily accessible.
The analyses are meant for IEDs. Therefore, a clue could imply that this functionality is meant for epileptic patients. Furthermore, the interface should prevent incorrect interpretations of the

results. Visual clues must inform users that the results are not infallible and strongly depend on factors such as the number of electrodes, the accuracy of the used head and cortex models and so on. Especially the depth of the dipoles is not infallible, so a visual clue could stress this. Furthermore, if the clusters size is too small, the interface could communicate this to the user.
The users will likely operate the interface with a mouse. Therefore, the design must account for usage with a mouse and account for subsequent control sensitivity. A main overview may use sliders, since this information is more general. Within the clusters and for the settings the adjustments are more specific, thus sensitivity is more important.
The interface must give clear clues to guide user behavior. It should use unambiguous symbols, so the user can guess their functionality before usage. Furthermore, the symbols should be tuned to the knowledge of neurologists.
Clear hierarchy within each functionality will prevent errors in navigation. Furthermore, color codes could signify related functions. Additionally, a help function could prevent mistakes and an undo button can help users recover from mistakes.

3.4.4 Visual design

Some principles of visual design can be used to help create a legible and functional design. The color palette will be important for coherence and familiarity with Neurocenter. Sharp shapes and open space are important for legibility. Vertical hierarchy in elements and space between clusters will create a clear distinction between clusters. Less open space and unity will create coherence and integration within one cluster. These principles are elaborated upon visually in Appendix I.

3.5 Interface design

The strategies above, combined with feedback provided by neurologists from the SEIN institute (see Appendix J) led to the conclusion that four main components must be present in each design: a main overview of the results, the cluster epochs in sensor space, the cluster sources in source space and an explanation of methods and settings. These components and their functionalities and requirements can be found in Figure 4 and are elaborated below.

Main overview
A main overview will present the most important information in a legible way. This must be the first page that users see and a central point to which they can return. It must contain the cluster signal averages and the dipoles of this cluster average. Furthermore, the page must show all detected clusters.

Cluster data
This page will provide more in-depth information about the clusters. It contains the individual epochs. Additionally, it could feature some thresholds for the data analysis. This page presents more data, thus legibility and navigation become more challenging and more important.

Sources
This page presents the sources of the individual epochs. Here, the user can alter the source localisation method, as well as display options such as sensitivity. The sources will be represented in a more intuitive way. Therefore, the visualisation method is an important consideration.

Settings
Since transparency is important for the end users, some way of altering the methods and thresholds must be provided. The most logical solution is a separate page, to ensure enough

space and legibility. This page provides insight into the different steps of the algorithm and their order. Furthermore, the user can make alterations to the algorithm and immediately see the results.

Two concepts were created based on these required components. These concepts were evaluated with the Nielsen User Interface design guidelines. Furthermore, semi-functional prototypes were created in Axure RP 9 (Axure Software Solutions, San Diego, CA, USA) to gather valuable input from neurologists. The process of usability testing is elaborated below and had a strong influence on concept selection.
The concept generation and evaluation led to a final design proposal. This is a continuation of one of the concepts, adapted based on the outcomes of the concept evaluations.

3.5.1 Usability testing

The semi-functional prototypes of the two concepts were presented to three participants; a clinical neurophysiologist and two training neurologists. An observer was present to guide the process and gather information. For each page, the observer posed several questions and asked the participant to complete a series of tasks (see Appendix K). Additionally, the participant was free to explore the interface on their own. All thoughts and feedback of the participant were noted. Furthermore, the interaction and usability patterns of the participant were observed.
Evaluation was based on the ability of the participant to navigate the interfaces. Furthermore, the participant was asked if the presented information and options were complete and concise. Other factors were intuitive understanding of the navigation, quick access to the desired information and ability to adjust settings. Finally, the preferences of the participant for a certain concept and certain functionalities were noted.

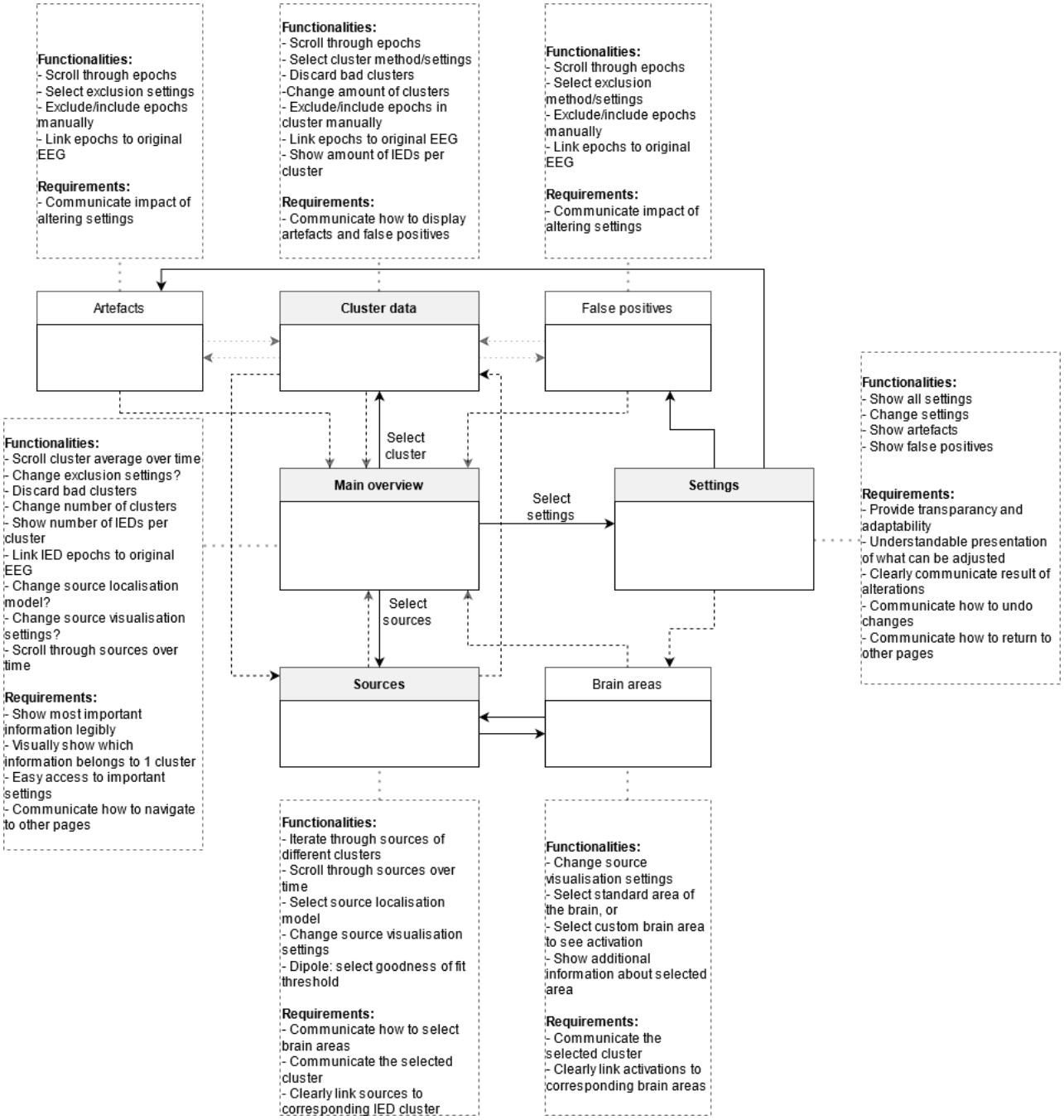

Figure 4: The different components that must be present in the designs, their functionalities and requirements and the ways in which they could interact. The first component is a main overview. From here direct navigation to other pages should be supported, which are the cluster data (individual epochs), the sources (individual sources) and the settings (algorithm parameters).

4 Results

4.1 Algorithms

4.1.1 Method 1

With clustering implemented, method 1 is unable to produce feasible results. Visual inspection of the results shows that too many clusters are generated per patient and feasible average IED shapes are scarce.
However, the algorithm can still perform IED localisation and source localisation for the Rolandic and other focal patients. This led to 16 correct, 5 incorrect and 1 inconclusive cluster averages. The results without clustering, for Rolandic and focal patients are shown in Figure 5. It shows the distributions of correct and incorrect clusters and the distribution of channels for correct clusters. Appendix L gives the full results. Method 1 finds ten correct clusters for the Rolandic (71%) and seven correct clusters for the other focal patients (88%). These correct clusters generally consist of a decent number of epochs (39.2 ± 38.4 (mean ± sd)), although this varies per patient. The correct clusters display IEDs in the temporal lobe (70%) and the central sulcus (30%) for Rolandic patients. The other focal patients show correct clusters in the temporal (71%) and frontal lobe (29%). The incorrect clusters often consist of artefacts.

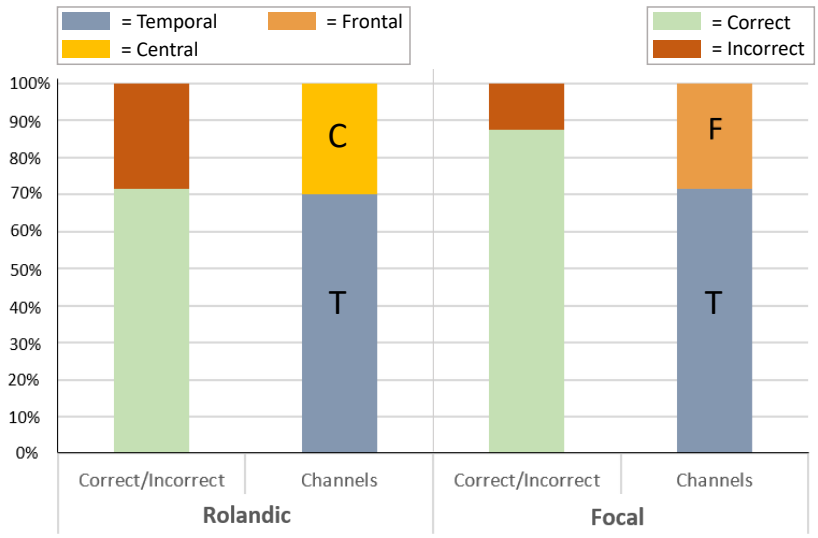

Figure 5: The results for method 1. For Rolandic and focal patients, the distribution of correct and incorrect clusters and the distribution of channels among correct clusters in shown. Channels are indicated with colors and a letter; C for central sulcus, T for temporal lobe and F for frontal and pre-frontal lobe. Approximately 71% of detected clusters were correct for Rolandic patients, and 88% for other focal patients. The correct clusters had IEDs in the central sulcus and temporal lobe for Rolandic patients and in the central sulcus and frontal lobe for the other focal patients.

4.1.2 Method 2

Method 2 implements clustering. The average results for each epilepsy type are shown in Figure 6. It shows the average number of detected clusters, the average number of correct clusters, the average number of incorrect clusters and the distribution of channels for correct clusters. Appendix M contains a full overview of the results.
The algorithm finds at least one correct cluster for each patient, with often a reasonable number of epochs (on average 45.6 detected IEDs ± 51.1), although this varies between patients. Overall,

more clusters were found for multi-focal patients (3.6 ± 1.8 versus 2.0 ± 1.6 in Rolandic and 2.5 ± 1.2 in other focal patients). For Rolandic patients, all correct clusters originate from the temporal lobe (50%) or the central sulcus (40%), with one exception (patient 12). For focal and Rolandic patients, either one correct cluster is found, or multiple correct clusters with channels mirrored in the hemispheres (a mirror-focus). Two focal patients (patient 15 & 19) display correct clusters in two different brain areas. For multi-focal patients, two or more correct clusters are found located in at least two different brain areas (not with mirror-focus), with one exception (patient 29).

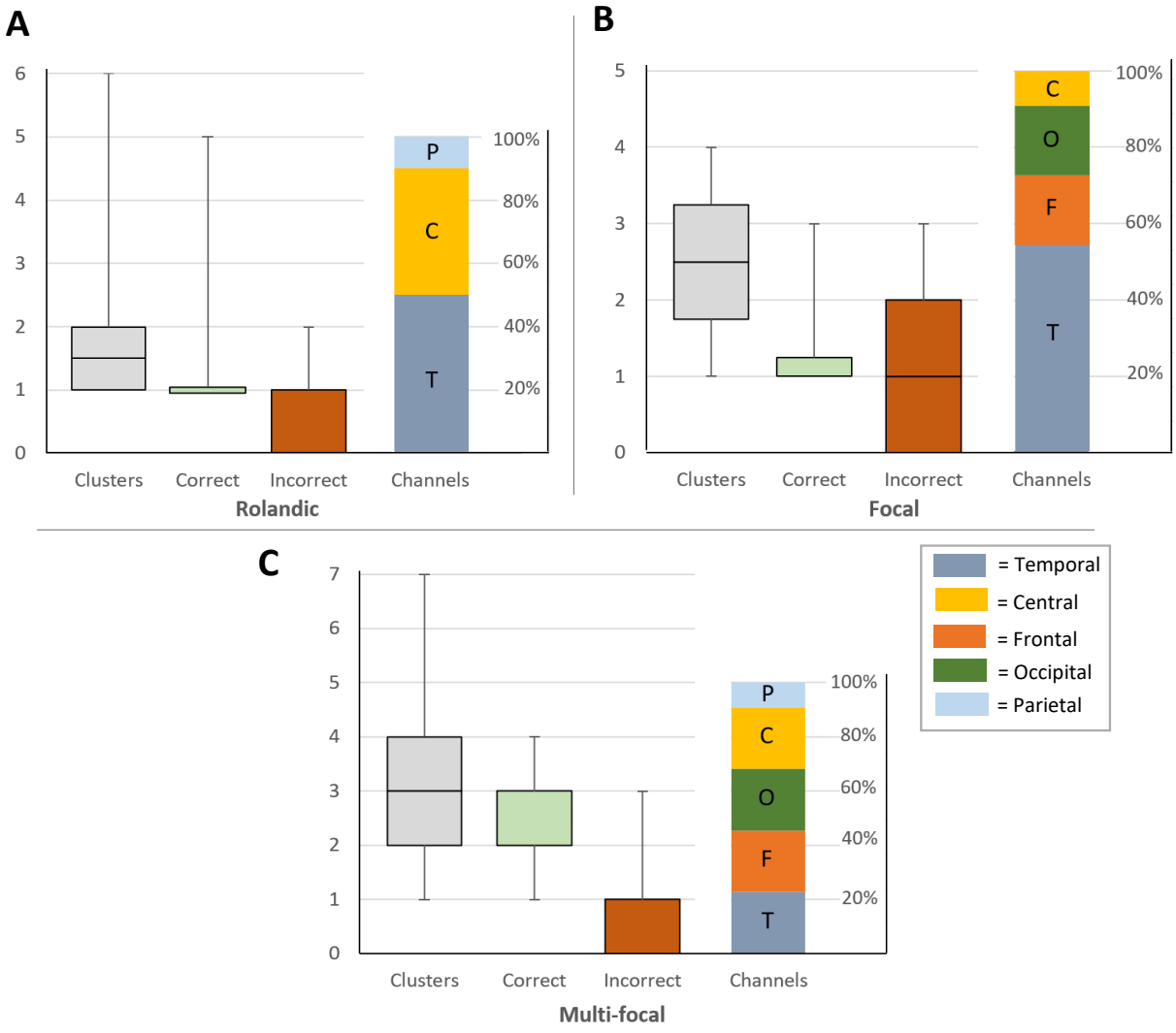

Figure 6: The results for method 2. For Rolandic (A), focal (B) and multi-focal patients (C), the average number of detected clusters (grey), the average number of correct clusters (green), the average number of incorrect clusters (red) and the distribution of channels among correct clusters in shown. Channels are indicated with a letter; C for central sulcus, T for temporal lobe, P for parietal lobe, F for frontal and pre-frontal lobe and O for occipital lobe. More clusters were found on average for multi-focal patients than for Rolandic and other focal patients. For Rolandic and focal patients the number of detected correct clusters is lower. Clusters for Rolandic patients were found in temporal and central sulcus, with one exception where the parietal lobe contained IEDs. Multi-focal patients show the largest variety in IED locations.

4.1.3 Influence of VGG sensitivity

The full results of varying the VGG sensitivity can be found in Appendix N. Figure 7 shows the result of varying the sensitivity on the total size of correct clusters, the number of correct clusters and the number of incorrect clusters for four patients. For most patients, the total size of correct clusters increases as the VGG sensitivity decreases, as seen in Figure 7A. At the same time, the number of incorrect clusters also increases with a decrease in sensitivity. There are also patients where a decrease in the sensitivity at some point results in an absence of correct clusters, as seen in Figure 7B. For some patients, the correct cluster sizes stay stable regardless of the sensitivity, as illustrated in Figure 7C. Patient 1 (Figure 7C) also shows an absence of correct clusters for only one sensitivity value (at 0.92). For patient 21, a decrease in the sensitivity leads to a decrease in the correct cluster sizes, as shown in Figure 7D.

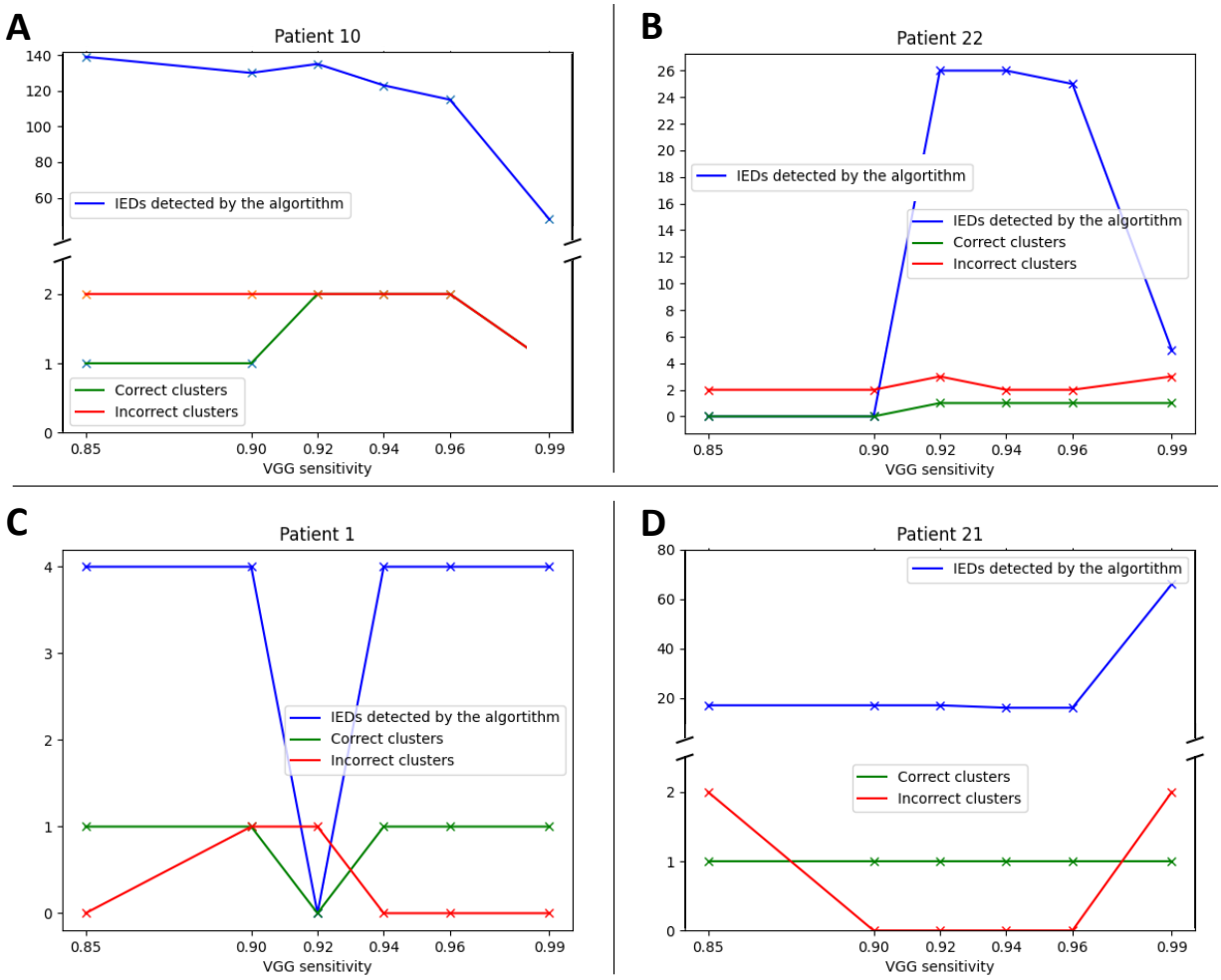

Figure 7: The result of varying the sensitivity of the VGG (x-axis) on the total number of detected IEDs (blue), the number of detected correct clusters (green) and the number of detected incorrect clusters (red). The lines do not represent data points, but only serve a visual purpose. Different results were found for different patients. For most patients, among which patient 10 (A) where an increase of VGG sensitivity decreases the number of IEDs detected by the algorithm. For some patients, such as patient 22 (B) a low sensitivity eventually led to a absence of correct clusters. Patient 1 (C) has a stable number of IEDs, except for one sensitivity value where the algorithm finds no correct clusters. Patient 21 (D) shows a decrease in the number of IEDs detected by the algorithm, with a decrease in sensitivity.

4.2 Source localisation

Since method 2 performed the best, the results of this method are used for subsequent source localisation. Source localisation calculates the dipoles for the first peak of the average IEDs of clusters (around 0.2 seconds).

4.2.1 Verification

Source localisation determined the average dipoles for 13 patients with Rolandic epilepsy (patient 5 was excluded because of the DB montage). Dipole modelling localised the source of the largest correct cluster for each patient. The results for all patients, represented in two different views, can be found in Appendix O. All Rolandic patients yield a dipole positioned at the centrotemporal area, with an orientation tangential to the skull. The result for one patient (patient 14) is shown in Figure 8. The dipole are plotted onto the MRI of the standard head model. The bottom image is the top of the head, the right is the side and the left is the back. The nose points towards the x-axis. The red dot indicates the dipole position and the arrow shows the orientation. The GoF, strength and location of the dipole are included at the top of the figure.

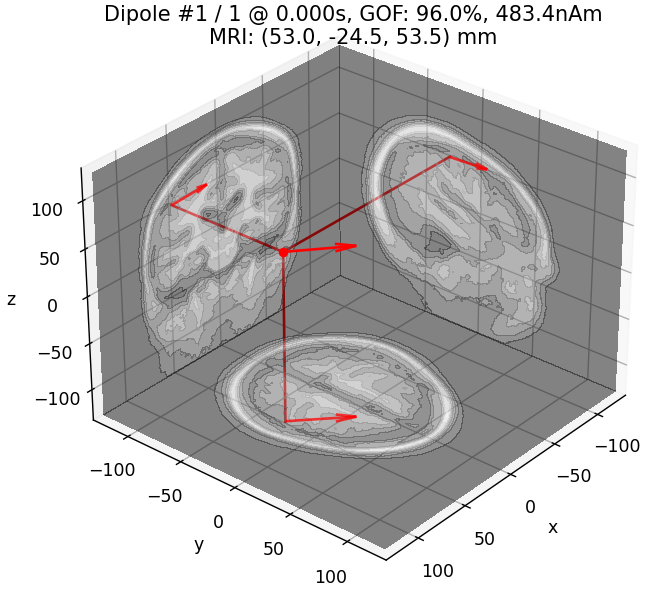

Figure 8: Dipoles for the first peak of the average IEDs of a Rolandic patient (patient 14). Dipole position and orientation are indicated with a red dot and arrow. The dipole GoF, strength and location in the MRI are indicated at the top. For this patient, the dipole is located at the centrotemporal are and oriented tangential to the skull, as is typical for patients with Rolandic epilepsy.

4.2.2 Dipole characteristics

Dipole modelling yields a dipole strength and GoF. The mean dipole strengths between correct and incorrect clusters are similar, with an average dipole strength of 336.9 nAm ± 174.0 for correct and 283.0 nAm ± 164.8 for incorrect clusters. The GoF does differ between correct and incorrect clusters. With an average GoF value of 84.0% ± 17.4 for correct clusters and an average of 64.7% ± 17.2 for incorrect clusters. Probability density functions for dipole strength and GoF for correct and incorrect clusters are shown in Figure 9. A table with the characteristics of the dipoles can be found in Appendix P.

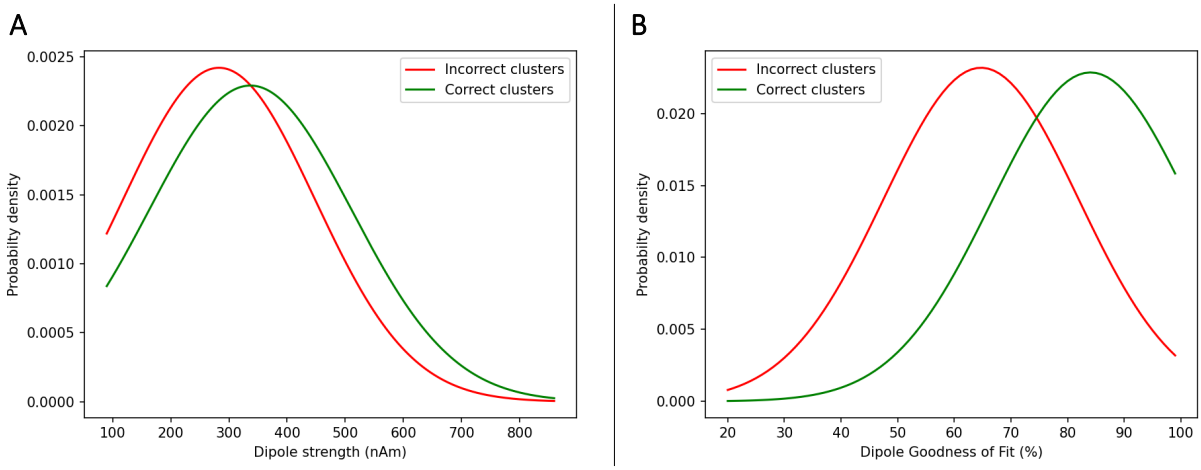

Figure 9: Probability density functions for dipole strength between correct (orange) and incorrect (blue) clusters (A) and dipole GoF between correct (orange) and incorrect (blue) clusters (B). The probabilities for the dipole strength between correct and incorrect are similar. The probabilities for GoF are higher for correct (84.0% ± 17.4) than for incorrect clusters (64.7% ± 17.2).

Some correct clusters with uncharacteristically low GoF values are shown in Figure 10. Likewise, some incorrect clusters with high GoF values are shown in Figure 11.

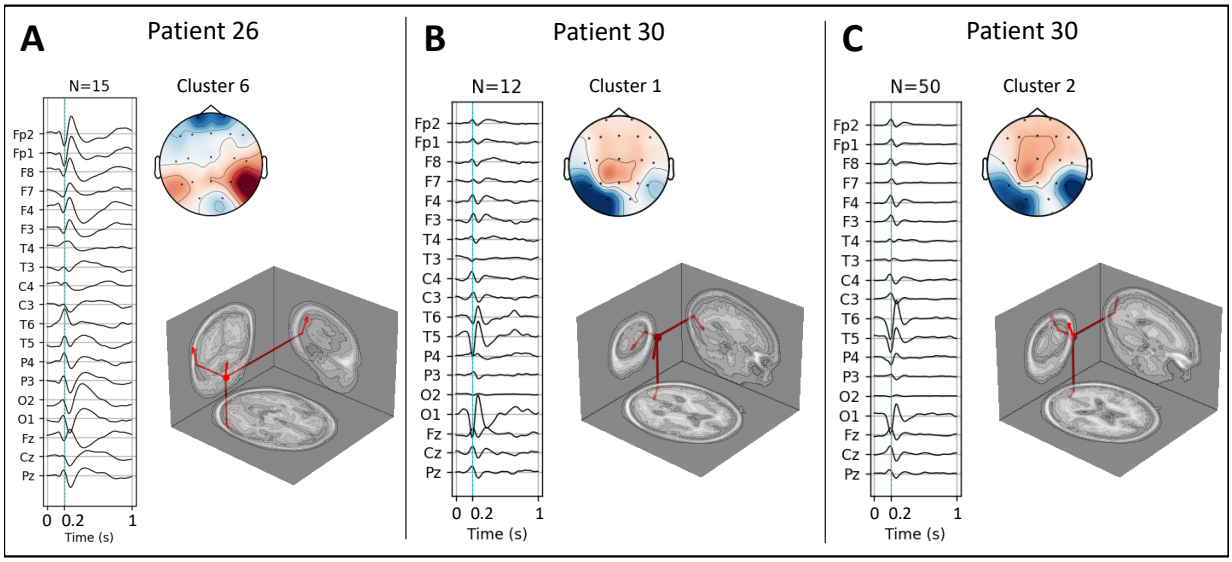

Figure 10: Correct clusters with low GoF values. Plotted are the average epochs, the dipoles of the average epochs at 0.2 seconds and the head topography at 0.2 seconds. Patient 26 (A) has a GoF of 37.6%, patient 30 (B & C) has GoF values of 23.9% and 20.1%. The expert classified all three clusters as IEDs.

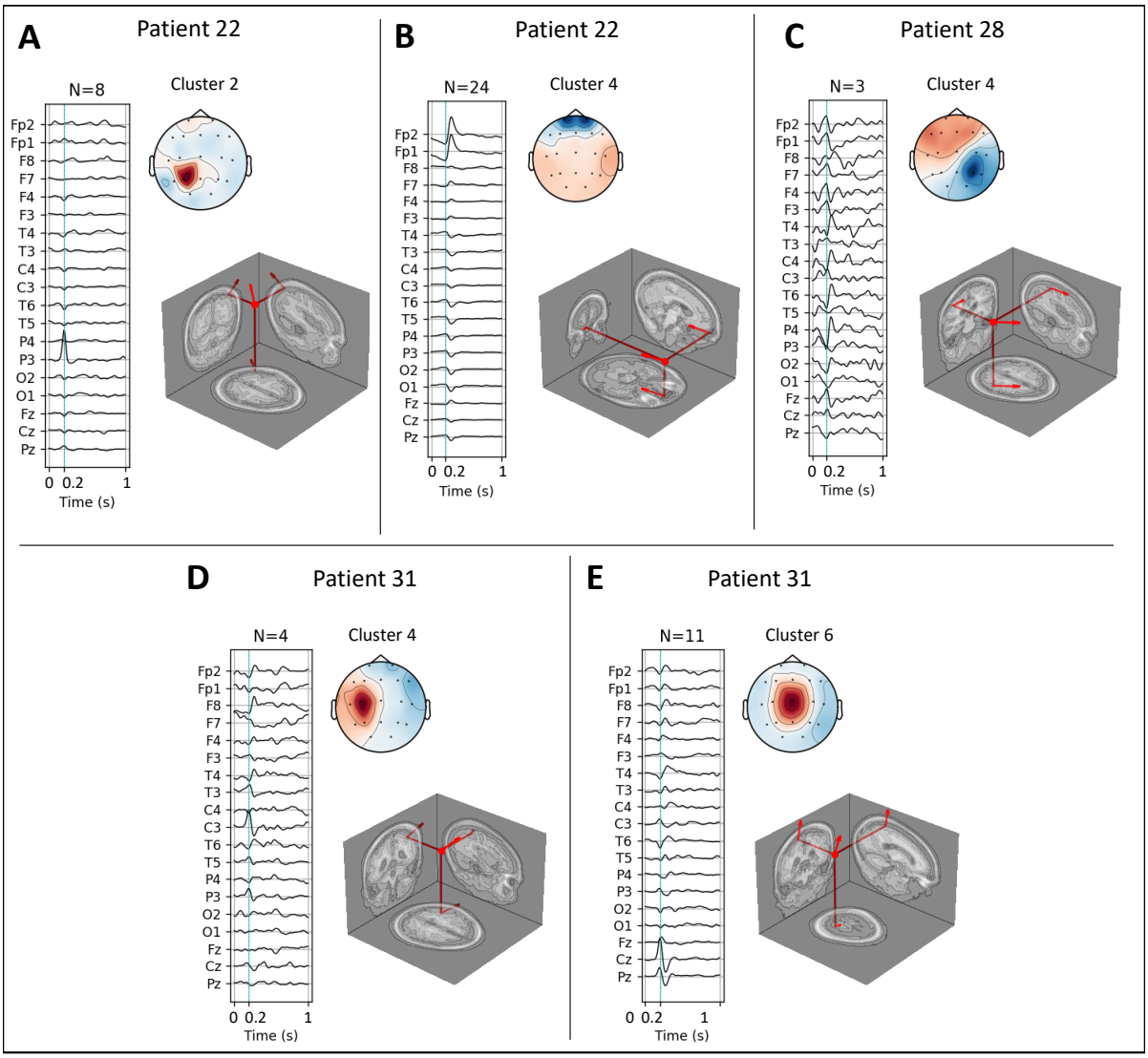

Figure 11: Incorrect clusters with high GoF values. Plotted are the average epochs, the dipoles of the average epochs at 0.2 seconds and the head topography at 0.2 seconds. Patient 22 (A & B) show artefacts with a GoF of 92.7% and 90.3% Patients 28 (C) and patient 31 (D & E) display other false positives with GoF values of 89.7%, 93.7% and 94.3%.

4.2.3 IED stability

For the home-recordings, the algorithm ran on all two hour segments. The resulting clusters were compared to the earlier classification. For each two hours, clusters coherent with the correct cluster of that patient (as classified by the expert) were used. The result for one patient (patient 7) is shown in Figure 12. For this patient, the IED shape shows a sharp valley followed by a slow wave for the first eight hours (11:15-17:15). After eight hours (19:15-05:15), the IED shape is a sharp valley with a sharp peak. The difference in IED morphology is also visible in source space. This presents itself as a shift in dipole location, where the dipole moves down the temporal lobe after the first eight hours (after 19:15). Results from two other patients (patients 10 & 13) can be found in Appendix Q. The dipole strength does not show significant change over time. The strength of the dipoles for all three patients over time are plotted in Appendix R.

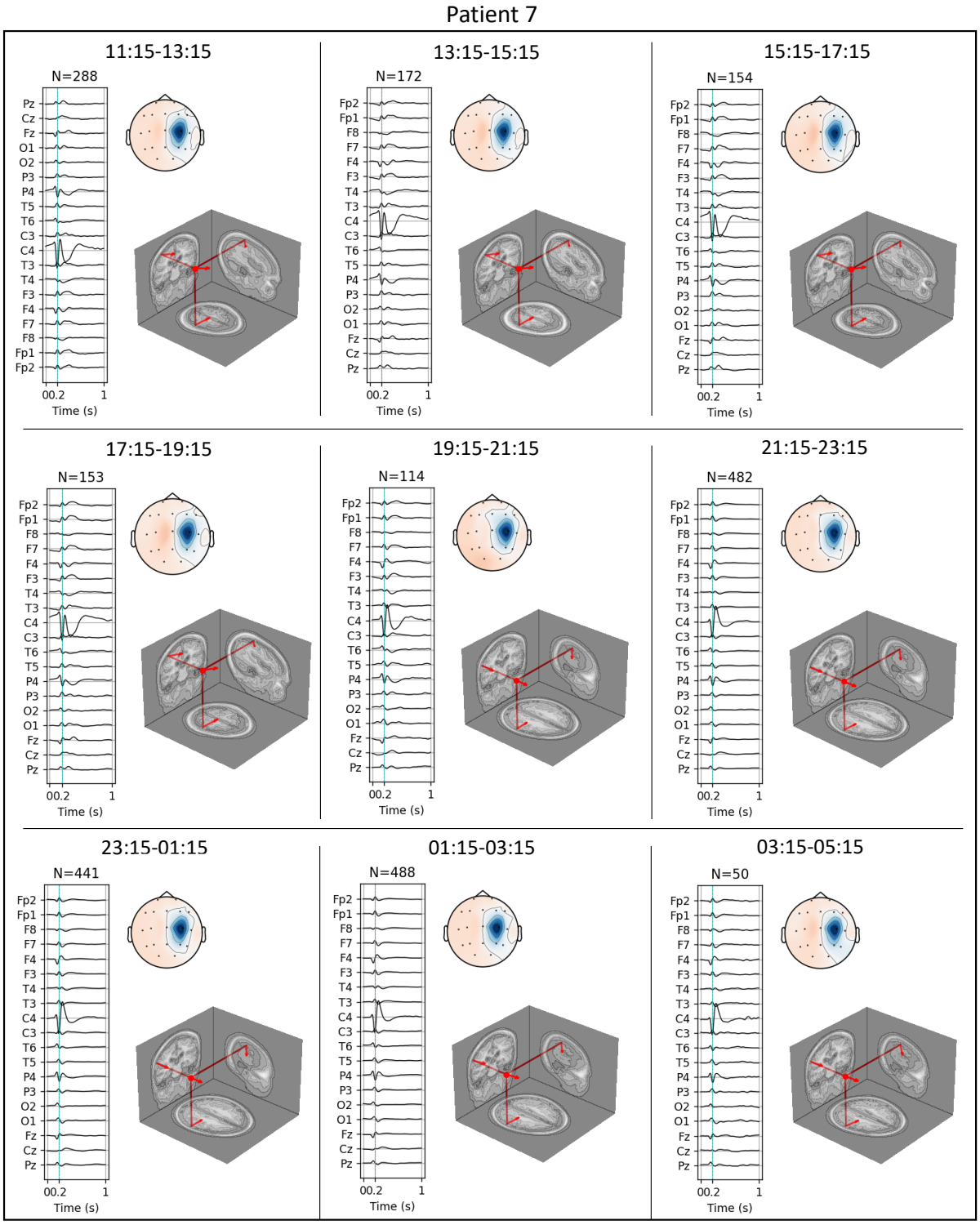

Figure 12: Average IED, dipole and head topography for the correct cluster for each two hours for patient 7. Current time is indicated at the top of the figures. The clusters sizes are indicated above the average IEDs. After 17:15-19:15, there is a change in the IED shape.

The number of detected IEDs per two hours does change over time, as seen in Figure 13. For patient 7, there is an increase in the number of detected IEDs from an average of 191.8 epochs ± 64.8 for the first eight hours (11:15-19:15) to an average of 470.3 epochs ± 25.6 between 10 and 16 hours (21:15-03:15).
Patient 10 shows an IED frequency of on average 34.0 epochs ± 12.9 for the first eight hours (13:45-21:45) to an average of 435.3 ± 73.6 between 10 and 16 hours (23:45-05:45).
Patient 13 shows an IED frequency of on average 15.3 epochs ± 6.1 for the first eight hours (11:30-19:30) to an average of 162.3 epochs ± 28.4 between 10 and 16 hours (21:30-03:30).

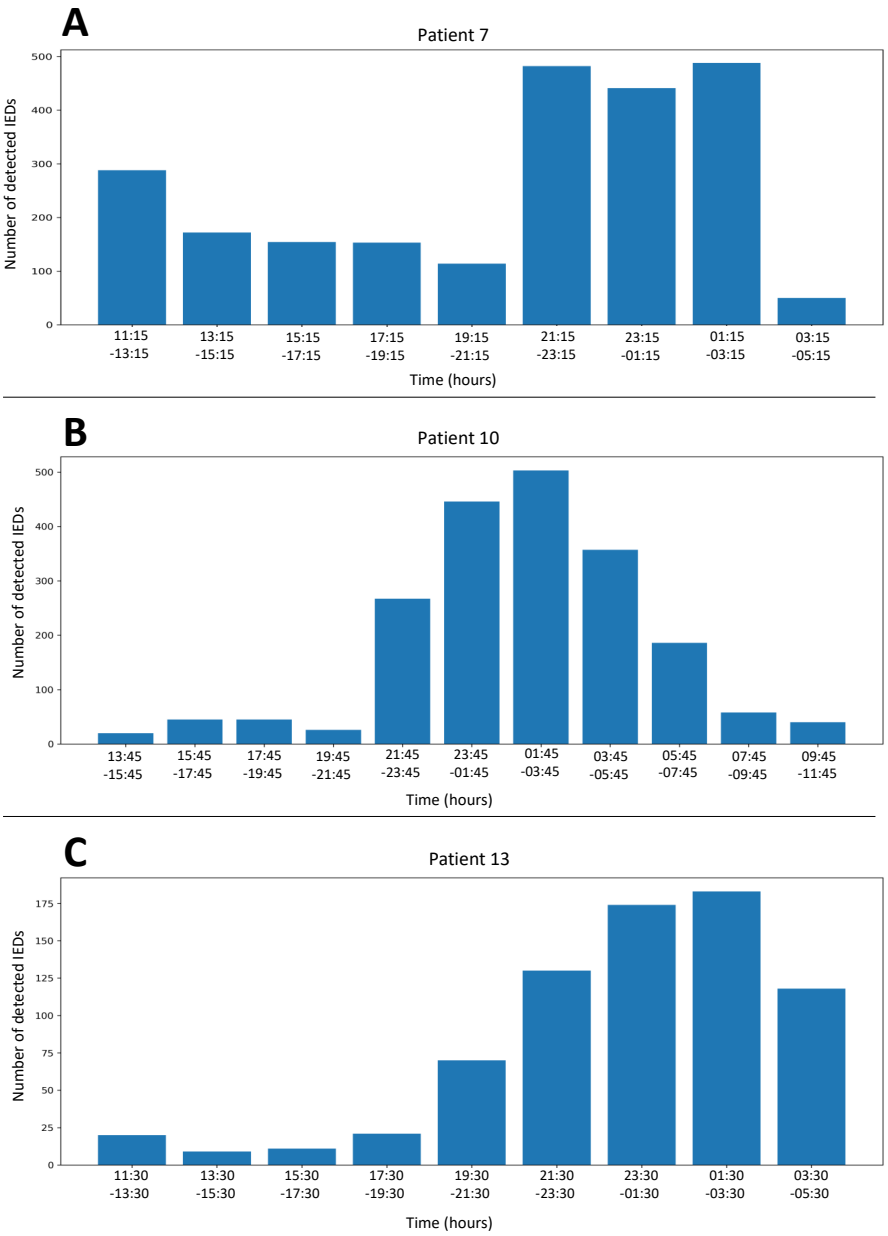

Figure 13: Number of detected IEDs per two hours for patient 7 (A), patient 10 (B) and patient 13 (C). The current time in steps of two hours is indicated on the x-axis. For all three patients an increase in the number of detected IEDs is seen over time.

4.3 Concepts

Design ideation led to two concepts which were detailed further. Some early sketches can be found inAppendix S. Besides aesthetic, the designs also incorporate user interaction.

4.3.1 Concept 1

Concept 1 has a clear separation between pages. The first page is the main page, with an overview of the most important information; average IEDs, dipoles and head topographies of clusters. From here the user can navigate to the epochs page, the sources page and the settings page. All pages allow the user to return to the homepage with a home icon. The interface indicates the selected cluster at the top. It also displays the other clusters that can be selected. A cluster page shows the cluster averages next to the individual epochs. An orange rectangle conveys whether the epochs or the sources are selected. The trash can icon removes epochs from clusters in the epochs or sources pages. The effect of removing an epoch is immediately visible since the average IED is displayed. Additionally, the thrash can icons next to clusters names remove entire clusters.

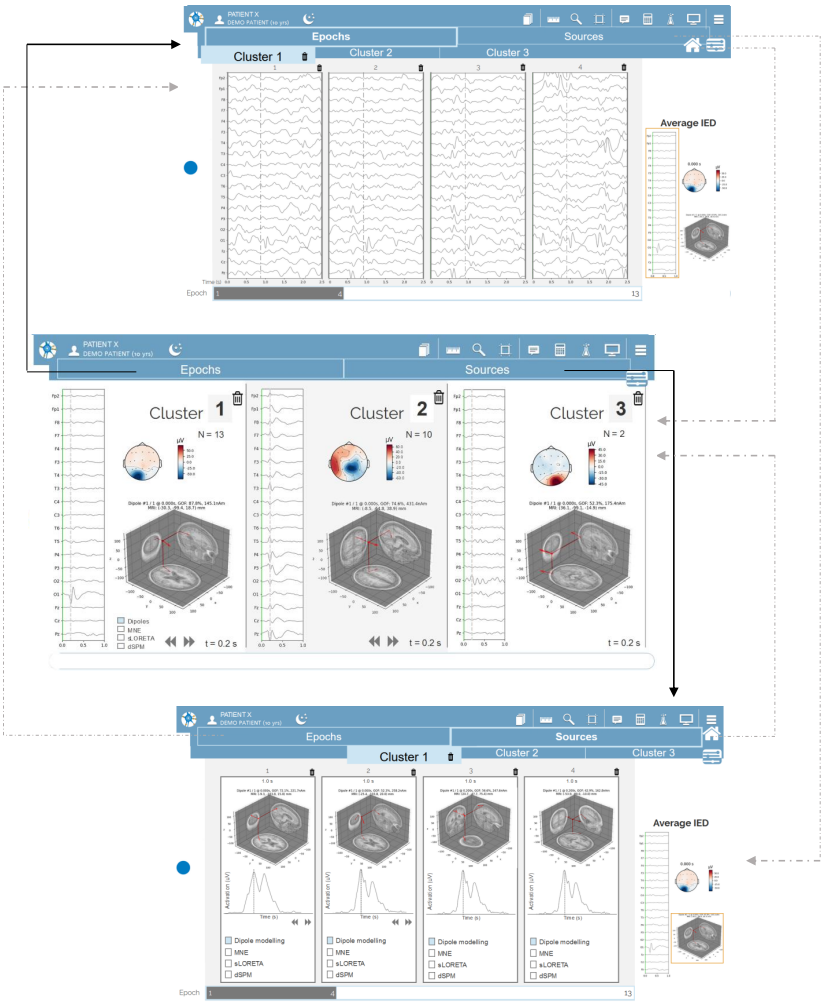

Figure 14: Pages belonging to concept 1. In the middle, the overview. From here, the user can navigate to the cluster page (upper) with the individual epochs and the sources page (bottom) with the sources of individual epochs. The top of the interface provides navigation and a home button.

4.3.2 Concept 2

Concept 2 has less direct separation between pages. Instead, the user can expand certain items to get more information about them. The first page again gives an overview of the cluster information. The user can adjust cluster settings here. Expanding a cluster shows the individual epochs within that cluster and its sources. In the same way, contracting the cluster info returns the user to the main page. An orange rectangle again indicates whether epochs or sources are selected. There are multiple ways to navigate between pages in this concept. The user can navigate by expanding and contracting the main page buttons, by scrolling to another cluster at the bottom or by selecting epochs or sources from the cluster average. Arrows and rectangles that appear when hovering are clues that indicate the ways in which the user can interact with the concept. For example, as the user hovers over the average dipole on the epoch page, an orange rectangle around this dipole indicates that clicking it will navigate to the source page. Again, the user can remove epochs with the thrash can icon.

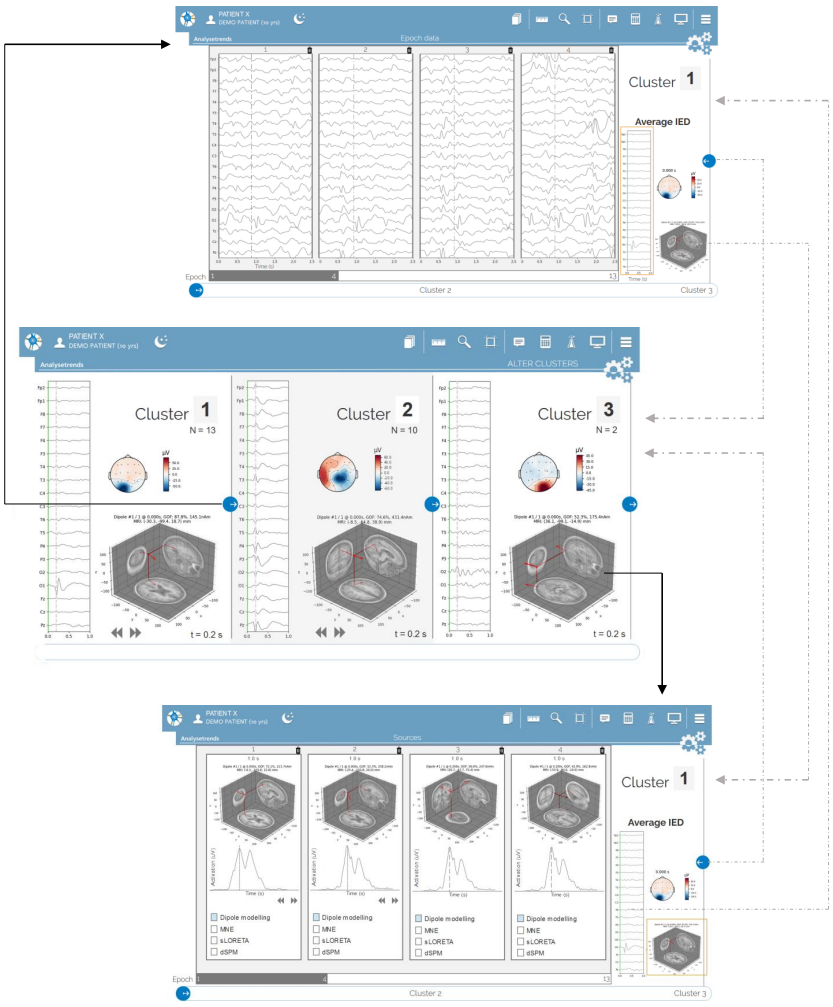

Figure 15: Pages belonging to concept 2. In the middle, the overview. Here, the user can alter cluster settings. The clusters can be expanded to get see the individual epochs in a cluster (upper) and the sources in a cluster (bottom). The user can also navigate to difference clusters at the bottom or between sources and epochs by clicking on the cluster averages.

The settings page is the same for both concepts and an impression of this page can be found in Figure 16. The page shows the sequential steps of the algorithm. The user can expand each step and make adjustments. The epochs immediately show the result of those adjustments. An undo button allows users to reverse their changes.

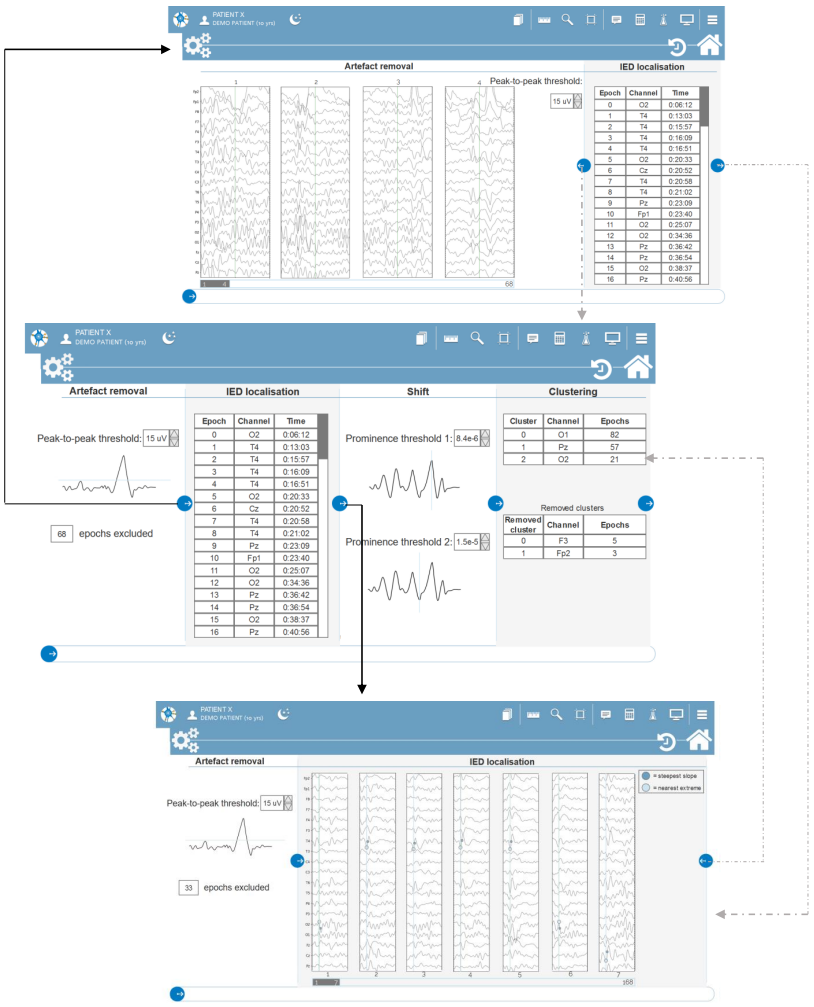

Figure 16: The separate settings page. All the steps of the algorithm are shown (middle). Individual steps can be expanded to show the results of that step in the epochs (bottom and top). The user can undo their adjustments and navigate to the main page with the icons on the top of the interface.

4.3.3 Additional features

Apart from the two main concepts, some additional features were explored to aid neurologists in several areas.

Moving pictures

This feature is inspired by early animation techniques. The epoch in a cluster slowly transforms into the next. This will highlight the similarities and differences between individual epochs. It may help identify false positives within a cluster. Furthermore, it makes it easier to compare epochs within one cluster. This feature is shown in Figure 17.

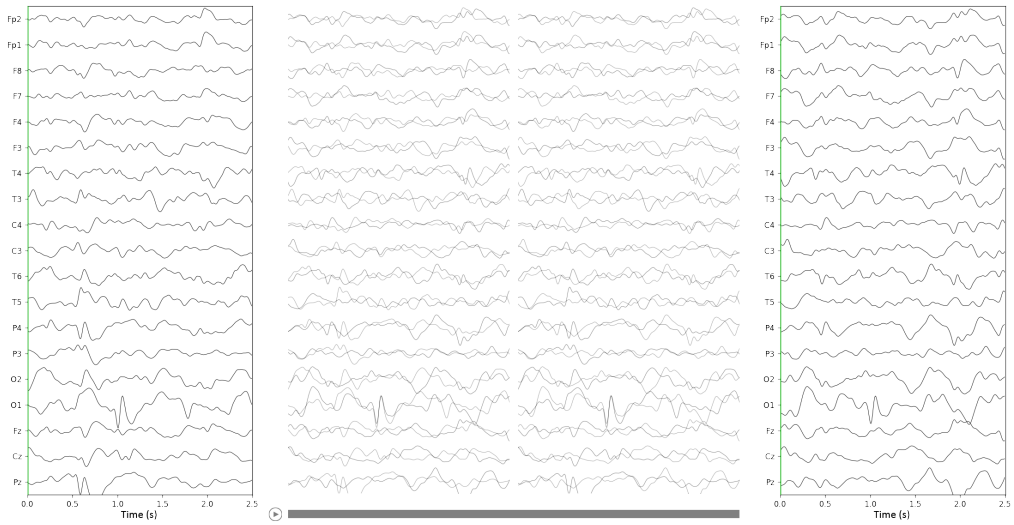

Figure 17: The first epoch (left) slowly transforms into the next epoch (right). This transition happens gradually over time (middle) to highlight differences and similarities between the two epochs.

Stylised brain images

It is standard for the MNE package to plot the dipole inside the MRI scan of a brain. However, this view may be hard to read. Therefore, more options are explored to discover the best presentation. One option with a minimalistic design to increase legibility is shown in Figure 18. It features image of the side, the top and the back of the head. Users can switch between these views.

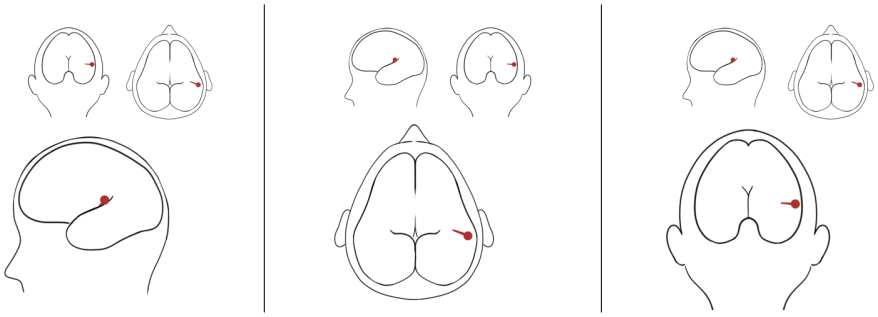

Figure 18: A different way to represent the dipole in the brain. The user can click on the view he wants to zoom in on; the side view (left), the top view (middle) or the back view (right).

Color coded GoF

To warn the user of the reliability of the dipole fit, the dipole could be color coded based on the GoF value. This gives a more intuitive display of the dipole accuracy. Furthermore, it can communicate expected GoF values, for example with a gradient that has its turning point around the first trustworthy value. Figure 19 shows this principle. High GoF values have a green dipole (Figure 19A) and low GoF values have a red one (Figure 19B). The change in gradient is rather high to signify that a GoF value should preferably be higher than 85%.

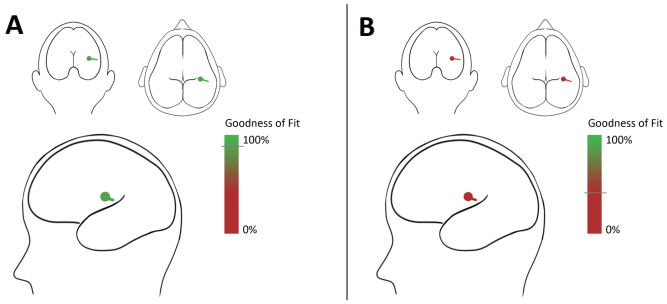

Figure 19: Indication of the GoF value, where a green dipole stands for a high GoF (A) and a red dipole belongs to a low GoF (B). The scalebar at the side show the color gradient belonging to different GoF values.

4.3.4 Concept evaluation

First, the two concepts were evaluated with the Nielsen interface design criteria. The full evaluation can be found in Appendix T. This evaluation identified promising areas of the concepts and areas with room for improvements. For example, the design maintains visibility of system status by displaying the currently selected cluster and its average IED. The designs are both consistent in their appearance, communication and navigation. Moreover, the designs are legible and minimalistic because of their color palette and a minimal number of functionalities. However, the designs adhere less to the principle of creating a match between the system and the real world. Other principles that lag behind are the error recognition, diagnosis and recovery and the help and documentation.
Additionally, users evaluated the prototypes with usability testing. This revealed strengths and weaknesses of the concepts. These can be found in Appendix U, along with scoring of the problems based on their impact and the frequency of occurrence.
Usability testing revealed that the participants needed little guidance in their navigation through the interface. The link to the raw EEG signal is an important element that the final design should preferably incorporate. Furthermore, the cluster IED averages on the main page posed a challenging view to the participants, who automatically interpreted them as a continuous signalf. Moreover, the sources of individual epochs were less valuable to the participants, who expressed that they were not likely to use them often. The settings page was a potentially interesting feature for the clinical neurophysiologist, but the training neurologists would not make any adjustments to the algorithm. Overall, the users experienced the interaction and navigation of concept 2 as more intuitive and more elegant.
Additionally, the participants said that they were not likely to use the moving pictures concept. The view of all epochs next to each other was more familiar to them and provided enough information. Also, they rather saw a cortex than an overly simplified head due to familiarity. However, both views were preferred above the 3D MRI view. Furthermore, they preferred to see a number for the GoF value, rather than to link it to the color of the dipoles.

4.4 Final design

Due to the preference of end users for concept 2, as revealed by the usability testing, the final design is an adaptation of this concept. The final design incorporates the feedback from usability testing. A new semi-function prototype was created of the final design. An impression is shown in Figure 20.

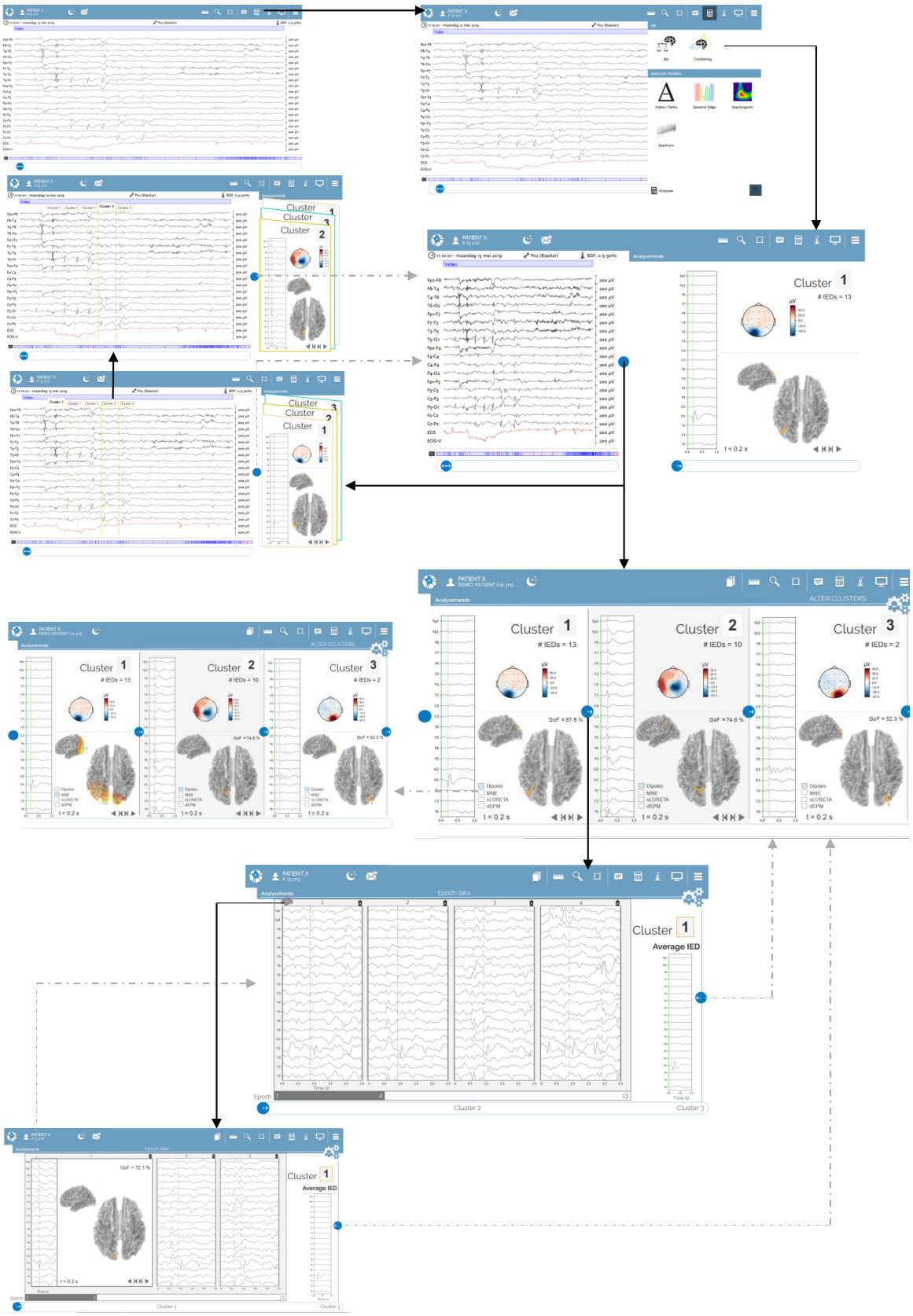

Figure 20: Pages belonging to the final design. At the top, the EEG viewer of Neurocenter. At the top right, the new functionality is selected. The clusters can be seen next to the EEG viewer (second row from the top). The main page can also be displayed in full screen (middle). The epochs within a cluster and their sources can be accessed from here (bottom).

5 Discussion

The goal of this work was to create a user interface for an algorithm that can localise, cluster and determine the sources of IEDs. IEDs are important for the epilepsy diagnosis and classification. Therefore, detection and clustering of IEDs will decrease analysis time and contribute to the diagnosis and classification of epilepsy. Source localisation can additionally aid the diagnosis and some of the results give insight into the nature and dynamic behaviour of IEDs. An interface proposal will improve clinical usage and acceptance of the algorithm.

5.1 IED localisation & clustering

The expert evaluated the average epoch of each cluster. Therefore, the exact number of false positives within the clusters is unknown. However, a convincing cluster average is a good indicator for the epochs in this cluster, especially for large clusters. Furthermore, the cluster average and the approximate number of IEDs in this cluster should provide enough information for an informed epilepsy diagnosis.

5.1.1 Method 1

For method 1, clustering results were insufficient. One reason could be fallibility of the initial IED localisation in method 1, since artefacts are also characterised by high amplitudes [93, 94]. The incorrect detection of the IED channels used for clustering could explain the unsatisfactory clustering results.
The results without clustering do not show a particularly high efficacy (16 of 22 clusters were correct). The lack of clustering reduces flexibility of the algorithm, which can explain this low efficacy. For the Rolandic patients, the correct clusters contain IEDs in centrotemporal channels, which corresponds to the Rolandic area as reported in literature [31, 95–97]. Incorrect clusters often consist of artefacts. Many contain eye blink artefacts, presenting in the pre-frontal channels (Fp1 and Fp2). These artefacts result from transretinal potential due to blinking [94, 98]. Since these signals have a consistent origin, they also present in similar shapes and thus correlate highly with each other. This is why the algorithm classifies them as IEDs. However, they are not neurobiological signals.

Overall, the algorithm of method 1 can detect clusters with IEDs. For some patients the algorithm detects clusters with artefacts instead. The algorithm detects epileptiform activity in 73% of the patients in this dataset.
Another drawback is that the algorithm contains many patient-specific exceptions (f.e. based on the found correlations with other epochs, or the number of channels that seem to contribute) and is thus less adaptable to new EEG signals.

5.1.2 Method 2

Method 2 uses the steepest slope for initial IED detection. This led to better results, suggesting that a steep slope is a more robust IED indicator than a high amplitude. Indeed, while artefacts often display high amplitude, their frequency is generally lower (in the delta-frequency range), resulting in a more gradual slope [94, 98].
The detection of correct clusters in all patients suggests that the algorithm is well suited for IED detection. For the Rolandic patients, correct clusters contain IEDs in the central sulcus or temporal lobe. Other focal clusters generally yield clusters in one brain area, as expected in focal epilepsies [99, 100]. When the algorithm finds multiple clusters for focal patients, it often concerns a mirror focus. This phenomenon where epileptiform activity is present in the same

area of both hemispheres is common for focal epilepsy patients [101, 102].
The algorithm found slightly more clusters for multi-focal than for focal patients. This slight difference may be due to the mirror-focus clusters in focal patients. The algorithm detects at least two clusters in different brain areas for multi-focal patients (with one exception), which is characteristic for multi-focal epilepsies [103]. This indicates that the algorithm is capable of detecting multiple clusters.
There are some divergent findings (patients 12, 15, 19 & 29), with multiple clusters in different brain areas for focal patients and only one cluster for a multi-focal patient. Since the expert identified those clusters as correct, the patients might have been wrongly diagnosed. This stresses the challenge clinicians face with manual IED detection and identification of IED locations. At the same time it verifies the importance of automated detection and clustering mechanisms.
The multi-focal patient with one correct cluster could also contain a low number of IEDs that belong to a second cluster, thus avoiding detection.

Overall, the results suggest that method 2 is successful at detecting and clustering IEDs. There are some clusters with false positives, but since they are captured in one cluster they are easily discarded. For this dataset, the maximum number of clusters that the neurologists would need to discard is 3 and the average number is 0.8 ± 0.9.
Others have explored automated IED detection, clustering and source localisation. Van 't Ent et al. (2003) presented clustering and source localisation results for magnetoencephalogram (MEG) signals for four patients [66]. Similarly, Rozendaal et al. (2015) presented a clustering and source localisation method for MEG of seven patients, with the same epilepsy type [65]. Van 't Ent et al. (2003) found at least one correct cluster for all patients and Rozendaal et al. (2015) found six correct clusters out of seven patients. The methods presented by both studies often returned several similar clusters, often with a low cluster size. This could be due to the clustering approach, which is based on discrete time instances and all channels and thus limited to a single point in time. Whereas method 2 uses a longer time signal and inherently separates clusters by IED channels. Another difference is that those studies used MEG data. MEG signals are generally better suited for IED detection and source localisation, because of a lower sensitivity to distributed and deep brain activity [65, 104].
Although MEG is preferred for source localisation, some studies use EEG signals. For example, van Mierlo et al. (2017) evaluated the Epilog PreOP (Epilog, Ghent, Belgium), which in turn uses the automated detection of Persyst Spike Detector P13 (Persyst, San Diego, CA, USA) on EEG signals of 32 patients [24]. In this work, van Mierlo et al. (2017) use the two clusters with the most epochs and discard all other clusters. They did not report total number of found clusters. Considering only the two largest clusters per patient, they still detected 20 incorrect clusters. In two of the 32 patients, no correct clusters were found. The downside to this method is that the number of clusters is naturally limited to two. In the work from this thesis, the algorithm finds three or more clusters in several instances, which illustrates the importance of limiting the number of incorrect clusters among the results. This is especially relevant for multi-focal patients, which is a patient group that Mierlo et al. (2017) did not consider in their work.
Overall, method 2 adds a new approach to automated IED detection, clustering and source localisation. While comparison can be difficult due to the difference in the study goal, dataset and evaluation of the results, some cautious conclusion can still be drawn. When compared to literature, method 2 seems as or more reliable in IED detection and clustering. The number of incorrectly detected clusters is generally lower and the algorithm is successful for a large number of patients and a larger variety of epilepsy types.

5.1.3 Influence of VGG sensitivity

Generally, a decrease in the VGG sensitivity leads to an increase in the cluster size and the number of clusters, as seen in Figure 7A. This is expected, since a decrease in sensitivity leads to an increase in the number of epochs used as input. This leads to an increase in the number of correctly detected IEDs, but also to an increase in the number of false positives.
Therefore, a decrease in sensitivity can also lead to a decrease (Figure 7D) or absence (Figure 7) of correctly detected IEDs. The decrease in detected IEDs indicates that the number of IEDs is low compared to the number of false positives. This impedes IED detection, as the assumption is that IEDs have a high correlation with many other epochs.
In one case, the algorithms finds no correct IEDs for one sensitivity value, as seen in Figure 7C. In this case, the ratio of IEDs within the cluster is lower for this specific sensitivity. This ratio is just below the IED detection threshold.
In the end, what probability threshold to use is a trade-off between quantity and quality. Overall, it seems that in the future the sensitivity threshold can be lower than 0.99. For this dataset, a probability of 0.96 or 0.94 will lead to an increase in the detected number of IEDs, without losing the accuracy for some of the patients.

5.2 Source localisation

5.2.1 Verification

The source localisation method was verified with EEG signals of patients diagnosed with Rolandic epilepsy. Typical spike topographies are reported as a negative potential field centrotemporally and a positive potential field frontally [95]. Furthermore, literature reports the dipoles in Rolandic epilepsy positioned around the central sulcus, causing motor or sensory symptoms. The orientation of the dipole is less consistent in literature, but dipoles are orientated tangential to the skull, either posteriorly or anteriorly [31, 95–97].
Inspection of the found dipoles (see Appendix O) shows that all are located in the centrotemporal area. The orientation is tangential to the skull surface for all patients, as demonstrated for one patient in Figure 8. Therefore, all dipoles show a location and orientation which is consistent with literature [31, 95–97]. This justifies the choice and implementation of the equivalent dipole model for these patients.

5.2.2 Dipole characteristics

Based on the probability density functions in Figure 9, there is no significant difference in dipole strength between correct and incorrect clusters. However, for the GoF the probability of finding a value higher than 85% is higher for correct clusters (47.6%) than for incorrect clusters (11.9%). A higher GoF for IEDs is as expected, as epileptiform activity originates from one or multiple sources in the brain, whereas background activity does not have discrete sources. Therefore, high GoF values for correct clusters suggest that the dipole modelling for these clusters is accurate. Furthermore, it suggests that a high GoF is synonymous with the credibility of a cluster. However, there are exceptions on both sides.
Some of the correct clusters show low GoF, as seen in Figure 10. The average IEDs of those clusters have similar dipole locations, close to the skull of the head model (see Figure 10). The used head model is a standard head model and thus not patient-specific. Therefore, the exact location and shape of the skull from the patient might differ from the used model [105,106]. More importantly, these patients often show epileptiform activity in non-adjacent brain lobes or even in different hemispheres at the same time. Therefore, one dipole may not suffice in explaining the IED, you might need 2 or 3 dipoles, or even distributed source models [107]. Both factors

could have contributed to the low GoF that was found.
On the other hand, some of the incorrect clusters also show a divergently high GoF. Upon inspection (see Figure 11) many of these clusters consist of artefacts. This suggests that the equivalent dipole model is confident that it can correctly detect the sources of artefacts. On one hand, this is to be expected as there are only one or two channels that significantly contribute to the measured signal. Thus it is not difficult to establish the origin of the supposed electrical activity. For patient 22, cluster 2, where the artefacts are present in channel F3, the model assumes that only one electrode (F3 in this case) contributes to the EEG signal. Indeed, the position of the dipole is precisely at the electrode displaying the artefact, pointing outward, towards the skull. However, biologically this is a very unlikely source. For the other patients, the artefacts are again eye blink artefacts. Therefore, the dipole model put the source of electric activity between the eyes. Again, visual inspection can easily confirm that this does not represent brain activity, since the source is not found in the cortex.

Overall, higher GoF values are found for correct clusters than for incorrect clusters. The exceptions can be explained with biological and mathematical arguments. The results suggest that the GoF value of the dipoles can be used to exclude incorrect clusters which do not consist of artefacts. However, one should take into account that the GoF value will only be high for IEDs where the electrical activity can be explained with a single dipole.

5.2.3 IED stability

For the three included patients, there is a change in IED morphology and dipole characteristics over time, as seen in Figure 12 and Appendix Q. Furthermore, the number of detected IEDs increases over time, as seen in Figure 13. The IED frequency shows an average increase of 250%, 1100% and 1300%.
Based on the inflection point (between 19:15-21:15, 21:45-23:45 and 21:30-23:30), this increase may relate to the difference in EEG between sleep and wake [108, 109]. It is known that NREM (non-Rapid Eye Movement) sleep often leads to an increase in IED frequency, while REM (Rapid Eye Movement) sleep leads to suppression of IEDs [110–120]. The general consensus is that this phenomenon is due to the high degree of cortical desynchronisation in EEG during REM sleep, while in NREM sleep the patterns are more synchronised, as witnessed in sleep spindles, delta waves and slow wave activity (SWA) [110, 113–116, 120, 121]. Furthermore, inhibitory influences during sleep may increase epileptiform activity [121, 122].
There is some additional evidence in literature that suggests that sleep also influences IED morphology [111, 118, 119]. For example, during REM sleep IEDs are generally shorter and more localised and the onset zone is more correlated to ictal (seizure) onset zone, when compared to NREM sleep [111, 118]. The hypothesis is that the interaction between sleep and EEG causes the increase in IED frequency and the shift in IED morphology.
What was not taken into account here is the effect of medication. However, AED usage can also interact with sleep patterns, leading to alteration of the IEDs during sleep [111].

5.3 Interface design

5.3.1 Design process

Gould and Lewis (1985) stated three principles for usability design [92]. The first is an early focus on users and tasks. In this work that encompassed a brand analysis, a stakeholder analysis, the information cycle and identification of users and their preferences and necessities through the user interface design principles. Furthermore, neurologists also gave direct input. This direct contact with end users is often forgotten but fundamental according to Gould and Lewis.
The second principle is empirical measurement, which refers to prototype testing. In this work users interacted with digital semi-functional prototypes for usability testing. The prototypes of the concepts yielded more feedback from the end users, while preserving focus on the design elements. Because of the interaction between the end users and the interface, the end users also get a more complete picture of the possible end product. This functionality contributed to gathering useful and precise user feedback. Apart from information about the interface, the interaction between users and the interface was also recorded, with is a recommended part of empirical measurement according to Gould and Lewis.
The third principle is iterative design. This refers to circular design, where design phases uncover problems which are fixed in the next iteration. The evaluation with the Nielsen design criteria and usability testing revealed strengths and weaknesses in the design. The final design incorporates these strengths, such as the visibility of system status, the intuitive navigation of concept 2 and the legible color palette. The revealed weaknesses are omitted or altered in the final design. For example, the ambiguous views were changed and the functionality was linked to the raw EEG signal. However, this work did not fully address all the weaknesses. For instance it did not completely fix the lack of error recognition, diagnosis and recovery and help and documentation. However, these features become increasingly important as implementation is nearing. In the current early phase it is more challenging to identify potential errors and thus less efficient to focus on this area. Further work could build on the challenges and gather more insight to aid implementation of these features.

5.3.2 Final design

The earlier design steps led to a final design. The prototype of the final design gives insight into a possible functional design. The design concisely presents the most important information for the end user. Furthermore, this design links the found IEDs to their location in the raw EEG signal. This provides more context, aiding the neurologists in the interpretation of the electrical activity. It also allows neurologists to easily verify the result, which improves usability and acceptance. Furthermore, it relates the new functionality to current practise, which will shorten the learning curve for the interface.
Usability testing revealed that familiarity is important to the end users. Therefore, the dipoles are now displayed inside the cortex, which helps the neurologists evaluate the dipole. Compared to the MRI 3D view of the concepts, the new representation is less ambiguous and more familiar to end users.
Furthermore, for time instances farther from the IED shape, the dipole is removed to convey that the dipole fit is not valuable when there is no epileptiform activity.
The user can access more in-depth information about clusters via intuitive navigation. The user can still access the sources of individual epochs, but it is a less dominant feature and does not have an individual page. Similarly, the user can still change parameters in the settings page, but the page itself is not a prominent feature. The opinions on adding a settings page were inconclusive. The (training) neurologists perceived the interface differently on this and other areas than the neurophysiologist. This difference is an important result. It indicates that future

work should focus on defining the exact target group. Johnson and Turley (2006) discussed the need for different design approaches for users with different backgrounds in health care [123]. They found cognitive differences between physicians and nurses, calling for different designs. The interface in this work may need a similar divide between neurologists, neurophysiologists and other clinicians. More research must reveal the different possible users and the intended target group. A preciser target group will help tune the design to their preferences and needs.
Another consideration for the settings page is that this function is a manual override that users will ideally not need. A further stadium with a better defined target group will have to reveal whether and in what sense a settings page is needed.
In the end, the misinterpretation of the horizontally aligned IEDs on the main page was not fixed. Breaking up this horizontal view by misaligning the average IEDs is detrimental for the consistency and aesthetic of the design. The end users may get used to this view over time. This is something further work can explore on a longer time scale with various end users. Furthermore, the final design provides an option to see the cluster information of only one cluster at a time, circumventing the issue.

The final design plays to the strengths and preferences of end users with visuals that are familiar to neurologists and by taking the perceived value of information to the end users into account. Multiple views and ways of navigation in the design increase flexibility and efficiency of use. The intended target group needs further exploration. Some elements of the design are underdeveloped, such as error handling and available settings. Further research must determine strategies to handle these features, based on end user preferences and challenges and opportunities identified through interaction.
Overall, the usability testing and the adaptions made in the final design show that there is a future for the presented work in a clinical environment.

6 Conclusion

This work presented two algorithms. The algorithm that localises IEDs by their steep slopes yielded the best results. This algorithm, in succession to the VGG adaptation of Catarina Lourenço [1], is able to create clusters of IEDs for all patients in the available dataset. The overall number of incorrectly determined clusters is low (0.8 ± 0.9 (mean ± sd)). As expected, the algorithm found clusters in different brain areas for multi-focal patients, whereas focal patients had one cluster or mirror-focus clusters.
The dipoles of the clusters revealed that correct clusters show a higher GoF value (84.0% ± 17.4) than incorrect clusters (64.7% ± 17.2).
Three long recordings revealed that there is a change in IED frequency, IED morphology and dipole location over time. This may reflect the interaction between sleep and epileptiform activity.
We created two prototypes for the interface design. Three end users evaluated the prototypes. The final design incorporates the user feedback. Despite the absence of a fully functional interface, the prototypes show possible functioning of the interface. This led to valuable feedback from the end users and it showed the possible clinical value of the algorithm in combination with the interface.
Automated detection, clustering and source localisation of IEDs is not common practise in the clinic. The goal of this work was to create an algorithm for automated IED localisation, clustering and source analysis and to present the results to neurologists in the clinic. The presented algorithm successfully creates clusters of IEDs and determines their sources. Usability testing and the subsequent final design show that the presented interface communicates the results according to preferences of end users. This combination could aid neurologists in setting the epilepsy diagnosis and classification in the future.
Furthermore, the algorithm could promote longer EEG recordings and encourage more common usage of source localisation in the epilepsy diagnosis and classification in the clinic.

7 Recommendations

7.1 VGG model

The VGG Convolutional Neural Network is continuously subject to improvements by Lourenço da Silva [1]. Since the start of this project, a new version of the VGG for 18-channel or 19-channel EEG signals was designed. Future works can use these new models as the input for the algorithm in this project, which should increase the number of detected IEDs.
Furthermore, the VGG seems to perform better on signals referenced with the Double Banana montage. This project used the average reference montage for most signals (with four exceptions), to allow source localisation. However, for future work it may be interesting to use the Double Banana montage for the labels, while running the algorithm on signals with an average reference.

Moreover, further work should explore the optimal value for the VGG sensitivity. In general, lower sensitivity thresholds should yield better results. The algorithm can be adjusted to support usage of lower probability thresholds. For example, the detection threshold (percentage of epochs an epoch should be highly correlated with) should likely be lower for lower sensitivities. Otherwise, the increasing number of false positives will decrease this percentage, making it more likely to exclude true positives. This was seen in practise for patient 1 for probability 0.92 (Figure 7C) and is likely what happened to patient 21 and 22 (Figure 7B and Figure 7D).

An alternative approach is to explore usage without the VGG output. Currently, the presented method relies on the performance of the VGG. Therefore, whenever the VGG detects a small number of epochs with IEDs or too many artefacts or false positives, this reflects back on the results from the algorithm. With some alterations it may be possible to use the algorithm on epochs of an EEG signal instead of the epoch generated by the VGG. If the approach is successful, this will likely lead to a higher number of detected IEDs, since the input is larger. The pitfall is that more false positives will be present amongst the epochs, making it more challenging to detect the IEDs.

7.2 IED detection & clustering

The first recommendation for further validation of the algorithm is to increase the sample size. With a larger dataset, the work can set more precise algorithm parameters. Instead of a more empirical approach in setting the thresholds, as is the case in this work, larger simulations should determine the optimal values.
Due to time constraints, this work did not quantify the exact number of false positives within each cluster. For further work, this is a recommended addition. Not only would the evaluation of the algorithm be more reliable, but it would also allow more exact comparison to results in literature.
Furthermore, in some cases the algorithm still yields multiple similar clusters. Further work can explore in what case clusters should be merged and how to implement this.

7.3 Source localisation

Future work can include extending the dipole modelling to multiple dipoles. This will lead to better results for a larger variety of EEG signals.
Future algorithms could use dipole GoF values to exclude clusters with false positives (f.e. GoF <85%). However, the work should be aware of possible fallibility of the dipole modeling, such as dipole position (close to the skull may lead to low GoF) or IED characteristics (origination from multiple sources). This would not exclude clusters with artefacts, but these are often easier to

distinguish from IEDs for neurologists, both because of shape, amplitude and (sometimes) dipole orientation and location.

7.4 IED stability

Since there can be a difference in IED shape over time, it may be interesting to implement hierarchical clustering in the future, to separate those shapes. Another option is to run the algorithm per 2/4 hours and then combine the results.
Furthermore, further work could explore the hypothesised relationship between sleep and IED frequency and morphology. Although literature reports the increase in IED frequency during sleep, the effect of sleep on IED morphology is largely unexplored. A larger dataset should be used, where sleep patterns of the patients are precisely annotated. This will produce more definite results. Furthermore, the influence of AEDs on these analyses should be investigated.

7.5 Interface design

The first recommendation is to create a fully functional interface design. Furthermore, usability testing should be performed on a larger scale, with more stakeholders (for example both neurologists and other clinicians from different institutions). More research must investigate the possible end users and define the intended target group. Direct contact with the clinicians involved in EEG analysis and more usability testing can help define the most relevant target group in this case.

Further work should incorporate the design into the current interface. While the final design contains interaction with the EEG viewer, this should be extended. For example, the clinician should be able to add their found IEDs from the raw signal to a cluster.
With a more functional design, opportunities arise to implement some features that may benefit usability. For example, a bottleneck in this project is that Axure RP (Axure Software Solutions, San Diego, CA, USA) does not support dragging of elements. However, it would be more intuitive to drag the scrollbars (to scroll between clusters and epochs) than to click them to the next page, which is currently the case. Furthermore, a more intuitive way of merging clusters would be to drag two clusters together on the main page.
The settings page needs further exploration. Further usability testing must determine the necessity of this page and more research must be conducted into clinical usage and what this means for the design. Furthermore, future work should focus more on potential errors and ways to avoid and fix them. Errors can be identified by creating (almost) fully functional prototypes and testing them with a large group of end user. Additionally it will be easier to design and evaluate user interaction with a fully-functional interface.

7.6 Implementation in the clinic

Before implementation of the algorithm in the clinic, several steps are needed. First, further work must prove that the VGG in combination with the algorithm is functional for a large number of patients. Furthermore, to increase user friendliness, the clinicians should not operate the algorithm with Python. Therefore, a design for the clinic should incorporate the algorithm. The interface design presented here gives an proposal on what information to present and how to present it. In the end, the design should be fully functional and preferably integrated into the current Neurocenter interface. Testing the completed algorithm with interface in hospitals may help clinicians see its added value. The implementation in the clinic must be gradual to let clinicians get used to the new interface. A trial phase can be added, in which the clinicians are

able to use the fully functional interface and give feedback. This feedback can immediately be implemented, to optimally tune the interface to the wants and needs of its users.
Once implemented, the end result may stimulate clinicians to use a larger number of IEDs in setting the epilepsy diagnosis. Furthermore, they may be more inclined to use the sources of IEDs for the IED evaluation as well, when the option is available and the design highlights its relevance. As a side effect, clinicians may be motivated to increase the standard time of EEG recordings, since they do not have to manually analyse the entire signal. These longer recordings will measure more IEDs and thus lead to more accurate results, in turn leading to a more accurate epilepsy diagnosis.

References

[1] C. Lourenço, M. C. Tjepkema-Cloostermans, L. F. Teixeira, and M. J. A. M. van Putten, "Deep learning for interictal epileptiform discharge detection from scalp eeg recordings," *IFMBE Proceedings*, vol. 76, pp. 1984–1997, 2020. doi:10.1007/978-3-030-31635-8_237.

[2] M. A. Jatoi, N. Kamel, A. S. Malik, I. Faye, and T. Begum, "A survey of methods used for source localization using eeg signals," *Biomedical Signal Processing and Control*, vol. 11, pp. 42–52, 2014. doi:10.1016/j.bspc.2014.01.009.

[3] J. Pillai and M. R. Sperling, "Interictal eeg and the diagnosis of epilepsy," *Epilepsia*, vol. 47, no. 1, pp. 14–22, 2006. doi:10.1111/j.1528-1167.2006.00654.x.

[4] S. J. M. Smith, "Eeg in the diagnosis, classification, and management of patients with epilepsy," *J Neurol Neurosurg Psychiatry*, vol. 76, no. 2, pp. 2–7, 2005. doi:10.1136/jnnp.2005.069245.

[5] E. K. Louis and L. C. Frey, *EEG in the Epilepsies*. American Epilepsy Society, 2011. doi:10.1002/14356007.a02_143.pub3.

[6] C. da Silva Lourenço, "Deep Learning for EEG Analysis in Epilepsy", M.S. Thesis, Clinical Neurophysiology Group, University of Twente, 2019.

[7] S. S. Lodder, J. Askamp, and M. J. A. M. van Putten, "Computer-assisted interpretation of the eeg backround pattern: A clinical evaluation," *PLOS ONE*, vol. 9, no. 1, pp. 1–8, 2014. doi:10.1371/journal.pone.0085966.

[8] R. Beach and R. Reading, "The importance of acknowledging clincal uncertainty in the diagnosis of epilepsy and non-epileptic events," *Arch Dis Child*, vol. 90, pp. 1219–1222, 2005. doi:10.1136/adc.2004.065441.

[9] C. Lourenço, "Machine learning for interictal epileptiform discharge detection - a review," *Clinical Neurophysiology*, vol. 132, no. 7, pp. 1433–1443, 2021. doi:10.1016/j.clinph.2021.02.403.

[10] M. L. Scheuer, A. Bagic, and S. B. Wilson, "Spike detection: Inter-reader agreement and a statistical turing test on a large data set," *Clinical Neurophysiology*, 2016. doi:10.1016/j.clinph.2016.11.005.

[11] F. E. A. El-Sami, T. N. Alotaiby, M. I. Khalid, S. A. Alshebeili, and S. A. Aldosari, "A review of eeg and meg epileptic spike detection algorithms," *Digital Object Identifier*, vol. 6, pp. 60673–6688, 2018. doi:10.1109/ACCESS.2018.2875487.

[12] S. B. Wilson and R. Emerson, "Spike detection: a review and comparison of algorithms," *Clinical Neurophysiology*, vol. 113, no. 12, pp. 1873–1881, 2002. doi:10.1016/S1388-2457(02)00297-3.

[13] M. W. Brown, B. E. Porter, D. J. Dlugos, J. Keating, A. B. Gardner, P. B. Storm, and E. D. Marsh, "Comparison of novel computer detectors and human performance for spike detection in intracranial eeg," *Clinical Neurophysiology*, vol. 118, no. 8, pp. 1744–1752, 2007. doi:10.1016/j.clinph.2007.04.017.

[14] R. Harner, "Automatic eeg spike detection," *Clinical EEG and Neuroscience*, vol. 40, no. 4, pp. 262–270, 2009. doi:10.1177/155005940904000408.

[15] F. L. Spijkerboer, "The cluster tool: Designing a clustering algorithm and graphical user interface for efficient clinical interpretation of Interictal Epileptiform discharges", M.S. Thesis, SEIN, University of Twente, 2019, https://essay.utwente.nl/79964/1/Spijkerboer_MA_TNW.pdf.

[16] Y. Roy, H. Banville, I. Albuquerque, A. Gramfort, T. H. Falk, and J. Faubert, "Deep learning-based electroencephalography analysis: a systematic review," *Journal of Neural Engineering*, vol. 16, pp. 1–37, 2019. doi:10.1088/1741-2552/ab260c.

[17] J. Thomas, L. Comoretto, J. Jin, J. Dauwels, S. S. Cash, and B. M. Westover, "Eeg classification via convolutional neural network-based interictal epileptiform event detection," *Conference Proceedings IEEE English Medical Biology Sociology*, pp. 3148–3151, 2018. doi:10.1109/EMBC.2018.8512930.

[18] J. Thomas, J. Jin, P. Thangavel, E. Bagheri, R. Yuvaraj, J. Dauwels, R. Rathakrishnan, J. J. Halford, S. S. Cash, and B. Westover, "Automated detection of interictal epileptiform discharges from scalp electroencephalogram by convolutional neural networks," *International Journal of Neural Systems*, vol. 30, no. 11, 2020. doi:10.1142/S0129065720500306.

[19] *Proc. Deep Learning for Interictal Epileptiform Discharge Detection from Scalp EEG Recordings (MEDICON, 2019)*, vol. 76 of *IFMBE Proceedings*, Springer, Cham, 2020.

[20] S. S. Lodder and M. J. A. M. van Putten, "A self-adapting system for the automated detection of inter-ictal epileptiform discharges," *PLoS ONE*, vol. 9, no. 1, p. e85180, 2014. doi:10.1371/journal.pone.0085180.

[21] V. Chavakula, I. S. Fernández, J. M. Peters, G. Popli, W. Bosl, S. Rakhade, A. Rotenberg, and T. Loddenkemper, "Automated quantification of spikes," *Epilepsy & Behavior*, vol. 26, pp. 143–152, 2013. doi:10.116/j.yebeh.2012.11.048.

[22] T. N. Alotaiby, S. R. Alrshoud, S. A. Alshebeili, M. H. Alhumaid, and W. M. Alsabhan, "Epileptic meg spike detection using statistical features and genetic programming with knn," *Journal of Healthcare Engineering*, vol. 2017, 2017. doi:10.1155/2017/3035606.

[23] A. Nonclercq, M. Foulon, D. Verheulpen, C. De Cock, M. Buzatu, P. Mathys, and P. Van Bogaert, "Cluster-based spike detection algorithm adapts to interpatient and intrapatient variation in spike morphology," *Journal of Neuroscience Methods*, vol. 210, pp. 259–265, 2012. doi:10.1016/j.jneumeth.2012.07.015.

[24] P. van Mierlo, G. Strobbe, V. Keereman, G. Birot, S. Gadeyne, M. Gschwind, E. Carette, A. Meurs, D. van Roost, K. Vonck, M. Seeck, S. Vlliémoz, and P. Boon, "Automated long-term eeg analysis to localize the epileptogenic zone," *Epilepsia Open*, vol. 2, no. 3, pp. 322–333, 2017. doi:10.1002/epi4.12066.

[25] J. Halford, M. Westover, S. Laroche, M. P. Macken, E. Kutluay, J. C. Edwards, L. Bonilha, G. P. Kalamangalam, K. Ding, J. L. Hopp, A. Arain, R. A. Dawson, G. U. Martz, B. J. Wolf, C. G. Waters, and B. C. Dean, "Interictal epileptiform discharge detection in eeg in different practice settings," *Journal of Clinical Neurophysiology*, vol. 5, no. 35, pp. 375–380, 2018. doi:10.1097/WNP.0000000000000492.

[26] T. Fuchigami, H. Mugishima, and Y. Fujita, "Relationship between migration and outcome in childhood epilepsy using dipole analysis," *Hong Kong Journal of Pediatrics*, vol. 17, pp. 167–173, 2012.

[27] S. Meckes-Ferber, A. Roten, C. Kilpatrick, and T. O'Brien, "Eeg dipole source localisation of interictal spikes acquired during routine clinical video-eeg monitoring," *Clinical Neurophysiology*, vol. 115, no. 12, pp. 2738–2743, 2004. doi:10.1016/j.clinph.2004.06.023.

[28] F. G. Awan, O. Saleem, and A. Kiran, "Recent trends and advantages in solving the inverse problem for eeg source localization," *Inverse Problems in Science and Engineering*, vol. 27, no. 11, pp. 1521–1536, 2018. doi:10.1080/17415977.2018.1490279.

[29] C. M. Michel and D. Brunet, "Eeg source imaging: A practical review of the analysis steps," *Frontiers in Neurology*, vol. 10, no. 325, 2019. doi:10.3389/fneur.2019.00325.

[30] C. S. Lessard, H.-i. Wu, and J. Winston, "Localization of current dipole within a sphere by magnetic measurements," *Computer Methods and Programs in Biomedicine*, vol. 20, pp. 45–49, 1985.

[31] H. Kim, I. H. Yoo, B. C. Lim, H. Hwang, J.-H. Chae, J. Choi, and K. J. Kim, "Averaged eeg spike dipole analysis may predict atypical outcome in benign childhood epilepsy with centrotemporal spikes (bcects)," *Brain & Development*, vol. 38, pp. 903–908, 2016. doi:10.1016/j.braindev.2016.06.001.

[32] S. Asadzadeh, T. Y. Rezaii, S. Beheshti, A. Delpak, and Meshgini, "A systematic review of eeg source localization techniques and their applications on diagnosis of brain abnormalities," *Journal of Neuroscience Methods*, vol. 339, pp. 1–23, 2020. doi:10.1016/j.jneumeth.2020.108740.

[33] Y.-H. Jun, T.-H. Eom, Y.-H. Kim, S.-Y. Chung, I.-G. Lee, and J.-M. Kim, "Changes in background electroencephalographic activity in benign childhood epilepsy with centrotemporal spikes after oxcarbazepine treatment: a standardized low-resolution brain electromagnetic tomography (sloreta) study," *BMC Neurology*, vol. 19, no. 3, pp. 1–8, 2019. doi:10.1186/s12883-018-1228-8.

[34] A. Endo, T. Fuchigami, Y. Fujita, and H. Mugishima, "Relationship between migration and outcome in childhood epilepsy using dipole analysis," *Hong Kong Journal of Paediatrics*, vol. 17, no. 3, pp. 167–173, 2012.

[35] C. Plummer, S. A. Harvey, and M. Cook, "Eeg source localization in focal epilepsy: Where are we now?," *Epilepsia*, vol. 49, no. 2, pp. 201–218, 2007. doi:10.1111/j.1528-1167.2007.01381.

[36] T. Eom, J. Shin, Y. Kim, S. Chung, I. Lee, and J. Kim, "Distributed source localization of interictal spikes in benign childhood epilepsy with centrotemporal spikes: A standardized low-resolution brain electromagnetic tomography (sloreta) study," *Journal of Clinical Neuroscience*, vol. 38, pp. 49–54, 2017. doi:10.1016/j.jocn.2016.12.047.

[37] A. Seeland, M. Krell, S. Straube, and E. Kirchner, "Empirical comparison of distributed source localization methods for single-trial detection of movement preparation," *Frontiers in Human Neuroscience*, vol. 12, no. 340, pp. 1–15, 2018. doi:10.3389/fnhum.2018.00340.

[38] A. P. Bagshaw, E. Kobayashi, F. Dubeau, G. B. Pike, and J. Gotman, "Correspondence between eeg-fmri and eeg sipole localisation of interictal discharges in focal epilepsy," *NeuroImage*, vol. 30, no. 2, pp. 417–425, 2006. doi:10.1016/j.neuroimage.2005.09.033.

[39] A. M. Lascano, S. Vulliemoz, G. Lantz, L. Spinelli, C. Michel, and M. Seeck, "A review on non-invasive localisation of focal epileptic activity using eeg source imaging," *Epileptologie*, vol. 29, pp. 80–88, 2012. doi:10.1016/j.jneumeth.2012.07.015.

[40] P. van Mierlo, B. J. Vorderwülbecke, M. Staljanssens, W an Seeck, and S. Vulliémoz, "Ictal eeg source localization in focal epilepsy: Review and future perspectives," *Clinical Neurophysiology*, vol. 131, no. 11, pp. 2600–2616, 2020. doi:10.1016/j.clinph.2020.08.001.

[41] S. Safi, T. Thiessen, and K. J. G. Schmailzl, "Acceptance and resistance of new digital technologies in medicine: Qualitative study," *JMIR Research Protocols*, vol. 7, no. 12, p. e11072, 2018. doi:10.2196/11072.

[42] J. Mares, "Resistance of health personnel to changes in healthcare," *Kontakt*, vol. 20, no. 5, pp. e262–e272, 2018. doi:10.1016/j.kontakt.2018.04.002.

[43] F. L. da Silva, "Eeg and meg: Relevance to neuroscience," *Neuron*, vol. 80, no. 5, pp. 1112–1128, 2013. doi:10.1016/j.neuron.2013.10.017.

[44] E. K. Louis and L. C. Frey, *Appendix 1. The Scientific Basis of EEG: Neurophysiology of EEG Generation in the Brain*. American Epilepsy Society, 2011. doi:10.1002/14356007.a02_143.pub3.

[45] P. L. Nunez and R. Srinivasan, *Electric fields of the brain: The neurophysics of EEF*. Oxford University Press, 2006. doi:10.1093/acprof:oso/9780195050387.001.0001.

[46] E. K. Louis and L. C. Frey, *Introduction: Brief History and Background*. American Epilepsy Society, 2011. doi:10.1002/14356007.a02_143.pub3.

[47] R. S. Fischer, C. Acevedo, A. Arzimanoglou, A. Bogacz, H. Cross, C. E. Elger, J. Engel, L. Forsgren, J. A. French, M. Glynn, D. C. Hesdorffer, B. I. Lee, G. W. Mathern, S. L. Moshé, E. Perucca, I. E. Scheffer, T. Tomson, M. Watanabe, and S. Wiebe, "Ilae official report: A practical clinical definition of epilepsy," *Epilepsia*, vol. 4, no. 55, pp. 475–482, 2014. doi:10.1111/epi.12550.

[48] E. B. Bromfield, J. E. Cavazos, and J. I. Sirven, *Basic Mechanisms Underlaying Seizures and Epilepsy*. American Epilepsy Society, 2006.

[49] J. S. Duncan, J. W. Sander, S. M. Sisodiya, and M. C. Walker, "Adult epilepsy," *Lancet*, vol. 367, pp. 1087–1100, 2006.

[50] C. E. Stafstrom and L. Carmant, "Seizures and epilepsy: An overview for neuroscientists," *Cold Spring Harb Perspect Med*, vol. 5, 2015. doi:10.1101/cshperspect.a022426.

[51] K. J. Staley and F. E. Dubek, "Interictal spikes and epileptogenesis," *Epilepsy Currents*, vol. 6, no. 6, pp. 199–202, 2006. doi:10.1111/j.1535-7511.2006.00145.x.

[52] H. M. Khoo, Y. Haom, N. von Ellenrieder, N. Zazubovits, J. Hall, A. Olivier, F. Dubeau, and J. Gotman, "The hemodynamic response to interictal epileptic discharges localizes the seizure-onset zone," *Epilepsia*, vol. 58, no. 5, pp. 811–823, 2017. doi:10.1111/epi.13717.

[53] E. D. Marsh, B. Peltzer, M. W. Brown III, C. Wusthoff, P. B. Storm Jr., B. Litt, and B. E. Porter, "Interictal eeg spikes identify the region of seizure onset in some, but not all pediatric epilepsy patients," *Epilepsia*, vol. 51, no. 4, pp. 592–601, 2010. doi:10.1111/j.1528-1167.2009.02306.x.

[54] J. W. Puspita, G. Soemarno, A. I. Jaya, and E. Soewono, "Interictal epiletiform discharges (ieds) classification in eeg data of epilepsy patients," *Journal of Physics: Conference Series*, vol. 943, 2017. doi:10.1088/1742-6596/943/1/012030.

[55] M. A. Kural, L. Duez, V. S. Hansen, P. G. Larsson, S. Rampp, R. Schilz, H. Tankisi, R. Wennberg, B. M. Bibby, M. Scherg, and S. Beniczky, "Criteria for defining interictal epileptiform discharges in eeg: A clinical validation study," *Neurology*, vol. 94, no. 20, pp. e2139–e2147, 2020. doi:10.1212/WNL.0000000000009439.

[56] J. Griffié, L. Boelen, G. Burn, A. P. Cope, and D. M. Owen, "Topographic prominence as a method for cluster identification in single-molecule localisation data," *Journal of Biophotonics*, vol. 8, no. 11-12, pp. 925–934, 2015. doi:10.1002/jbio.201400127.

[57] B. Kashyap, M. Horne, P. N. Pathirana, L. Power, and D. Szmulewicz, "Automated topographic prominence based quantitative assessment of speech timing in cerebellar ataxia," *Biomedical Signal Processing and Control*, vol. 57, pp. 1–11, 2020. doi:10.1016/j.bspc.2019.101759.

[58] M. Choi, J. Ahn, D. J. Park, S. M. Lee, K.-H. Kim, D. Cho, S. Senok, K. Koo, and Y. Goo, "Topographic prominence discriminator for the detection of short-latency spikes of retinal ganglion cells.," *Journal of neural engineering*, vol. 14, no. 1, p. 016017, 2017. doi:10.1088/1741-2552/aa5646.

[59] J. Yoo and H. H. Tae, "Fast normalized cross-correlation," *Circuits System Signal Processing*, vol. 28, pp. 819–843, 2009. doi:10.1007/s00034-009-9130-7.

[60] R. Siedenberg, D. S. Goodin, M. J. Aminoff, H. A. Rowley, and T. P. L. Roberts, "The correlation coefficient and the goodness of fit in source localization of noise recorded by magnetoencephalography," *Brain Topography*, vol. 9, no. 14, pp. 95–100, 1996. doi:10.1007/BF01200709.

[61] R. T. Dean and W. T. M. Dunsmuir, "Dangers and uses of cross-correlation in analyzing time series in perception, performance, movement and neuroscience: The importance of constructing tranfer function autoregressive models," *Behavioural Research*, vol. 48, pp. 783–802, 2015. doi:10.3758/s13428-015-0611-2.

[62] F. Murtagh and P. Contreras, "Methods of hierarchical clustering," no. 2, pp. 1–21, 2011. doi:arXiv:1105.0121v1.

[63] W. H. E. Day and H. Edelsbrunner, "Efficient algorithms for agglomerative hierarchering clustering methods," *Journal of Classification*, no. 1, pp. 7–24, 1984. doi:.

[64] E. Blair, "Semi-supervised clustering methods," *WIREs Computer Statistics*, vol. 5, pp. 349–361, 2013. doi:10.1002/wics.1270.

[65] Y. J. W. Rozendaal, G. van Luijtelaar, and O. P. P. W, "Spatiotemporal mapping of interictal epileptiform discharges in human absence epilepsy: A meg study," *Epilepsy Research*, vol. 119, pp. 67–76, 2016. doi:10.1016/j.eplepsyres.2015.11.013.

[66] D. van 't Ent, I. Manshanden, P. Ossenblok, D. N. Velis, J. C. de Munck, J. P. A. Verbunt, and F. H. Lopes da Silva, "Spatiotemporal mapping of interictal epileptiform discharges in human absence epilepsy: A meg study," *Epilepsy Research*, vol. 119, pp. 67–76, 2016. doi:10.1016/j.eplepsyres.2015.11.013.

[67] G. J. Székely, "Hierarchical clustering via joint between-within distances: Extending ward's minimum variance method," *Journal of Classification*, vol. 22, pp. 151–1831, 2005. doi:10.1007/s0037-005-0012-9.

[68] F. Pittau, F. Dubeau, and J. Gotman, "Contribution of eeg/fmri to the definition of the epileptic focus," *Neurology*, vol. 78, pp. 1479–1487, 2012. doi:10.1212/WNL.0b013e3182553bf7.

[69] R. Grech, T. Cassar, J. Muscat, K. P. Camilleri, S. G. Fabri, M. Zervakis, P. Xanthopoulos, V. Sakkalis, and B. Vanrumste, "Review on solving the inverse problem in eeg source analysis," *Journal of NeuroEngineering and Rehabilitation*, vol. 5, no. 25, 2008. doi:10.1186/1743-0003-5-25.

[70] R. J. Ilmoniemi, "Models of source currents in the brain," *Brain Topography*, vol. 5, no. 4, 1993. doi:10.1007/BF01128686.

[71] A. M. Dale, A. K. Liu, B. R. Fischl, R. L. Buckner, J. W. Belliveau, J. Lewine, and E. Halgren, "Dynamic statistical parametric mapping: Combining fmri and meg for high-resolution imaging of cortical activity," *Neuron*, vol. 26, no. 1, pp. 55–67, 2000. doi:10.1016/s0896-6273(00)81138-1.

[72] *Interface Design for Health Care Environments: The Role of Cognitive Science*, Proceedings, AMIA Annual Symposium, (Quebec), McGill University, 1998.

[73] *Designing Interfaces for Healthcare Workers: A Case Study of the Electronic Partogram*, ACM International Conference Proceeding Series, (Bangalore, India), 2013. doi:10.1145/2525194.2525268.

[74] J. Horsky, G. D. Schiff, D. Johnston, L. Mercincavage, D. Bell, and B. Middleton, "Interface design principles for usable decision support: A targeted review of best practices for clinical prescribing interventions," vol. 45, pp. 1202–1216, 2012. doi:10.1016/j.jbi.2012.09.002.

[75] C. M. Johnson, T. R. Johnson, and J. Zhang, "A user-centered framework for redesigning health care interfaces," vol. 38, pp. 75–87, 2005. doi:10.1016/j.jbi.2004.11.005.

[76] L. Rosenfield, P. Morville, and J. Arango, *Information Architecture: For the Web and Beyond*. Sebastopol, California, USA: O'Reilly Media Inc, 2015.

[77] D. Farkas and J. Farkas, "Guidelines for designing web navigation," *Technical Communication*, vol. 341, 2000.

[78] Y. Rogers, H. Sharp, and J. Preece, *Interaction Design: Beyond Human-Computer Interaction*. West Sussex, United Kingdom: John Wiley & Sons Ltd, 2011.

[79] D. Saffer, *Designing for Interaction: Creating Innovative Applications and Devices*. Berkeley, California, USA: New Riders, 2010.

[80] M. L. Wong, C. W. Khong, and H. Thwaites, "Applied ux and ucd design process in interface design," *Procedia - Social and Behavioral Sciences*, vol. 51, pp. 703–708, 2012. doi:10.1016/j.sbspro.2012.08.228.

[81] A. W. White, *The Elements of Graphic Design*. New York, USA: Allworth Press, 2011.

[82] K. Tomita, "Principles and elements of visual design: A review of the literature on visual design of instructional materials," *Educational Studies (IERS, International Christian University)*, vol. 57, pp. 167–174, 04 2015.

[83] J. Nielsen, "Enhancing the explanatory power of usability heuristics," *Human Factors in Computing Systems*, pp. 24–18, 04 1994.

[84] J. Bastien, "Usability testing: a review of some methodological and technical aspects of the method," *International Journal of Medical Informatics*, vol. 79, no. 4, pp. e18–e23, 2010. doi:10.1016/j.ijmedinf.2008.12.004.

[85] J. Chisman, K. Diller, and S. Walbridge, "Usability testing: A case study," *College and Research Libraries*, vol. 6, no. 6, pp. 552–569, 1999. doi:10.5860/crl.60.6.552.

[86] A. W. Kushniruk, V. L. Patel, and J. J. Cimino, "Usability testing in medical informatics: Cognitive approaches to evaluation of information systems and user interfaces," *Journal of the American Medical Informatics Association*, vol. 4, pp. 218–222, 1997.

[87] J. Lewis, *Usability Testing*, pp. 1275 – 1316. 02 2006.

[88] A. Gramfort, M. Luessi, E. Larson, D. Engemann, D. Strohmeier, C. Brodbeck, L. Parkkonen, and M. Hämäläinen, "Mne software for processing meg and eeg data," *Neuroimage*, vol. 86, pp. 446–460, 2014. doi:10.1016/j.neuroimage.2013.10.027.

[89] *Mind the noise covariance when localizing brain sources with M/EEG*, International Workshop on Pattern Recognition in Neuroimaging, (United States), Stanford, 2015.

[90] K. Sekihara, K. Abraham-Fuchs, H. Stefan, and E. Hellstrandt, "Suppression of background brain activity influence in localizing epileptic spike sources from biomagnetic measurements," *Brain Topography*, vol. 8, no. 3, pp. 323–328, 1996. doi:10.1007/BF01184792.

[91] K. Whittingstall, G. Stroink, L. Gates, J. F. Connolly, and A. Finley, "Effects of dipole position, orientation and noise on the accuracy of eeg source localisation," *BioMedical Engineering OnLine*, vol. 2, no. 2, 2003. doi:10.1186/1475-925X-2-14.

[92] J. D. Gould and C. Lewis, "Designing for usability: Key principles and what designers think," *Communications of the ACM*, vol. 28, no. 3, pp. 300–311, 2008. doi:10.1145/3166.3170.

[93] E. K. Louis and L. C. Frey, *Appendix 4. Common Artifacts During EEG Recording*. American Epilepsy Society, 2011. doi:10.1002/14356007.a02_143.pub3.

[94] A. Tandle, N. Jog, P. D'cunha, and M. Chheta, "Classification of artefacts in eeg signal recordings and eog artefact removal using eog subtraction," *Communications on Applied Electronics*, vol. 4, no. 1, pp. 2394–4714, 2016.

[95] M.-L. Tsai and K.-L. Hung, "Topographic mapping and clinical analysis of benign childhood epilepsy with centrotemporal spikes," *Brain & Development*, vol. 20, pp. 27–32, 1998. doi:10.1016/s0387-7604(97)00089-2.

[96] W. van der Meij, G. H. Wieneke, and A. C. van Huffelen, "Dipole source analysis of rolandic spikes in benign rolandic epilepsy and other clinical syndromes," *Brain Topography*, vol. 5, no. 3, pp. 203–213, 1993. doi:10.1007/BF01128988.

[97] H. Yoshinaga, R. Amano, E. Oka, and S. Ohtahara, "Dipole tracing in childhood epilepsy with special reference to rolandic epilepsy," *Brain Topography*, vol. 4, no. 3, pp. 193–199, 1992. doi:10.1007/BF01131150.

[98] O. G. Lins, T. W. Picton, P. Berg, and M. Scherg, "Ocular artifacts in eeg and event-related potentials i: Scalp topography," *Brain Topography*, vol. 6, no. 1, pp. 51–63, 1993. doi:10.1007/BF01234127.

[99] J. I. Sirven, "Epilepsy: A spectrum disorder," *Cold Spring Harbor Perspectives in Medicine*, vol. 5, no. 9, p. a022848, 2015. doi:10.1101/cshperspect.a022848.

[100] C. E. Stafstrom, "Seizures and epilepsy: An overview for neuroscientists," *Cold Spring Harbor Perspectives in Medicine*, vol. 5, no. 6, p. a022426, 2015. doi:0.1101/cshperspect.a022426.

[101] S. J. Choi, E. Y. Joo, and S. B. Hong, "Mirror focus in a patient with intractable occipital lobe epilepsy," *Journal of Epilepsy Research*, vol. 4, pp. 34–37, 2014. doi:10.14581/jer.14009.

[102] M. A. Falconer and W. A. Kennedy, "Epilepsy due to small focal temporal lesions with bilateral independent spike-discharging foci: A study of seven cases relieved by operation," *Journal of Neurosurgical Psychiatry*, vol. 24, pp. 205–212, 1961.

[103] A. A. Asadi-Pooya, M. Farazdahi, and M. Shahpari, "Clinical significance of bilateral epileptiform discharges in temporal lobe epilepsy," *Acta Neurologica Scandinavica*, vol. 143, no. 6, pp. 608–613, 2020. doi:10.1111/ane.13402.

[104] P. Ossenblok, J. C. de Munck, A. Colon, W. Drolsbach, and P. Boon, "Magnetoencephalography is more successful for screening and localizing fronal lobe epilepsy than electroencephalography," *Epilepsia*, vol. 48, no. 11, pp. 2139–2149, 2007. doi:10.1111/j.1528-1167.2007.01223.x.

[105] Z. A. Acar and S. Makeig, "Effects of forward model errors on eeg source localization," *Brain Topography*, vol. 26, no. 3, pp. 378–396, 2013. doi:10.1007/s10548-012-0274-65.

[106] Y. Céspedes-Villar, J. D. Martinez-Vargas, and G. Castellanos-Dominguez, "Influence of patient-specific head modeling on eeg source imaging," *Computational and Mathematical Methods in Medicine*, pp. 1–15, 2020. doi:10.1155/2020/5076865.

[107] X. Bai and B. He, "On the estimation of the number of dipole sources in eeg source localization," *Clinical Neurophysiology*, vol. 116, no. 9, pp. 2037–2043, 2005.

[108] C. Cirelli and G. Tononi, "Cortical development, eeg rhythms, and the sleep/wake cycle," *Biological Psychiatry*, vol. 77, no. 12, pp. 1071–1078, 2015. doi:10.1016/j.biopsych.2014.12.017.

[109] J. R. L. Schwartz and T. Roth, "Neurophysiology of sleep and wakefulness: Basic science and clinical implications," *Current Neuropharmacology*, vol. 6, pp. 367–378, 2008. doi:10.2174/157015908787386050.

[110] L. Nobili, F. Ferillo, M. G. Baglietto, M. Beelke, F. De Carli, E. De Negri, G. Schiavi, G. Rosadini, and M. De Negri, "Relationship of sleep interictal epileptiform discharges to sigma activity (12-16 hz) in benign epilepsy of childhood with rolandic spikes," *Clinical Neurophysiology*, vol. 110, pp. 39–46, 1999.

[111] L. Mohan, J. Singh, Y. Singh, R. Kathrotia, and A. Goel, "Association of interictal epileptiform discharges with sleep and anti-epileptic drugs," *Annuals of Neurosciences*, vol. 23, no. 4, pp. 230–234, 2016. doi:10.1159/000449483.

[112] M. G. Baglietto, F. M. Battaglia, L. Nobili, S. Tortorelli, E. De Negri, M. G. Calevo, E. Veneselli, and M. De Negri, "Neuropsychological disorders related to interictal epileptic discharges during sleep in benign epilepsy of childhood with centrotemporal or rolandic

spikes," *Developmental Medicine and Child Neurology*, vol. 43, no. 6, pp. 407–412, 2001. doi:10.1111/j.1469-8749.2001.tb0022.

[113] B. A. Malow, X. Lin, R. Kushwaha, and M. S. Aldrich, "Interictal spiking increases with sleep depthin temporal lobe epilepsy," *Epilepsia*, vol. 39, no. 12, pp. 1309–1316, 1998. doi:10.1111/j.1528-1157.1998.tb01329.x.

[114] L. Nobili, M. G. Baglietto, M. Beelke, F. De Carli, E. De Negri, G. Rosadini, M. De Negri, and F. Ferrillo, "Modulation of sleep interictal epileptiform discharges in partial epilepsy of childhood," *Clinical Neurophysiology*, vol. 110, no. 5, pp. 839–845, 1999. doi:10.1016/S1388-2457(99)00021-8.

[115] C. Marcus, "Orexin and epilepsy: Potential role of rem sleep," *Sleep*, vol. 40, no. 3, 2017. doi:10.1093/sleep/zsw061.

[116] P. Halász, "How sleep activates epileptic networks?," *Epilepsy Research and Treatment*, pp. 1–19, 2013. doi:10.1155/2013/425697.

[117] A. Natarajan, M. L. Marzec, X. Lin, D. Minecan, and B. A. Malow, "Interictal epileptiform discharges do not change before seizures during sleep," *Epilepsia*, vol. 43, no. 1, pp. 46–51, 2002. doi:10.1046/j.1528-1157.2002.24301.x.

[118] X. Kang, M. Boly, G. Findlay, B. Jones, K. Gjini, R. Maganti, and A. F. Struck, "Quantitative spatio-temporal characterization of epileptic spikes using high density eeg: Differences between nrem sleep and rem sleep," *Scientific reports*, vol. 10, no. 1, p. 1673, 2020. doi:10.1038/s41598-020-58612-4.

[119] J. Pastor and L. V. Zelaya, "Sleep and epilepsy: a bidirectional influence," *Sleep Medicine and Disorders: International Journal*, vol. 2, no. 1, pp. 12–13, 2018. doi:10.15406/smdij.2018.02.00033.

[120] S. A. Gibbs and P. Nobili, L nd Halász, "Interictal epileptiform discharges in sleep and the role of the thalamus in encephalopathy related to status epilepticus during slow sleep," *Epileptic Disorders*, vol. 21, no. 1, pp. 554–561, 2019. doi:10.1684/epd.2019.1058.

[121] J. Moehring, F. Moeller, J. Jacobs, S. Wolff, R. Boor, O. Jansen, U. Stephani, and M. Siniatchkin, "Non-rem sleep influences results of fmri studies in epilepsy," *Neuroscience Letters*, vol. 443, no. 2, pp. 61–66, 2008. doi:10.1016/j.neulet.2008.07.044.

[122] C. Gottesmann, "Brain inhibitory mechanisms involved in basic and higher integrated sleep processes," *Brain Research Reviews*, vol. 45, no. 3, pp. 230–249, 2004. doi:10.1016/j.brainresrev.2004.04.003.

[123] C. M. Johnson and J. P. Turley, "The significance of cognitive modeling in building healthcare interfaces," *International Journal of Medical Informatics*, vol. 75, pp. 163–172, 2006. doi:10.1016/j.ijmedinf.2005.06.003.

[124] D. G. Lowe, "Distinctive image features from scale-invariant keypoints," *International Journal of Computer Vision*, vol. 60, pp. 91–110, 2004. doi:10.1023/B:VISI.0000029664.99615.94.

A Assignment description

Implementation of a generic algorithm to perform automated source localisation of detected IEDs in EEG signals, designed for a clinical setting

MSc Assignment

Background

Epilepsy is a prevalent neurological disease, defined by recurrent seizures. Diagnosis of epilepsy can be based on interictal EEG, as the presence of Interictal Epileptiform Discharges (IEDs) indicate an underlaying epileptic disorder. Neural Networks can be used to automate IED detection (da Silva Lourenco, n.d.; Duncan et al., 2002; St.Louis & Frey, 2002; Thomas et al., 2018). Additional information can be extracted from these detected IEDs with source localisation.

State of the Art

Source localisation methods reconstruct the sources in the brain underlaying a certain EEG signal. This entails a forward and an inverse solution. The EEG forward problem explains how pyramidal cortical neurons create current sources that are measured on the scalp by electrodes, resulting in an EEG signal. The inverse problem starts with an EEG signal and determines a corresponding simulated source inside the brain (Asadzadeh et al., 2020; Awan et al., 2019; Grech et al., 2008; Jatoi et al., 2014). Since the inverse problem is ill-posed, there are several mathematical models which provide a solution. The models return the optimal location and orientation of simulated source(s). They differ in a priori assumptions and constraints (Grech et al., 2008). The advantages of source localisation are its non-invasive nature, the usage of readily available tools (EEG measurements), the addition of spatial insight to the EEG signal and the intuitive presentation of results. Various authors discussed source localisation of EEG data. However, these studies are mainly experimental and conducted on a small-scale dataset. Research into source localisation of specifically IED signals is limited. Furthermore, research is often limited to specific epilepsy syndromes, specific spike patterns and/or specific tasks (Bagshaw et al., 2006; Eom et al., 2017; Meckes-Ferber et al., 2004; Seeland et al., 2018). Currently, source localisation used in a clinical setting requires an extensive and specific set-up. Overall, there is a lack of generic implementations of source localisation models that are suitable for use in the clinic.

Goal of the project

The goal is to create and implement a generic source localisation algorithm, which can automatically provide complementary information, based on IEDs in an EEG signal, to support the neurologist in setting a more extensive epilepsy diagnosis.

Research activities

The accuracy and performance of different source localisation methods will be investigated and one or more methods will be chosen. These will be implemented into an algorithm to automate source localisation of detected IEDs. Useful functions for neurologists will be determined to improve the performance of the implementation. Preferences of neurologists will be used to aid the design of the user interface for clinical usage.

Expected results

The expected result is an automated algorithm which can determine the source localisation of the average IED from all IEDs detected in an EEG signal. Additionally, the design of an implementation specifically tuned to the needs of neurologists will be delivered. **References**

1. Asadzadeh, S., Yousefi Rezaii, T., Beheshti, S., Delpak, A., & Meshgini, S. (2020). A systematic review of EEG source localization techniques and their applications on diagnosis of brain abnormalities. Journal of Neuroscience Methods, 339, 1–23. https://doi.org/10.1016/j.jneumeth.2020.108740

2. Awan, F. G., Saleem, O., & Kiran, A. (2019). Recent trends and advances in solving the inverse problem for EEG source localization. Inverse Problems in Science and Engineering, 27(11), 1521–1536. https://doi.org/10.1080/17415977.2018.1490279

3. Bagshaw, A. P., Kobayashi, E., Dubeau, F., Pike, G. B., & Gotman, J. (2006). Correspondence between EEG-fMRI and EEG dipole localisation of interictal discharges in focal epilepsy. NeuroImage, 30(2), 417–425. https://doi.org/10.1016/j.neuroimage.2005.09.033

4. da Silva Lourenco, C. (n.d.). Machine learning for Interictal Epileptiform Discharge detection - a review. NOT PUBLISHED YET

5. Duncan, J. S., Sander, J. W., Sisodiya, S. M., & Walker, M. C. (2002). Adult epilepsy. 1087–1100.

6. Eom, T. H., Shin, J. H., Kim, Y. H., Chung, S. Y., Lee, I. G., & Kim, J. M. (2017). Distributed source localization of interictal spikes in benign childhood epilepsy with centrotemporal spikes: A standardized low-resolution brain electromagnetic tomography (sLORETA) study. Journal of Clinical Neuroscience, 38, 49–54. https://doi.org/10.1016/j.jocn.2016.12.047

7. Grech, R., Cassar, T., Muscat, J., Camilleri, K. P., Fabri, S. G., Zervakis, M., Xanthopoulos, P., Sakkalis, V., & Vanrumste, B. (2008). Review on solving the inverse problem in EEG source analysis. Journal of NeuroEngineering and Rehabilitation, 5, 1–33. https://doi.org/10.1186/1743-0003-5-25

8. Jatoi, M. A., Kamel, N., Malik, A. S., Faye, I., & Begum, T. (2014). A survey of methods used for source localization using EEG signals. Biomedical Signal Processing and Control, 11(1), 42–52. https://doi.org/10.1016/j.bspc.2014.01.009

9. Meckes-Ferber, S., Roten, A., Kilpatrick, C., & O'Brien, T. J. (2004). EEG dipole source localisation of interictal spikes acquired during routine clinical video-EEG monitoring. Clinical Neurophysiology, 115(12), 2738–2743. https://doi.org/10.1016/j.clinph.2004.06.023

10. Seeland, A., Krell, M. M., Straube, S., & Kirchner, E. A. (2018). Empirical Comparison of Distributed Source Localization Methods for Single-Trial Detection of Movement Preparation. Frontiers in Human Neuroscience, 12(September). https://doi.org/10.3389/fnhum.2018.00340

11. St.Louis, E. K., & Frey, L. C. (2002). Electroencephalography: An introductory Text and Atlas of Normal and Abnormal Findings in Adults, Children and Infants. In Cerebral Cortex (Vol. 62, Issue 12). https://doi.org/10.1093/cercor/bhm213

12. Thomas, J., Comoretto, L., Jin, J., Dauwels, J., Cash, S. S., & Westover, M. B. (2018). EEG Classification via Convoltional Neural Network-Based Interictal Epileptiform Event Detection. Conf Proc IEEE Eng Med Biol Soc, 3148–3151. https://doi.org/10.1109/EMBC.2018.8512930

B Information cycle

Figure 21 shows the process of patient admittance and subsequent information collection and analysis. The patient experiences symptoms and consults the hospital. At the hospial the EEG measurement are made. The neurologists revises the EEG with additional patient information. This leads to a diagnosis and classification on the epilepsy characteristics, which will determine the management or treatment options. This work will add information and relieve some parts of the analysis, to aid the neurologist in determining an epilepsy classification.

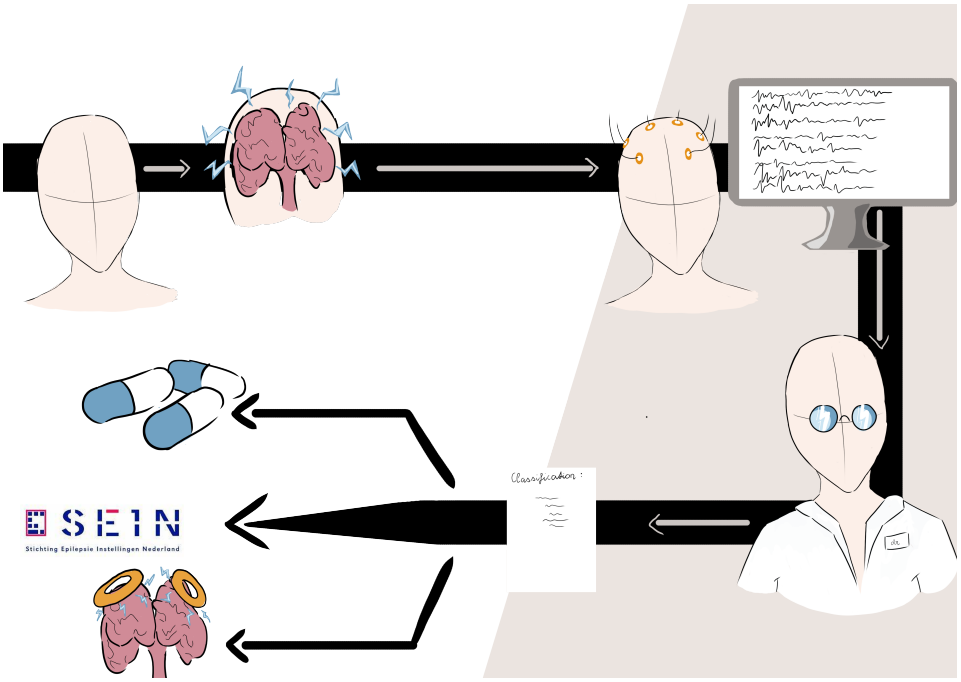

Figure 21: The information cycle in the clinic. A patient has certain symptoms and the neurologists suspects an underlaying epilepsy disorder. To confirm this suspicion, EEG signals of the patient are measured. The neurologists analyses these EEG signals, looking for epileptiform activity. Based on the presence and presentation of IEDs, the neurologists determines the epilepsy diagnosis and classification. This results in treatment or management strategies. The work presented here is targeted at the EEG analysis, leading to a diagnosis and classification. This part is indicated with a different background color.

C Usability Heuristics

Below are ten general principles for user interface design, formulated by Jakob Nielsen. They are called "heuristics" because they are more in the nature of rules of thumb than specific usability guidelines.

1. Visibility of system status
The system should always keep users informed about what is going on, through appropriate feedback within reasonable time.
2. Match between system and the real world
The system should speak the users' language, with words, phrases and concepts familiar to the user, rather than system-oriented terms. Follow real-world conventions, making information appear in natural and logical order.
3. User control and freedom
Users often choose system functions by mistake and will need a clearly marked "emergency exit" to leave the unwanted state without having to go through an extended dialogue. Support undo and redo.
4. Consistency and standards
Users should not have to wonder whether different words, situations, or actions mean the same thing. Follow platform conventions.
5. Error prevention
Even better than good error messages is a careful design which prevents a problem from occurring in the first place. Either eliminate error-prone conditions or check for them and present users with a confirmation option before they commit to the action.
6. Recognition rather than recall
Minimize the user's memory load by making objects, actions, and options visible. The user should not have to remember information from one part of the dialogue to another. Instructions for use of the system should be visible or easily retrievable whenever appropriate.
7. Flexibility and efficiency of use
Accelerators – unseen by the novice user – may often speed up the interaction for the expert user such that the system can cater to both inexperienced and experienced users. Allow users to tailor frequent actions.
8. Aesthetic and minimalist design
Dialogues should not contain information which is irrelevant or rarely needed. Every extra unit of information in a dialogue competes with the relevant units of information and diminishes their relative visibility.
9. Help users recognize, diagnose, and recover from errors
Error messages should be expressed in plain language (no codes), precisely indicate the problem, and constructively suggest a solution.
10. Help and documentation
Even though it is better if the system can be used without documentation, it may be necessary to provide help and documentation. Any such information should be easy to search, focused on the user's task, list concrete steps to be carried out, and not be too large.

D Data

Table 1: Used EEG signals, consisting of 14 patients with Rolandic epilepsy, 8 patients with another focal epilepsy and 9 patients with multi-focal epilepsy. The used number of epochs and when applicable the total number of epochs (indicated with a dash) are shown. Furthermore, the number of epochs in which the VGG found an IED and the number of those epochs excluded due to artefacts are also shown.

Patient	**M/V**	**Epilepsy type**	**Used epoch no. / total epoch no.**	**Epochs from VGG**	**Artefact no.**
1	M	Rolandic	614	29	12
2	M	Rolandic	581	130	84
3	V	Rolanic	599	63	39
4	M	Rolandic	609	123	17
5	M	Rolandic	5000 / 30302	58	7
6	V	Rolandic	602	77	11
7	M	Rolandic	5000 / 38159	1220	659
8	M	Rolandic	3110	595	409
9	M	Rolandic	605	11	2
10	M	Rolandic	5000 / 42061	207	111
11	M	Rolandic	603	26	17
12	V	Rolandic	606	383	236
13	M	Rolandic	10000 / 36667	982	722
14	M	Rolandic	2634	1536	1260
15	M	Other focal	599	201	29
16	M	Other focal	599	37	18
17	M	Other focal	599	105	56
18	M	Other focal	18253	14	0
19	V	Other focal	25818	180	2
20	M	Other focal	24417	6	0
21	M	Other focal	44463	3252	3107
22	V	Other focal	10000 / 39669	1527	1396
23	M	Multi-focal	544	79	25
24	M	Multi-focal	599	301	270
25	V	Multi-focal	564	47	16
26	M	Multi-focal	640	173	4
27	V	Multi-focal	651	308	168
28	V	Multi-focal	10000 / 33659	3424	3383
29	M	Multi-focal	37259	649	516
30	V	Multi-focal	30535	4873	4777
31	M	Multi-focal	629	373	298

E Algorithm flowcharts

Method 1

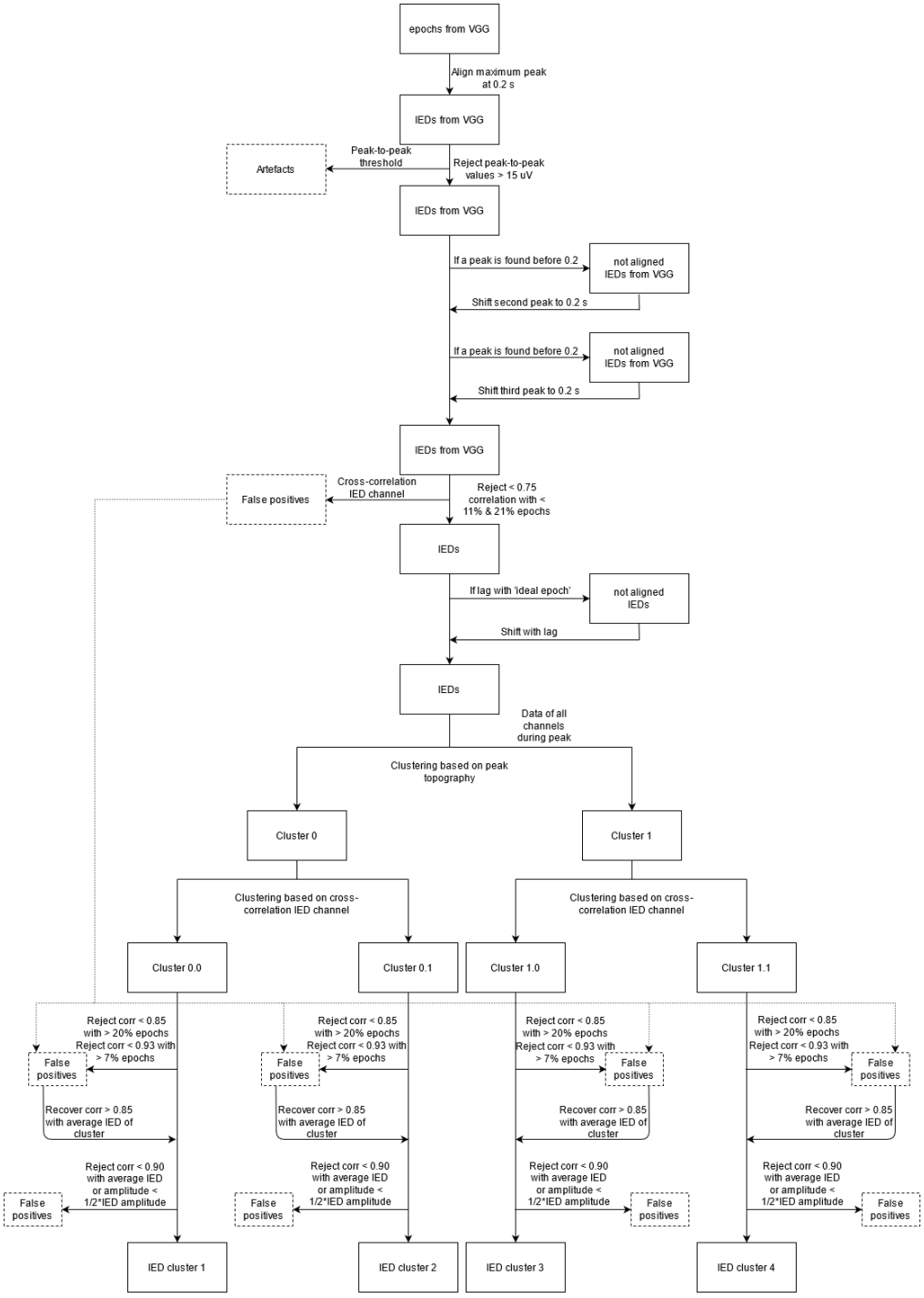

Figure 22: Simplified IED acquisition flow for method 1. IEDs are detected by high amplitudes. Artefacts are removed from the VGG epochs with a peak-to-peak threshold. High peaks are shifted to 0.2 seconds. False positives are removed with cross-correlation. The epochs are realigned with lags. The epochs are first clustered by IED channel. Hierarchical clustering splits these clusters into two. False positives are removed within a cluster. As a last step, some false positives are retrieved.

Method 2

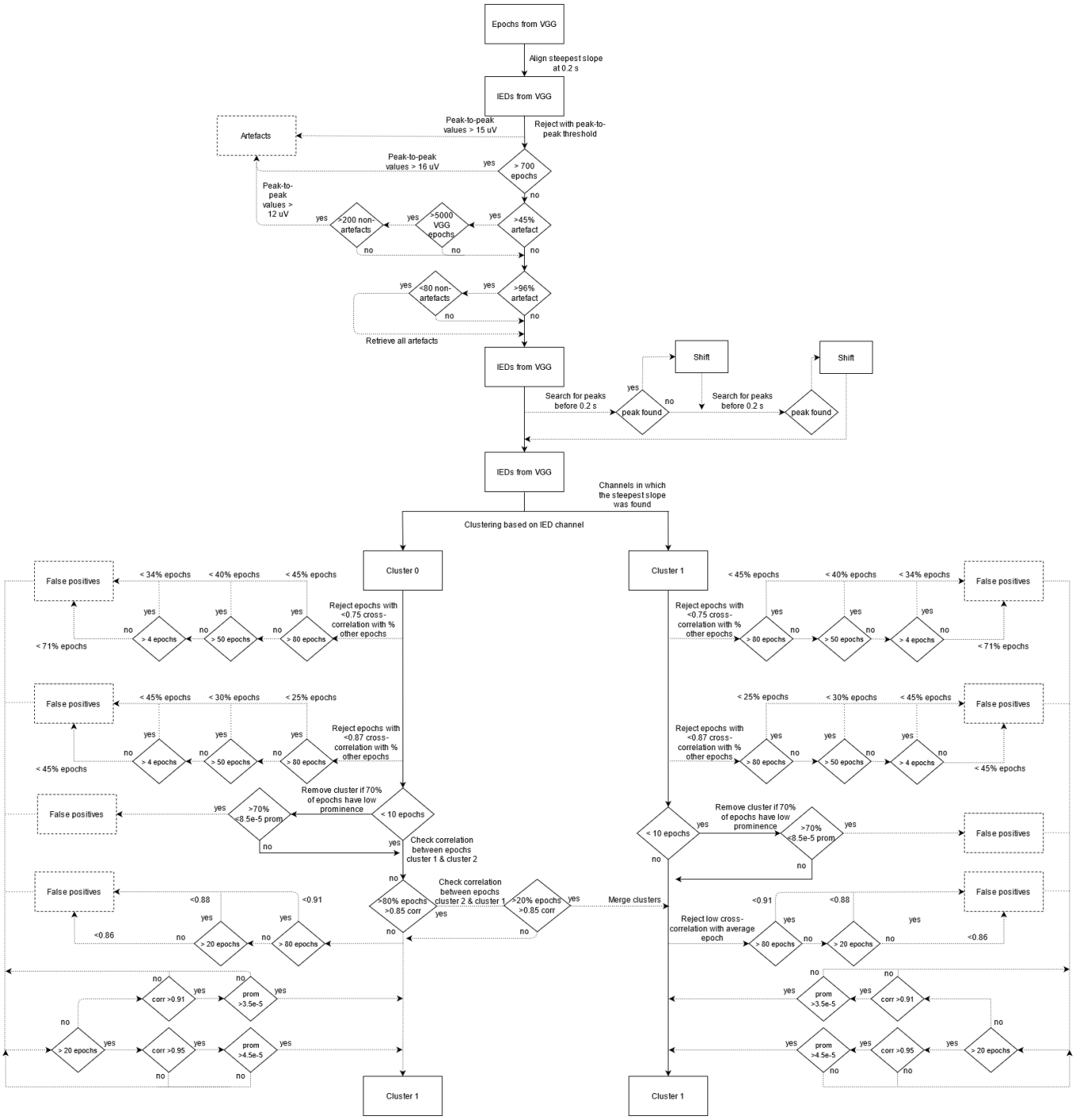

Figure 23: IED acquisition flow for method 2. IEDs are detected by steep slopes. Artefacts are removed from the VGG epochs with a peak-to-peak threshold. High peaks are shifted to 0.2 seconds. The epochs are clustered by IED channel. False positives are removed with cross-correlation. The epochs are realigned with lags. Similar clusters are merged together. As a last step, some false positives are retrieved.

F Methods exploration

False positive removal

Several methods for exclusion of false positives were explored, such as scale-invariant feature transform (SIFT), heatmaps, peak amplitude and cross-correlation.

An attempt was made to perform SIFT on EEG signals. SIFT is an algorithm designed to find similar features between pictures [124]. First results suggested that SIFT is unfit for usage on EEG signals. Figure 24A shows the matches between keypoints of an epoch with itself. Figure 24B shows matches of the same epoch with other epochs. SIFT often led to no matches (figure 24B (left)), or a few matches with keypoints that were not part of IED shapes (figure 24B (middle & right)). The results imply that the algorithm responds to intersecting lines. This hypothesis was tested with sines and cosines. Figure 24C shows the performance of SIFT on a series of sines and cosines. At first no keypoints are found. An increase of scaling and subsequent increase of intersecting lines creates new keypoints. The matches found between the sinoids and shifted versions appeared random, as seen in figure 24D. Therefore, SIFT was abandoned.

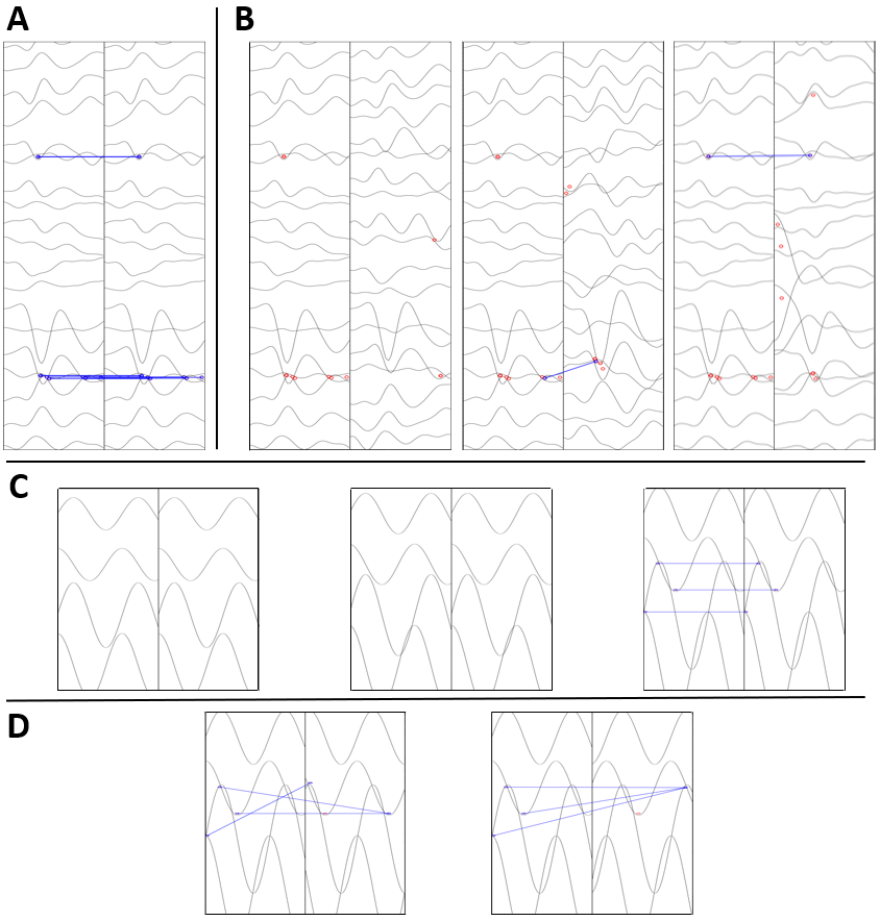

Figure 24: SIFT determines keypoints of epochs and matches them to keypoints in other epochs. The epoch on the left is matched to the epoch on the right. Epochs matched to themselves display as matches between the same epochs (A). An epoch matched with another epoch (B) shows the keypoints without matches as red dots (left) and matches between epochs are connected by a blue line (middle & right). Little matches were found and they were not located at the IED shapes. SIFT was also performed on sinoids (C). No matches are found (left & middle) until the scaling is increased and lines intersect (right). Matching sinoids to shifted versions (D) did not lead to matches between similar shapes.

Another option is to create heatmaps of the EEG data and compare these images by subtracting pixel intensity values around the IEDs. Trial-and-error with this method did not prove promising. A possible explanation could be that this approach does not account for small shifts between signals, and is thus less forgiving to small deviations from the earlier steps. This combination between early attempts and theoretical background led to this method being dropped.

Clustering

The first method is based on the assumption that the highest peak is an important part of the IED. The IEDs are clustered based on their data during the highest peak, resulting in an array of length R^C, containing the voltage of each channel at the time of the highest peak. A distance matrix is created, of size $R^{E \times E}$, with the Euclidean distances between all epochs. This distance matrix is the input to Wards hierarchical clustering method [65, 66]. This method will prevent clustering different peak polarities together, which will prevent that the peaks even each other out when the epochs are averaged later. However, upon seeing more data and evaluation with neurologists, it seems that if the IEDs are located in the same channel and shifted correctly, it is unlikely that there is still a significant difference between their peaks. If true, this method is not useful for the purpose of IEDs, since clustering on only one time sample does not reveal anything about the shape aside from this peak.

G Stakeholder analysis

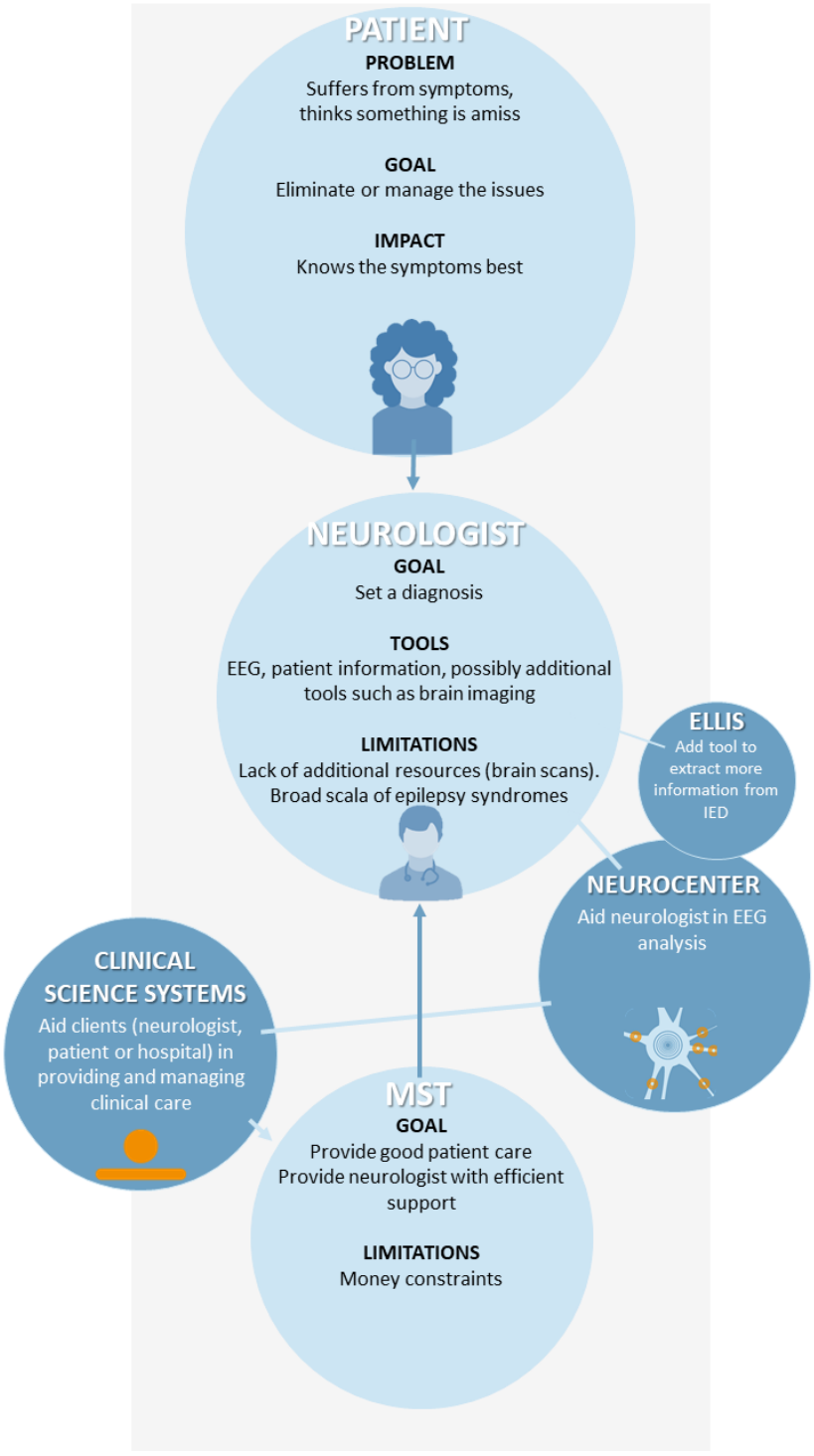

Figure 25: Stakeholder analysis. The patient has a certain problem, presenting as symptoms. The neurologists has a goal to treat these symptoms, in the first place by setting a diagnosis. To achieve this goal, the Neurologist uses EEG signals. Neurocenter is a system from Clinical Science Systems, which can help the neurologists with the EEG analysis. The tool presented in this work may lead to addition of a new tool to the current Neurocenter system, to additionally aid the EEG analysis. MST may be interested in this tool because it improves patient care.

H Brand analysis

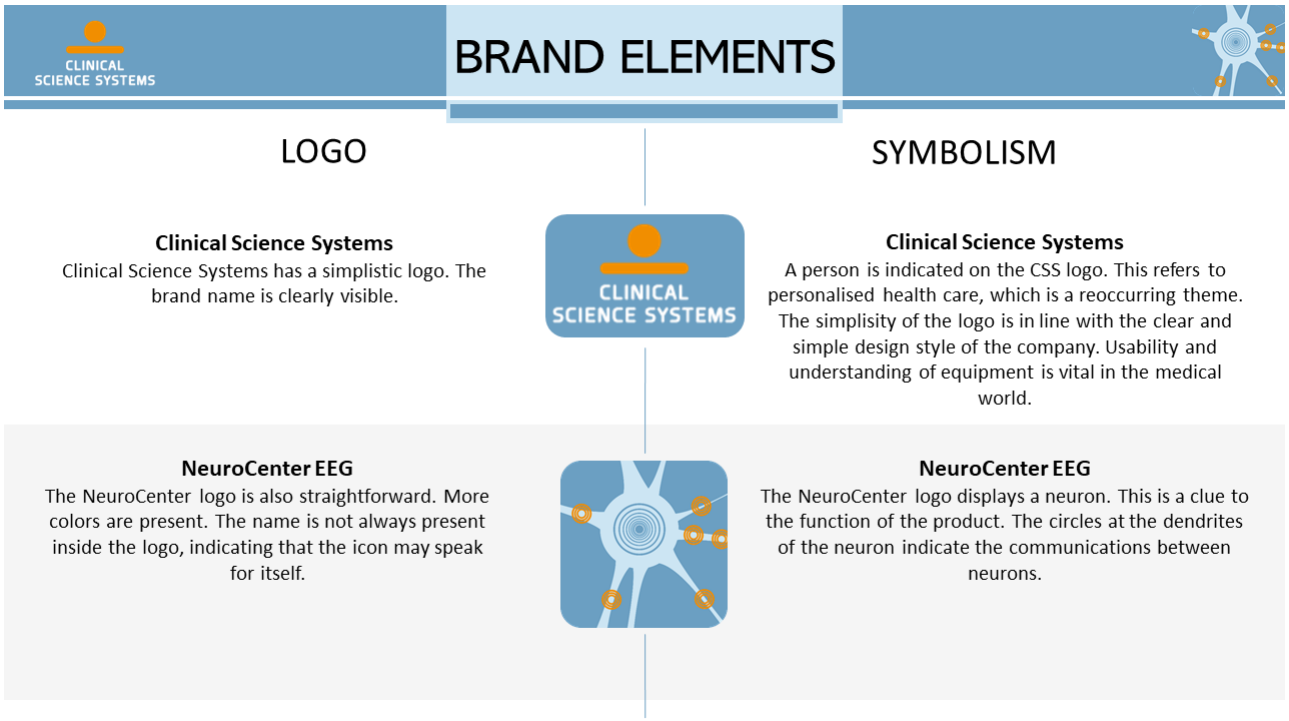

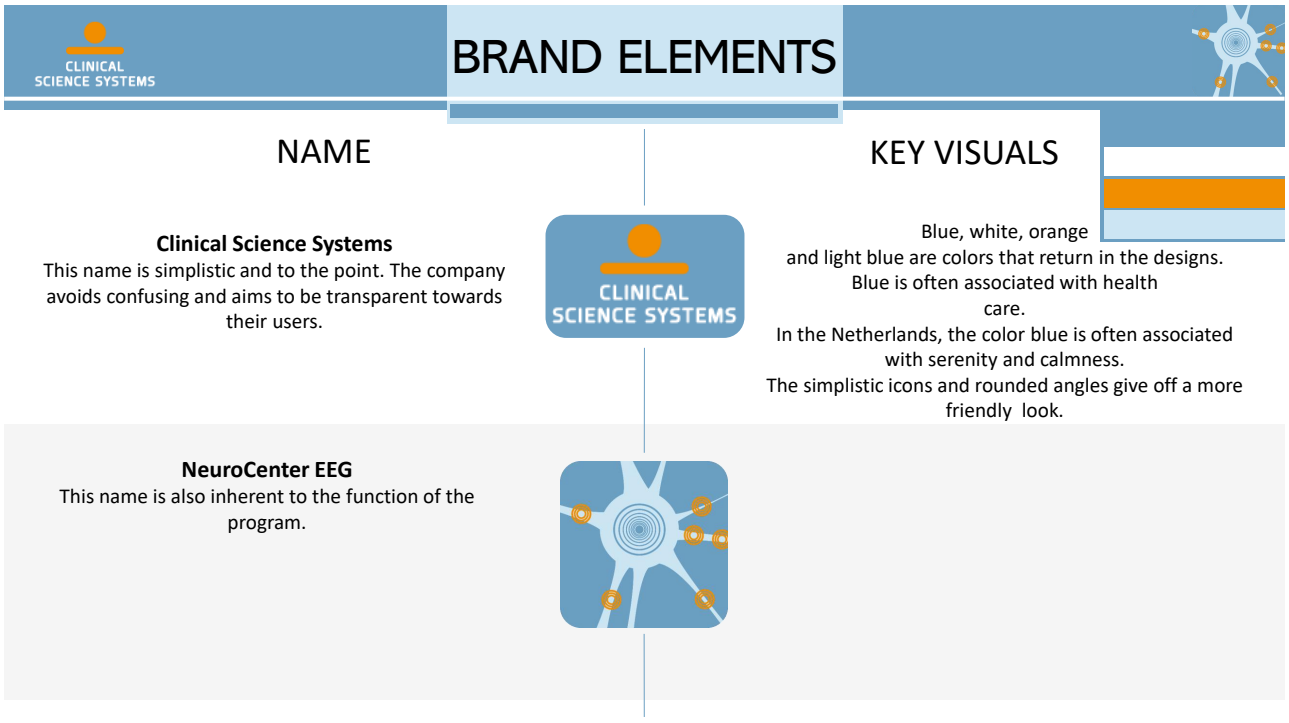

CLINICAL SCIENCE SYSTEMS

BRAND ELEMENTS

PRODUCTS

BrainStatus

BrainStatus is an EEG acquisition product. It consists of an electrode set which can be used quickly and is disposable. It is most useful in emergency situations.

NeuroCenter EEG

Neurocenter is a software to read and analysis EEG signals. An USP is the mobility and flexibility of the system. Furthermore, the simplification of performing analyses on the data is an important aspect.

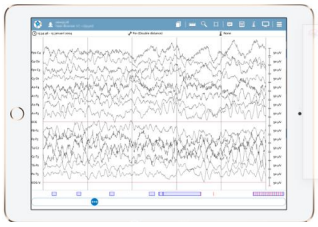

MDOrganizer

MDOrganizer organizes and shares patient data. The system integrates with existing environment and equipment. The USP is the easy usability.

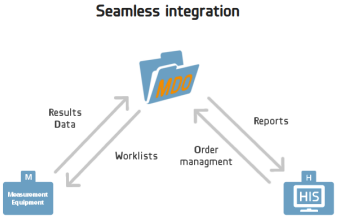

CLINICAL SCIENCE SYSTEMS

BRAND ELEMENTS

NEUROCENTER EEG

The NeuroCenter userface is displayed on the right. The main clinical applications are for patients with brain injury, patients in coma, patients with epilepsy and patients waiting to undergo carotid surgery.

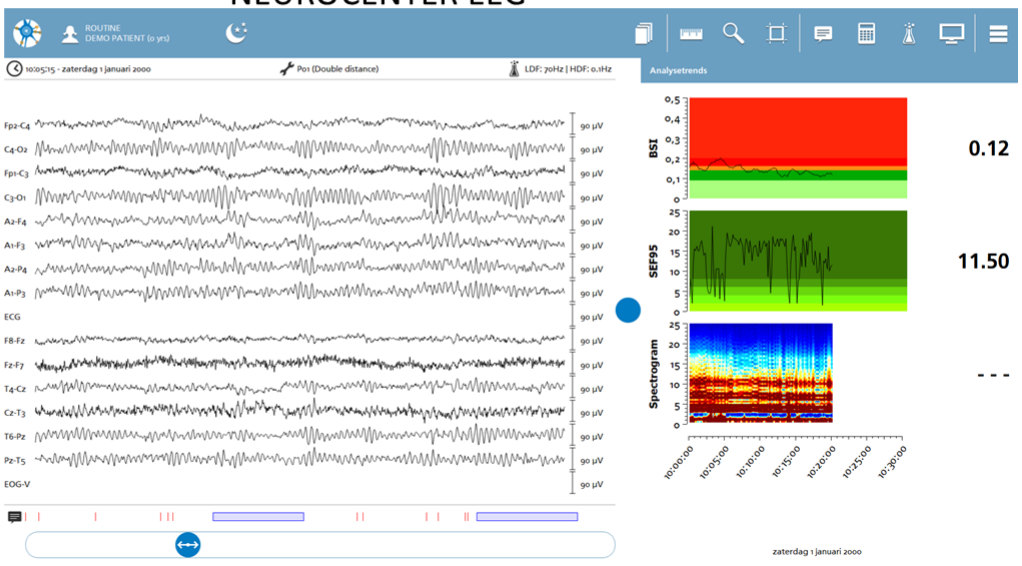

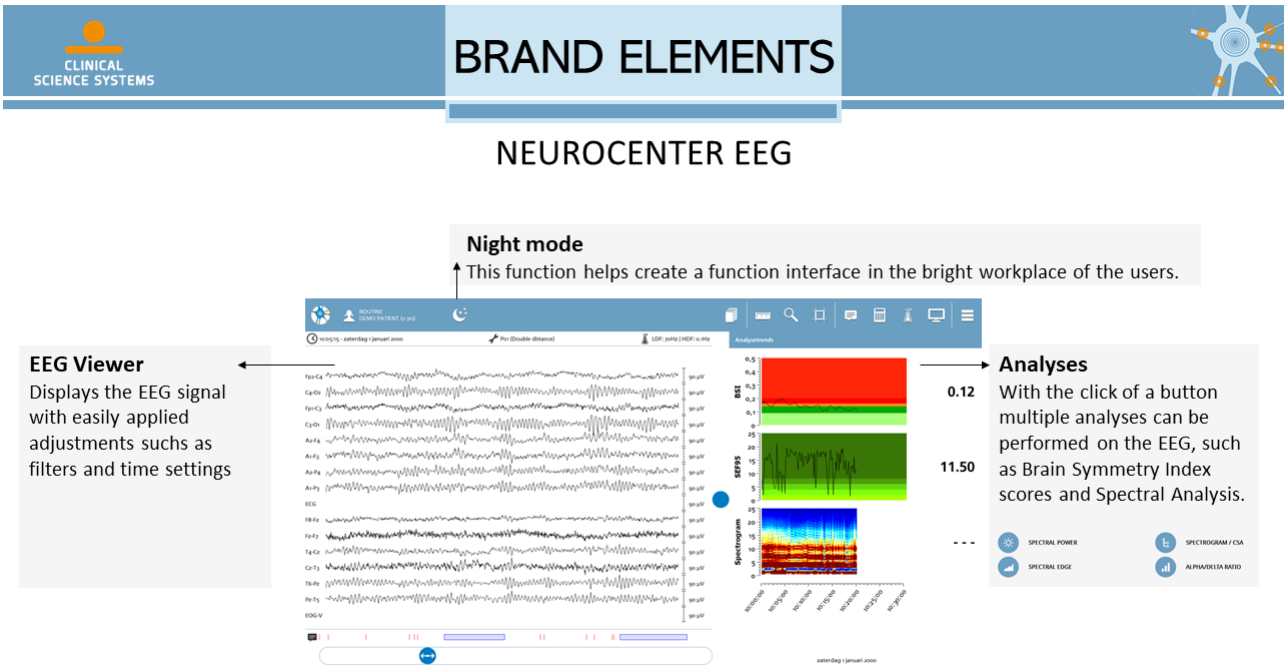

Figure 26: Brand analysis. Clinical Science Systems is a company that develops products and services for the clinic. Both have use a consistent color palette of a dark and light blue with orange accents. The company provides several neuro-imaging and analysis products. One of those is Neurocenter. Neurocenters is used for the analysis of EEG signals. It contains an EEG viewer and provides several analysis techniques for EEG signals.

I Visual design elements

Color palette

The color can create familiarity with other Neurocenter products. Furthermore, the colors should fit the environment. In the hosptal, blue and white are common colors. The orange can be used to set the Neurocenter style apart from other clinical interfaces.

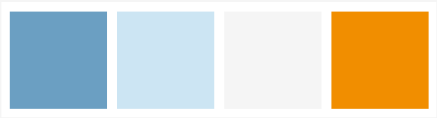

Shapes

Soft, rounded shapes will be avoided to create a more professional look. Furthermore, sharp shapes will increase legibility.

Hierarchy

A visual hierarchy can help create a distinction between clusters. Vertical orientation seem to help create more legibility

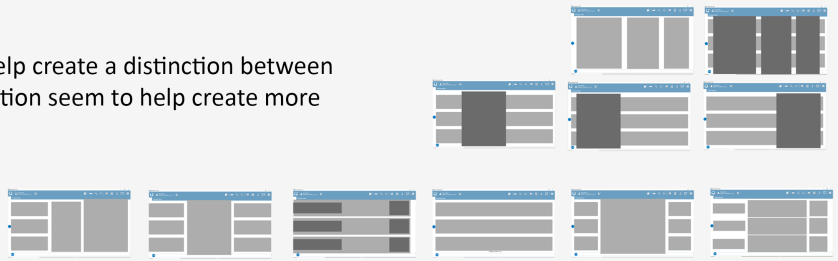

Balance

Balance can be used between and within clusters. An asymmetrical balance within a cluster, where weight is not equally distributed but still visually balances, will.
Symetrical balance between clusters will intuitive show that all cluster contain the same elements.

Rythm

Open space is also important for legibility. Furthermore, arrangement of open space can be used to create a division.

Space

Open space is also important for legibility. Furthermore, arrangement of open space can be used to create a division between clusters. Elements within one cluster will be close together, whereas the space between clusters will be large.

Unity

Elements within one cluster should be composed in a way that creates visual wholeness. This will help the user see how elements are connected and decide on a focus point.

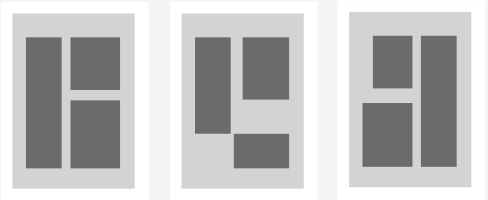

Figure 27: Visual design elements. These principles can be used to create a consistent and legible design. The principles are described and examples of the implementation are included on the right.

J Input from neurologists

The interviewees noted that examples of source localisation show a nice interactive view. On first sight, this seems to have added value. Also, it is a nice addition to the temporal EEG.
Some concerns were voiced over the limitation of the sources to the cortex. However, this tool is meant for surface EEG, which does not measure deeper sources. As opposed to MEG, which does measure sources deeper than the cortex. Since the tool uses surface EEG, you may want to be hesitant in determining the sources, since it is more difficult to measure depth from surface EEG. At SEIN they compare the EEG with depth measurements. This tool may be more suited for general neurologists, who do not have access to depth measurements. However, if you only find superficial sources (approximately 3 cm underneath the surface) these sources would not be very valuable.
The source localisation is not a sole tool in setting the epilepsy diagnosis. However, as a neurologist you may have a suspicion that the epilepsy originates from a certain brain area. You can verify this suspicion with source localisation.
At SEIN, they use Epilog. This is a collaboration where the parties help each other to further develop the program. The neurologists give input about new developments in the program. A problem they encounter with Epilog is that when the program gives a source with a high accuracy, the neurologists could have found this source as well, based on the signal. Thus, Epilog often yields the same result as neurologists. This means that the source localisation is accurate. However, the the system is then not really needed.
Sometimes the result will be a-specific: the epilepsy type can not be determined. In that case, the algorithm would also not be able to determine a diagnosis.
If you have a short EEG signal, there could be hardly any epileptiform activity. For recordings of longer than half an hour you can expect to find IEDs. However, currently most EEG signals are shorter than that. The current application may be more suited to specialised centra, where longer EEGs are recorded. On the other hand, this product could encourage measurement of longer EEGs in all clinics. Another incentive for longer EEG recordings is that more IEDs will lead to more accurate and useful source localisation.

K Usability testing protocol

For each page, several tasks (indicated with a T) and questions (indicated with a Q) were prepared, which can be found below.

Main page
T: Delete cluster 3. Then undo / add a new cluster.
T: Scroll through the average epoch of cluster 1.
T: Navigate to the epochs inside cluster 1.
Q: Do you have all the information needed for a first impression?
Q: Is it clear which information belongs to which cluster?
Q: Is the navigation clear / intuitive?

Epochs
T: Delete epoch 1 from cluster 1. Then undo.
T: Navigate to the sources of the current cluster.
T: Navigate back to the main page.
T: Navigate to the other clusters.
T: Delete the epochs from cluster 3. Then undo.
Q: Will you use this page / the individual pages?
Q: How do you feel about this representation of the epochs (2 second epochs)?
Q: Is the navigation clear / intuitive?

Sources
T: Scroll through the activations of epochs 1 & 2 in cluster 1.
T: Navigate to the epochs of the current cluster.
T: Navigate back to the main page.
T: Navigate to the other clusters.
T: Delete the epochs from cluster 3. Then undo.
Q: Will you use this page / the individual sources?
Q: How do you feel about this representation of the sources?
Q: Will you use the activation of the sources (strength of the dipole)?
Q: Is the navigation clear / intuitive?

Settings
T: Alter the thresholds.
T: Look at the epochs with artefacts.
T: Look at the epochs with slopes. Change the detected steepest slope of epoch 1. Then undo.
T: Navigate to the other pages.
T: Merge clusters 0 & 1. Then undo.
T: Toggle visibilities in the source localisation visualisations.
T: Switch to the MRI view & the cortex view.
T: Navigate to the main page.
Q: Will you use the explanatory figures?
Q: Do you have enough freedom to make alterations?
Q: Is there too much information / is it still legible?
Q: Do you want this on a separate page?
Q: Is the navigation clear / intuitive?

Moving pictures
T: Navigate to the functionality.
T: Scroll through the epochs.
Q: Will you use this functionality?

Stylised cortex
T: Scroll through the epoch average.
T: Switch between head views.
Q: Will you use this functionality?
Q: Do you mind / like that the dipole is only visible near the IED shape?

Color coded GoF
Q: How do you feel about this addition?

Miscellaneous
Q: Were you always aware of the current system status (epochs/sources/main page)?
Q: Are the used symbols & terminology clear?
Q: Were you able to make all the changes you wanted? Was it clear how to reverse changes?
Q: Was the design consistent? Did you learn how to use it over time?
Q: How much explanation did you need before using the interface?
Q: Was the interface efficient & flexible in accomplishing your tasks?
Q: How did you feel about the amount of information?
Q: What are your thoughts on the aesthetic of the design?

L Results for method 1

Table 2: Data analysis results for method 1. For each patient, the channel in which IEDs were found, the number of found epochs and whether the cluster is correct are included.

Patient	Epilepsy type	Channel	Epochs	Correct
1	Rolandic	T4	38	yes
2	Rolandic	T4	8	yes
3	Rolanic	Fp1	6	no
4	Rolandic	T4	4	maybe
5	Rolandic	Fp1-F3	19	no
6	Rolandic	T3	36	yes
7	Rolandic	C4	115	yes
8	Rolandic	T3	78	yes
9	Rolandic	T4	8	yes
10	Rolandic	Fp1	37	no
11	Rolandic	T4	4	yes
12	Rolandic	C4	40	yes
13	Rolandic	Fp1	69	no
14	Rolandic	C4	126	yes
15	Other focal	T4	38	yes
16	Other focal	T4	8	yes
17	Other focal	Fp1	11	no
18	Other focal	T3-T5	12	yes
19	Other focal	Fp2-F8	115	yes
20	Other focal	Fp2-F8	6	yes
21	Other focal	T4	41	yes
22	Other focal	T6	43	yes

Average IED (left), map topography at 0.2 seconds (top-right) and dipole at 0.2 seconds (bottom-right).

Patient 1

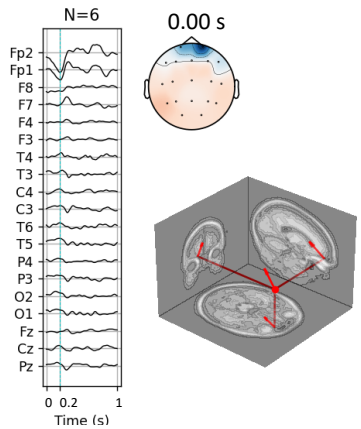

Patient 2

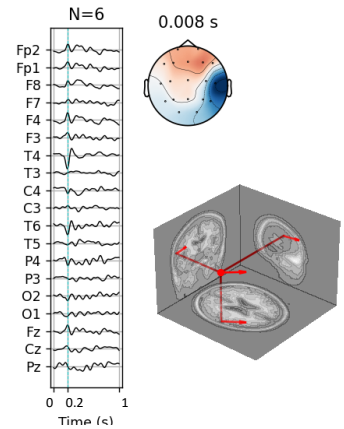

Patient 3

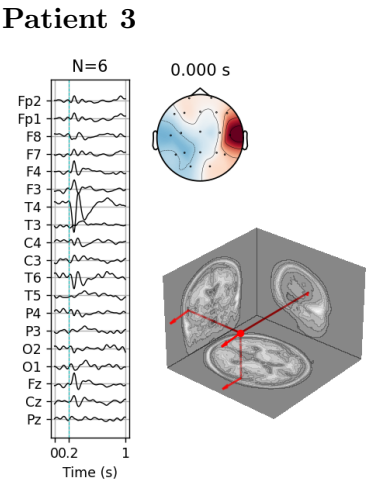

Patient 4

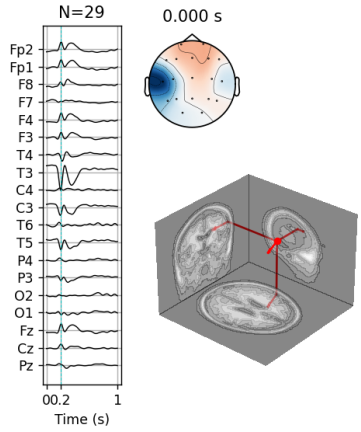

Patient 5

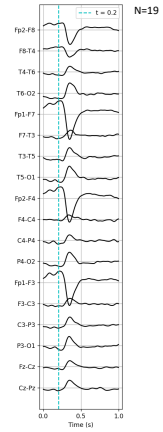

Patient 6

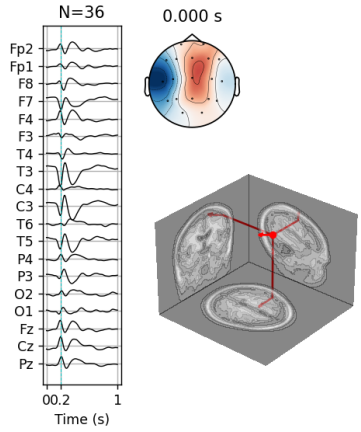

Patient 7

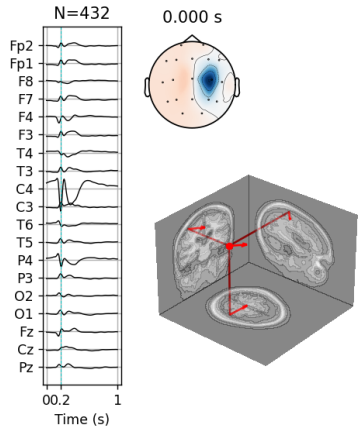

Patient 8

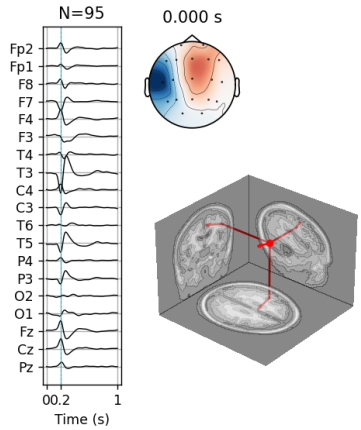

Patient 9

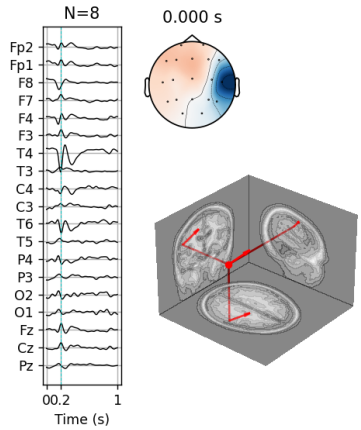

Patient 10

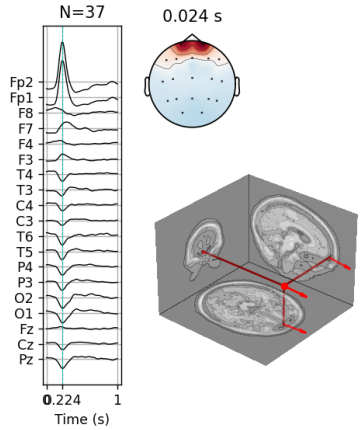

Patient 11

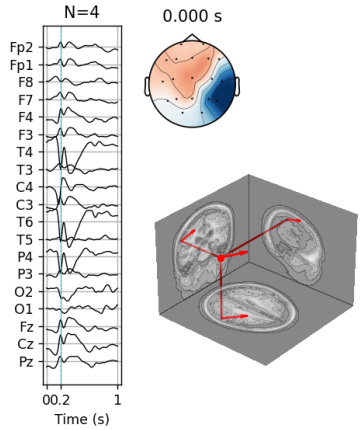

Patient 12

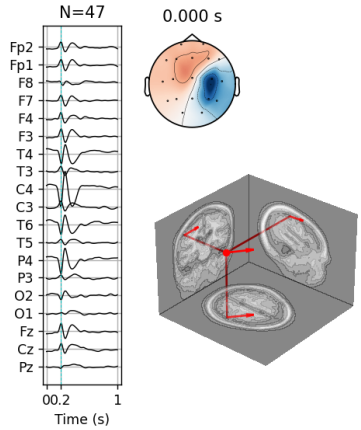

Patient 13

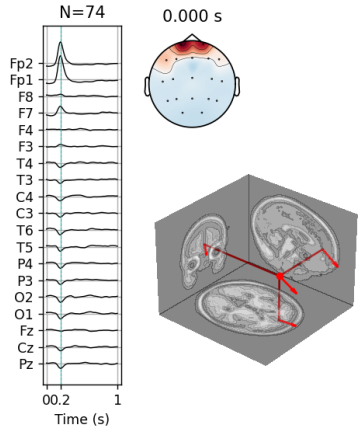

Patient 14

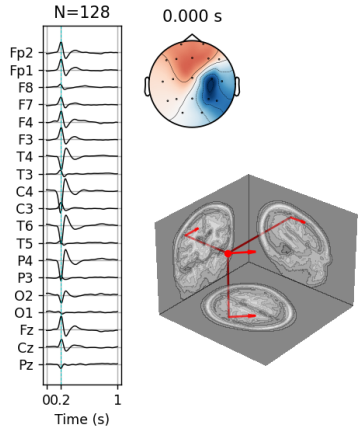

Patient 15

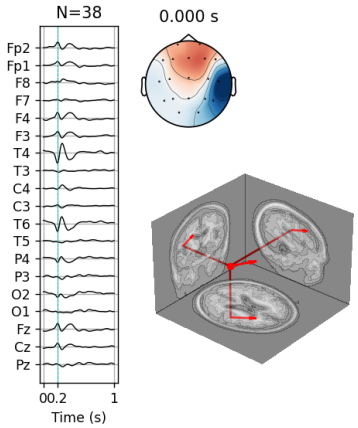

Patient 16

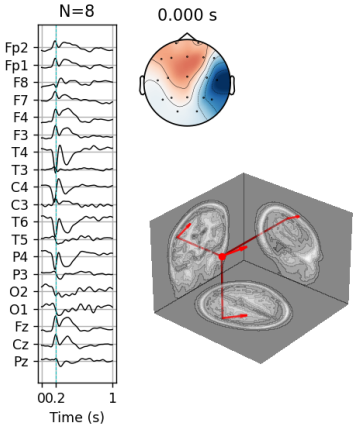

Patient 17

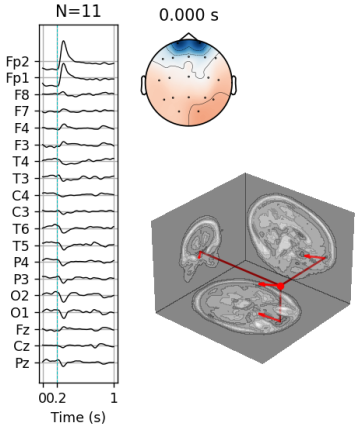

Patient 18

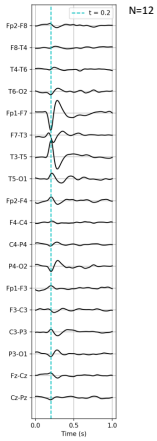

Patient 19

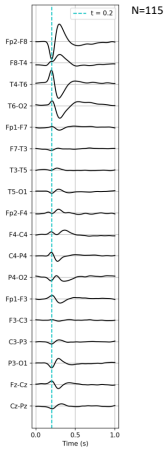

Patient 20

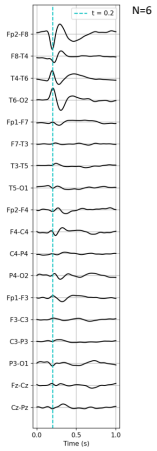

Patient 21

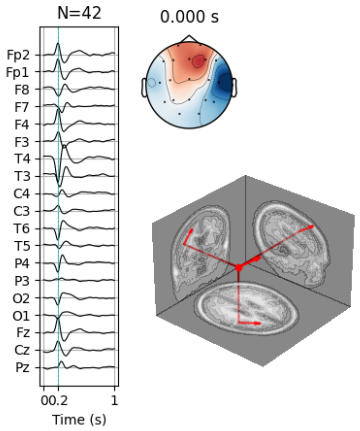

Patient 22

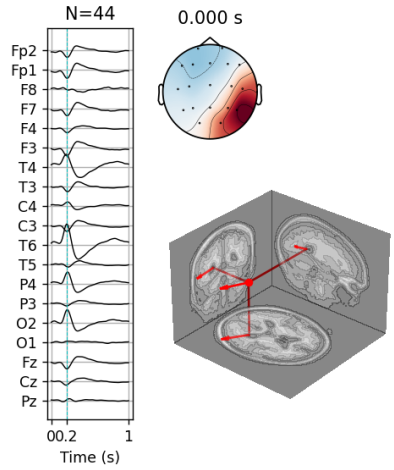
N=44
0.000 s
Fp2
Fp1
F8
F7
F4
F3
T4
T3
C4
C3
T6
T5
P4
P3
O2
O1
Fz
Cz
Pz
0
0.2
1
Time (s)

M Results for method 2

Table 3: Data analysis results for method 2. For each patient, the number of clusters, the channel in which IEDs were found, the number of found epochs and whether the cluster is correct are included. Table continues on the next page.

Patient	Epilepsy type	Cluster	Channel	Epochs	Correct
1	Rolandic	1	T3	4	yes
2	Rolandic	1	T4	11	yes
3	Rolanic	1	T4	10	yes
4	Rolandic	1	T3	35	yes
		2	T6	8	maybe
		3	T5	2	no
5	Rolandic	1	F4-C4	13	yes
		2	F3-C3	5	yes
6	Rolandic	1	C3	45	yes
7	Rolandic	1	Fp1	3	no
		2	C4	141	yes
8	Rolandic	1	T3	166	yes
9	Rolandic	1	T4	5	yes
10	Rolandic	1	T3	48	yes
		2	Pz	3	no
11	Rolandic	1	T6	2	yes
12	Rolandic	1	T4	3	yes
		2	T5	5	yes
		3	P3	27	yes
		4	O1	2	no
		5	C3	17	yes
		6	P4	53	yes
13	Rolandic	1	Fp1	10	no
		2	F8	11	no
		3	T3	6	maybe
		4	C4	34	yes
		5	C3	6	yes
14	Rolandic	1	F8	2	no
		2	C4	190	yes
15	Other focal	1	T5	3	no
		2	O2	30	yes
		3	Cz	2	no
		4	T6	52	yes
16	Other focal	1	O2	2	no
		2	C4	8	yes
17	Other focal	1	Fp2	3	no
		2	T3	19	yes
18	Other focal	1	T3-T5	12	yes

Patient	Epilepsy type	Cluster	Channel	Epochs	Correct
19	Other focal	1	T6-O2	12	yes
		2	T3-T5	13	yes
		3	Fp2-F8	114	yes
20	Other focal	1	Fp2-F8	5	yes
21	Other focal	1	F8	4	no
		2	Pz	2	no
		3	T4	66	yes
22	Other focal	1	T4	3	no
		2	P3	8	no
		3	O2	5	yes
		4	Fp1	3	no
23	Multi-focal	1	Fp1	17	yes
		2	T4	5	yes
24	Multi-focal	1	T3	4	yes
		2	C4	4	yes
		3	Cz	8	yes
25	Multi-focal	1	Fp1	7	yes
		2	O2	5	yes
		3	O1	2	yes
26	Multi-focal	1	F8	15	yes
		2	T6	16	maybe
		3	P3	4	no
		4	O2	6	yes
		5	Pz	4	no
		6	Fp1	15	yes
27	Multi-focal	1	T6	4	no
		2	O1	14	yes
		3	Pz	11	yes
28	Multi-focal	1	T3	3	maybe
		2	C4	8	yes
		3	C3	11	yes
		4	P4	3	no
29	Multi-focal	1	F8	4	no
		2	P4	32	yes
30	Multi-focal	1	O1	12	yes
		2	T6	50	yes
31	Multi-focal	1	F8	16	yes
		2	T4	5	yes
		3	C4	2	yes
		4	C3	4	no
		5	T5	8	yes
		6	Cz	11	no
		7	Fp2	4	no

Average IED (left), map topography at 0.2 seconds (top-right) and dipole at 0.2 seconds (bottom-right).

Patient 1

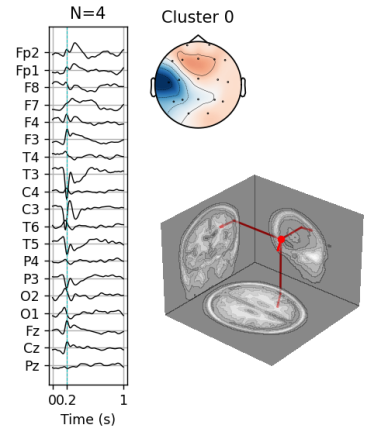

Patient 2

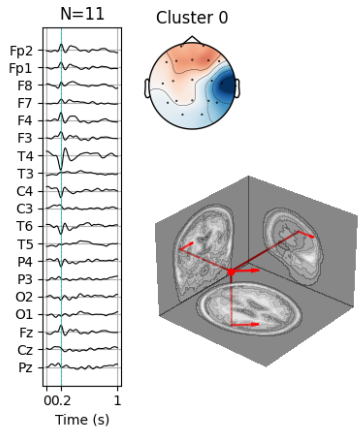

Patient 3

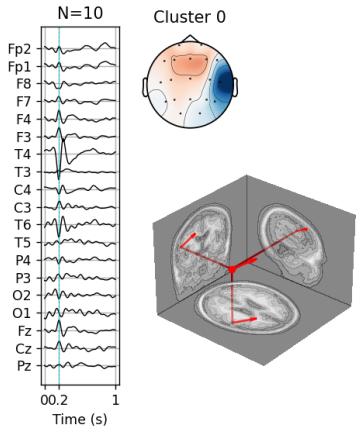

Patient 4

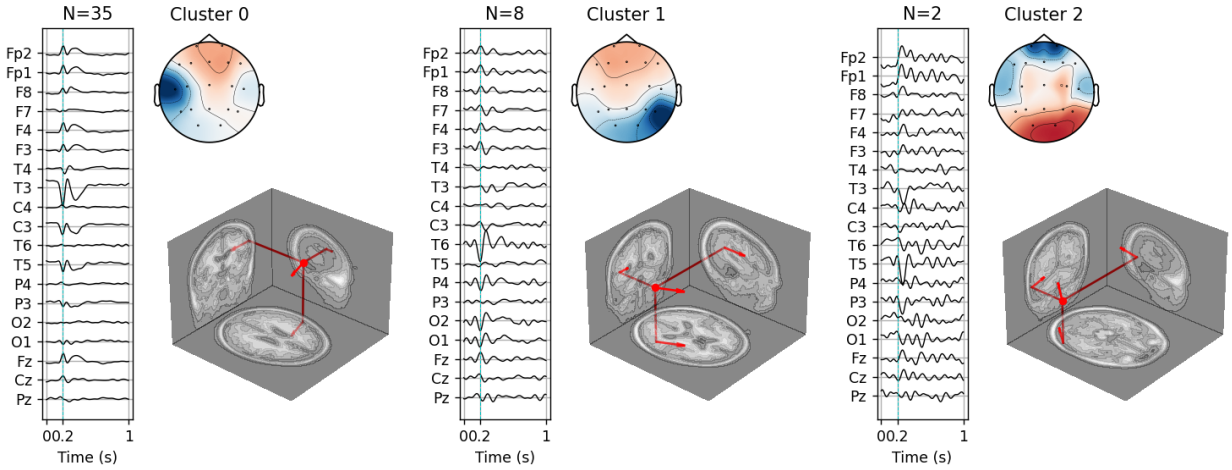

Patient 5

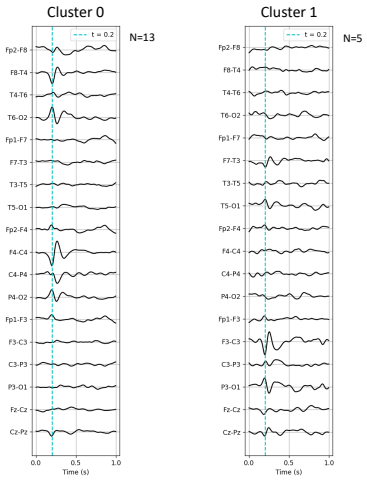

Patient 6

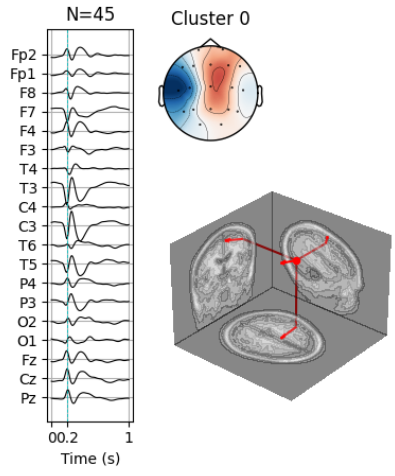

Patient 7

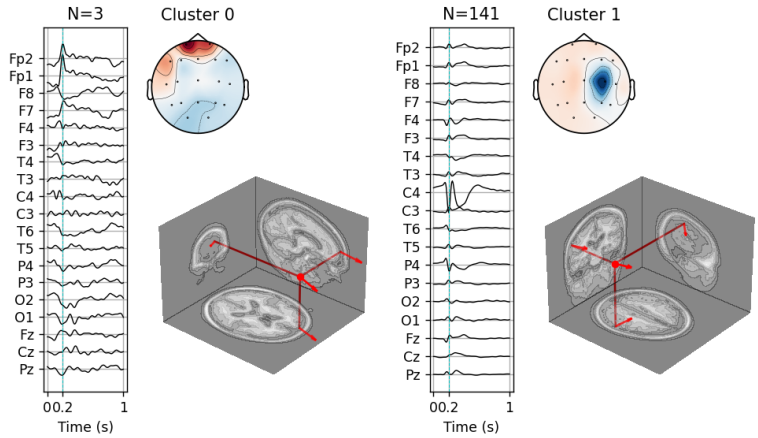

Patient 8

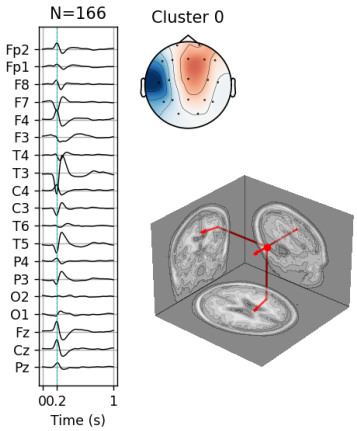

Patient 9

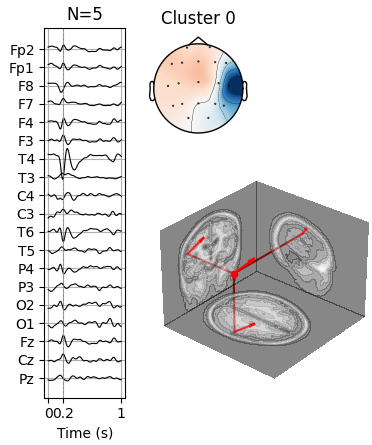

Patient 10

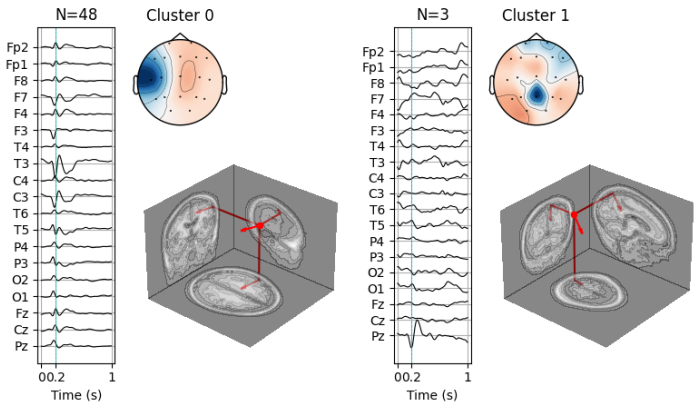

Patient 11

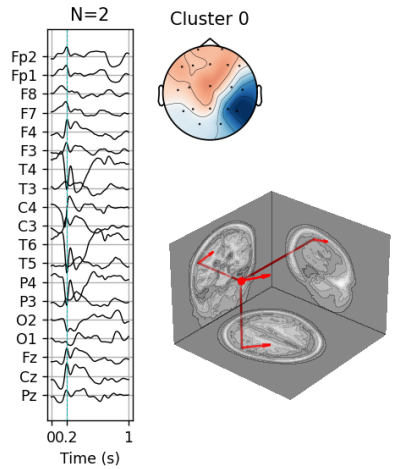

Patient 12

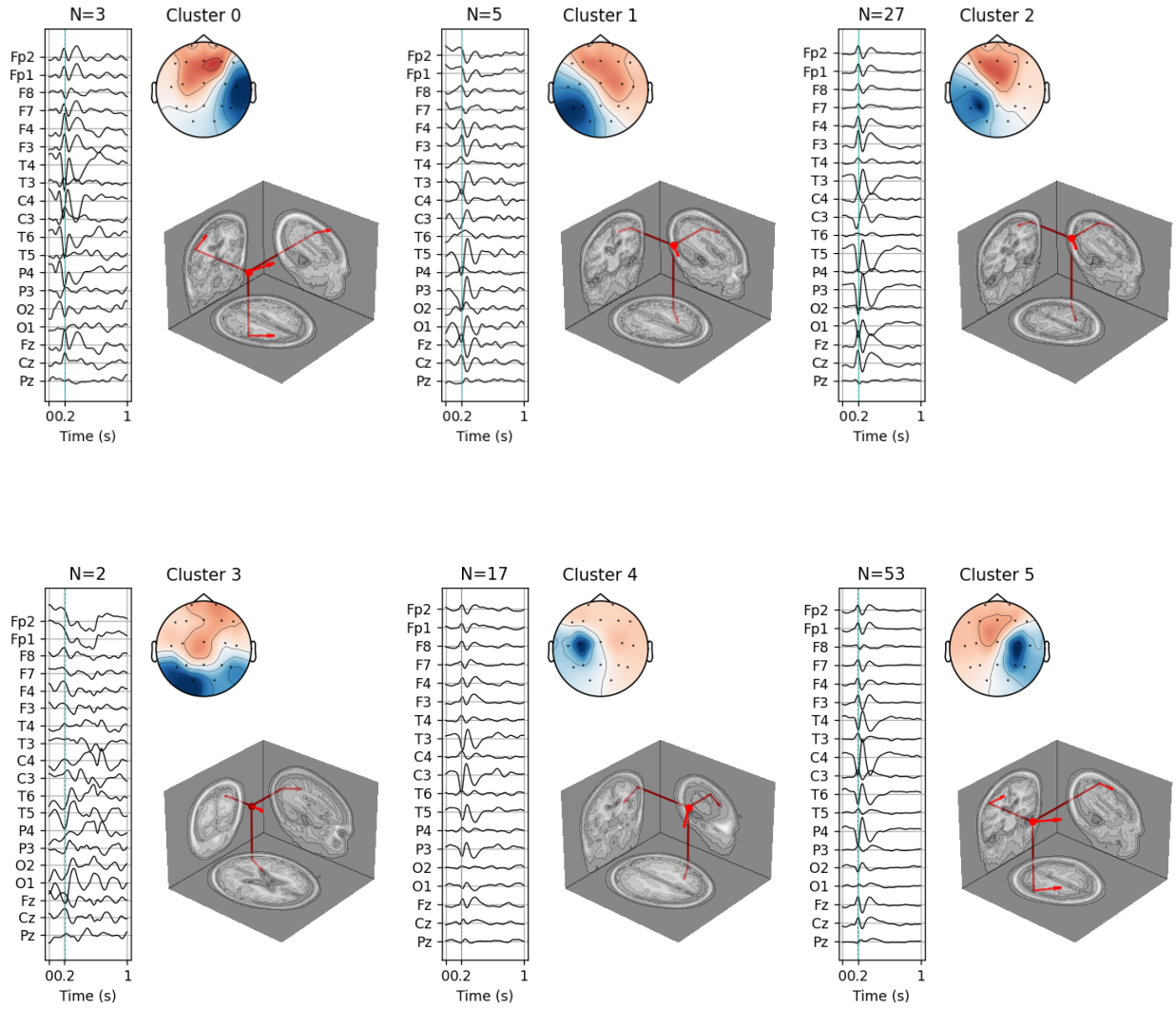

Patient 13

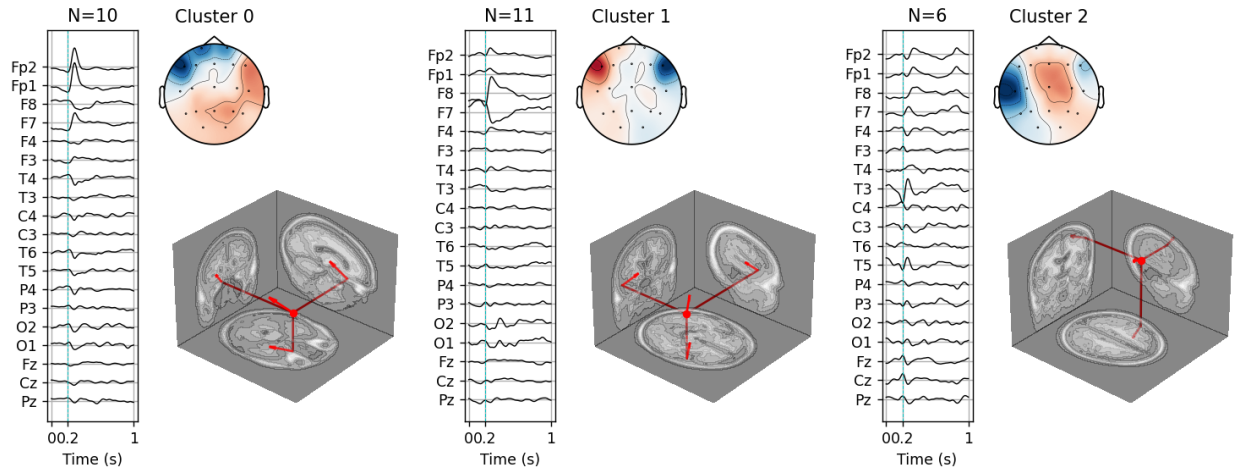

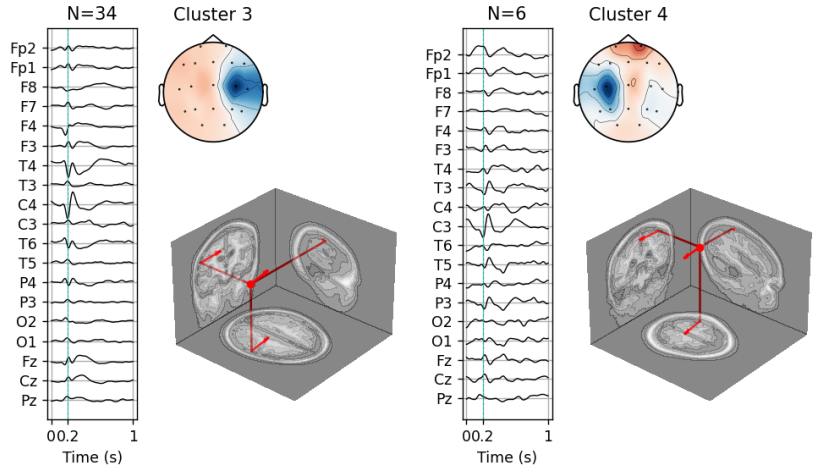

Patient 14

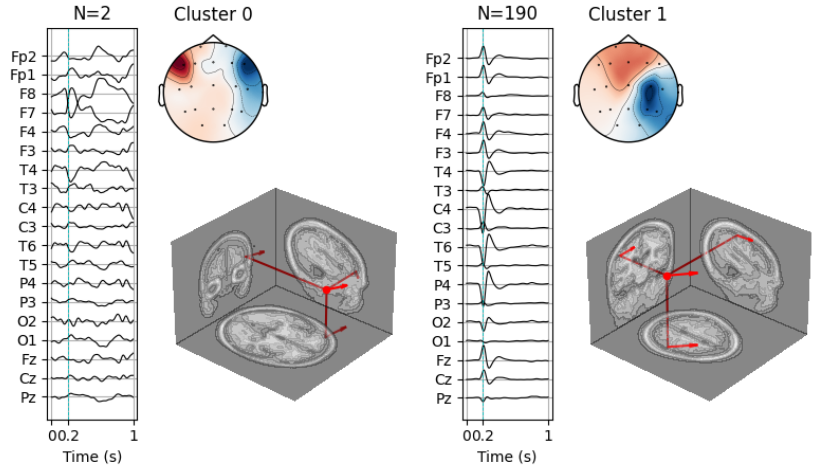

Patient 15

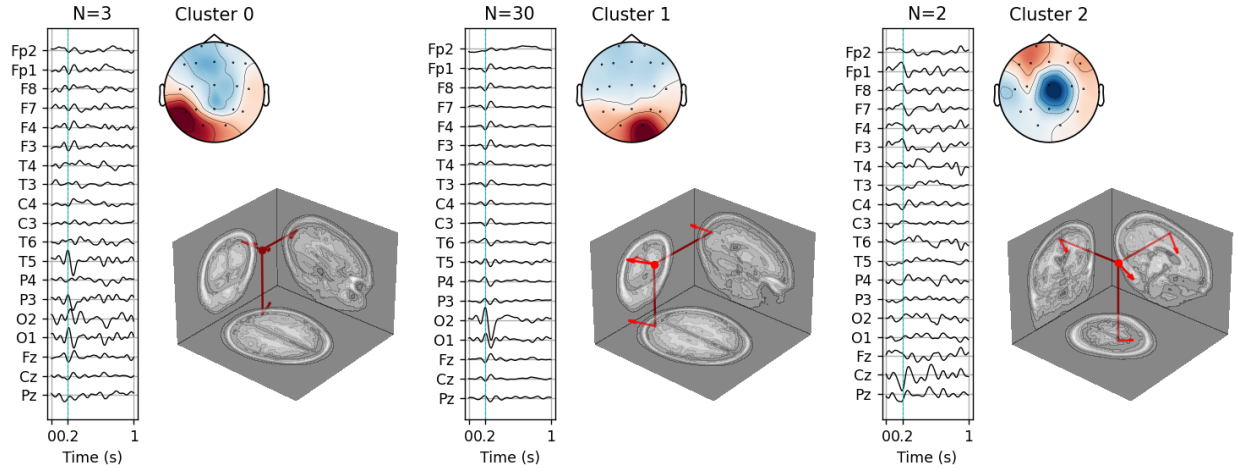

Patient 16

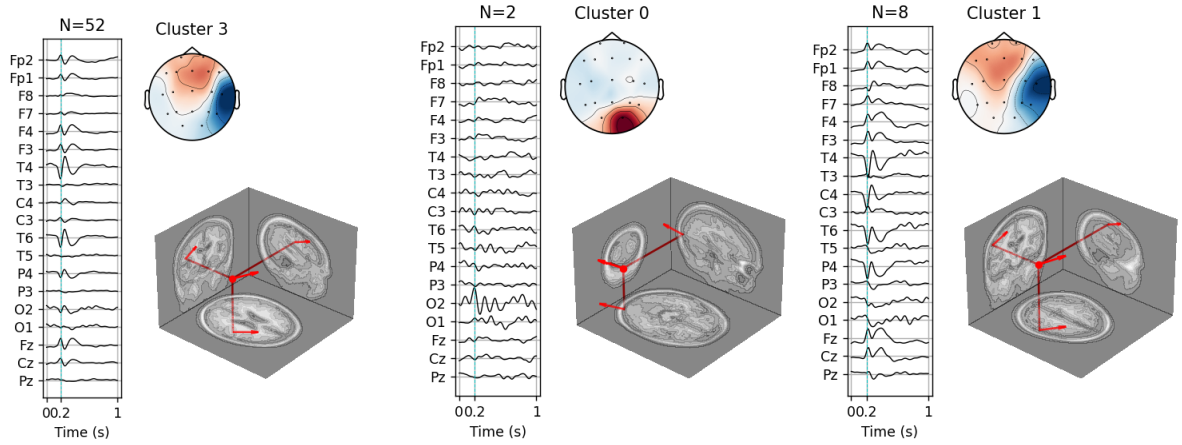

Patient 17

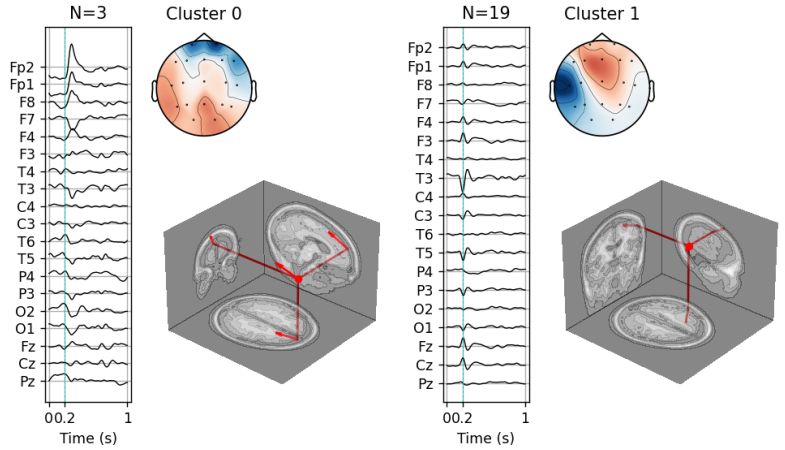

Patient 18

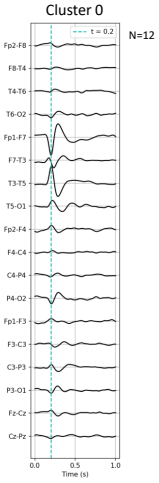

Patient 19

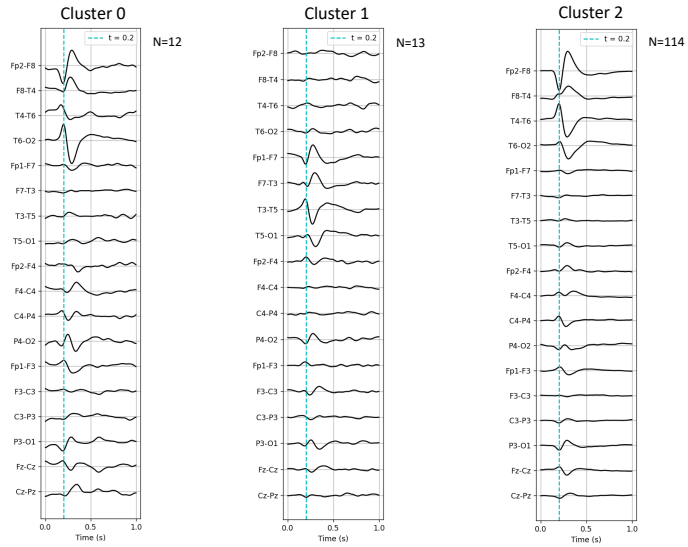

Patient 20

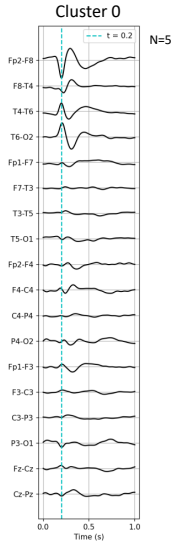

Patient 21

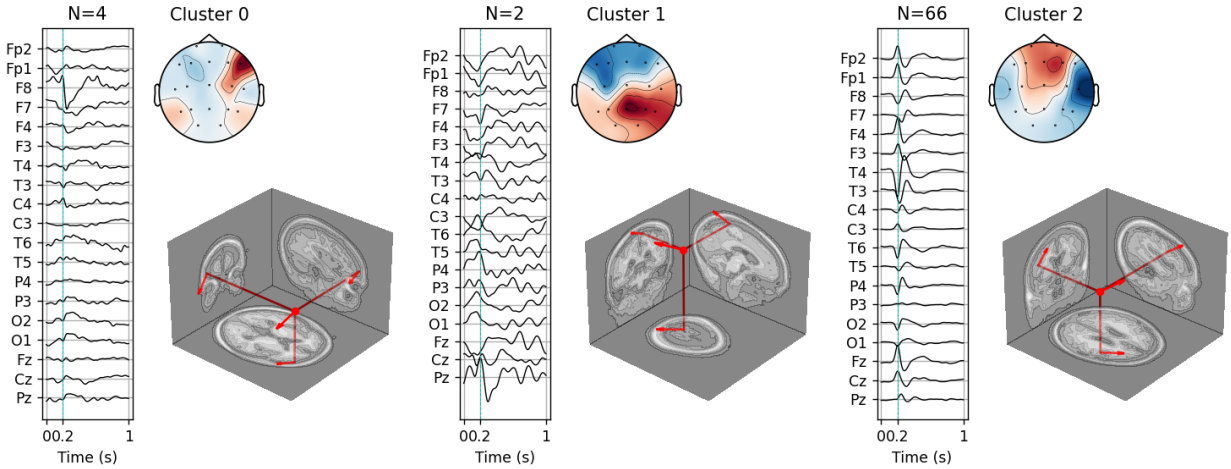

Patient 22

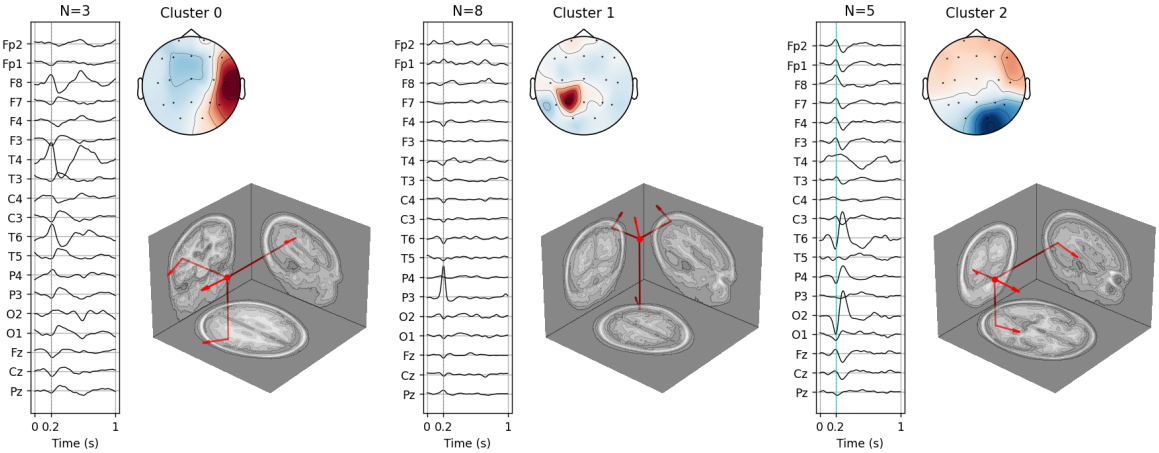

Patient 23

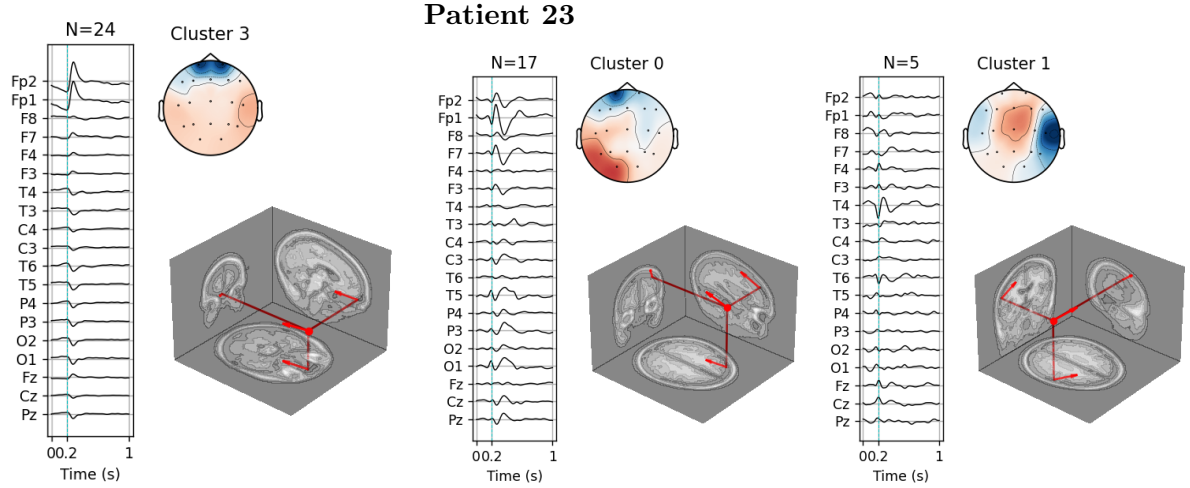

Patient 24

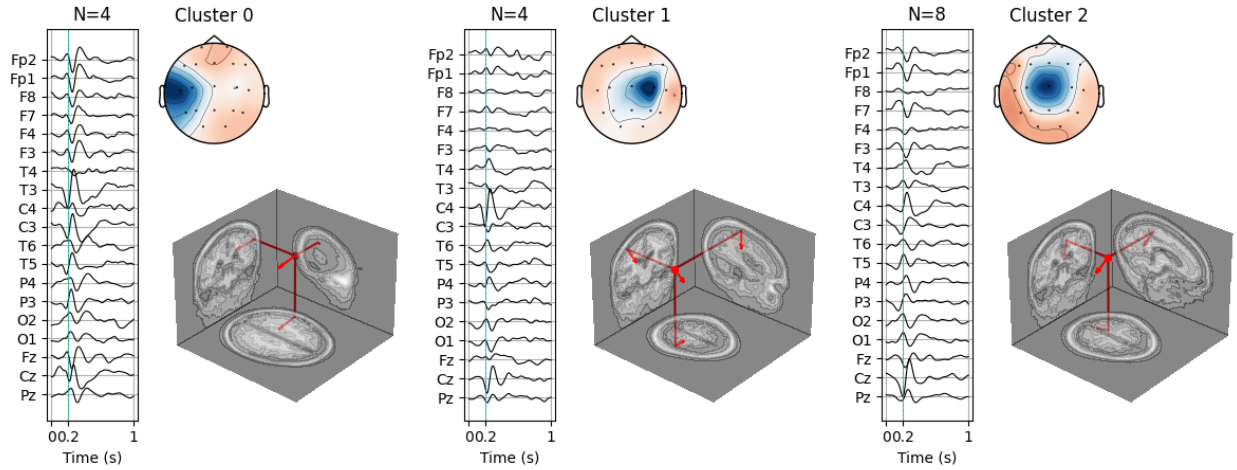

Patient 25

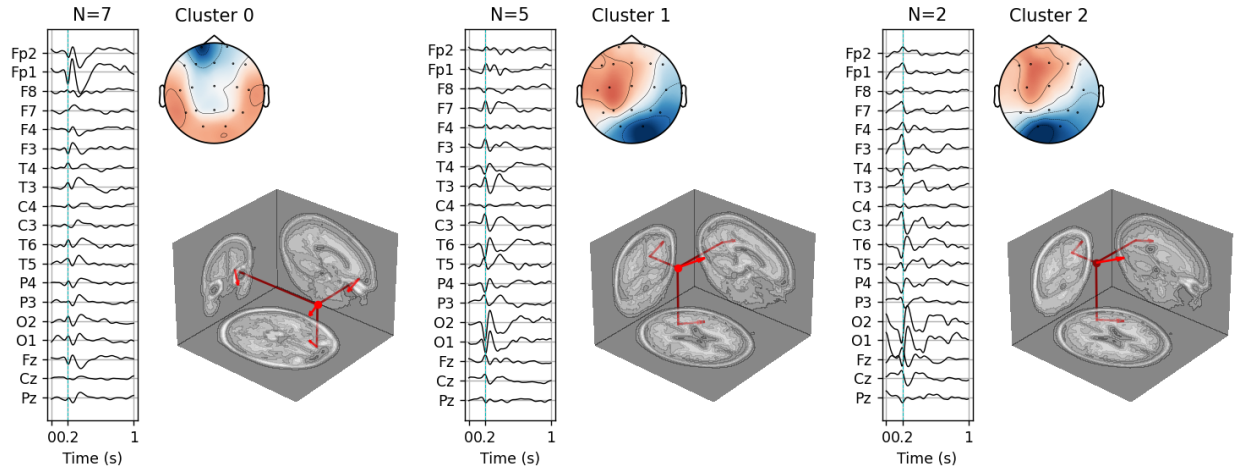

Patient 26

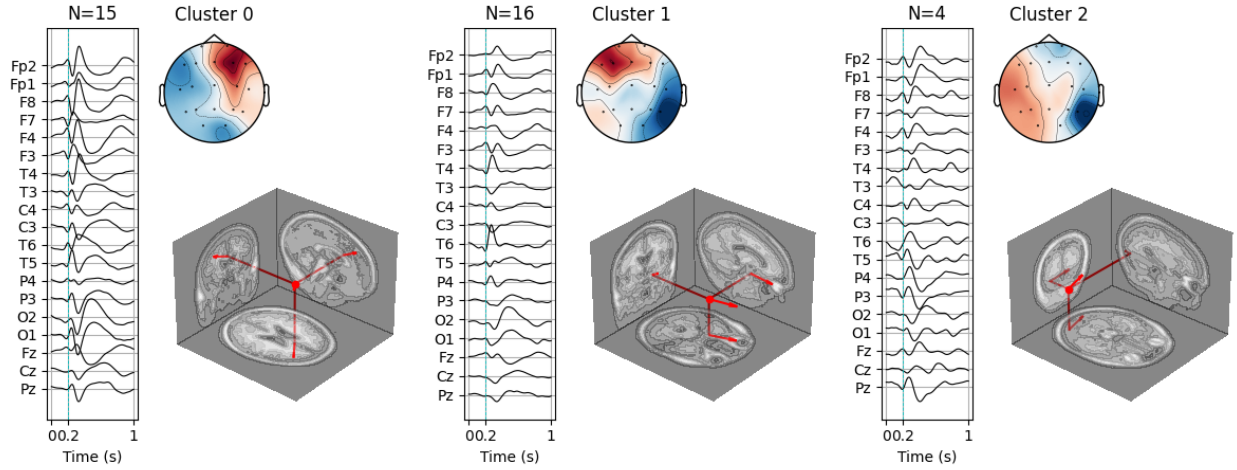

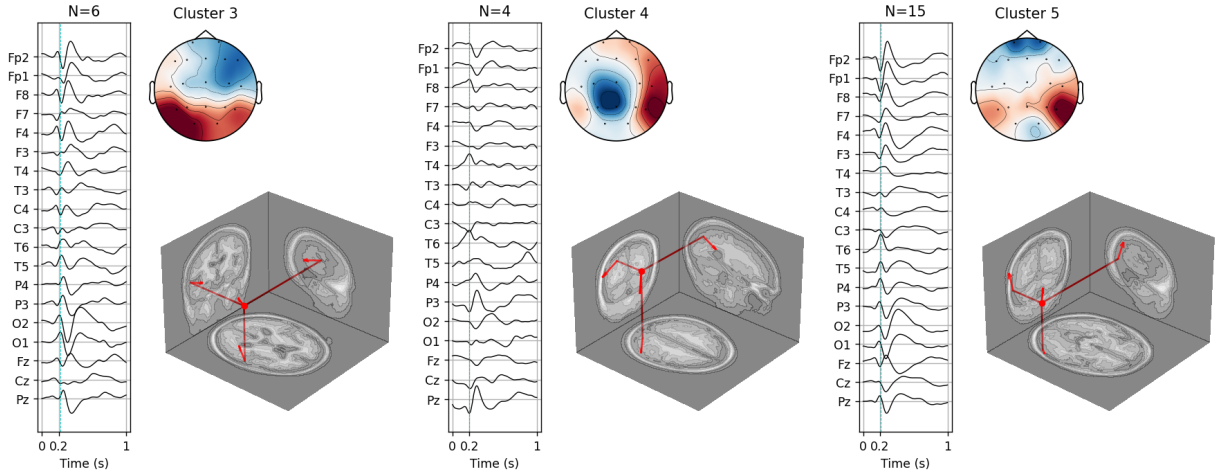

Patient 27

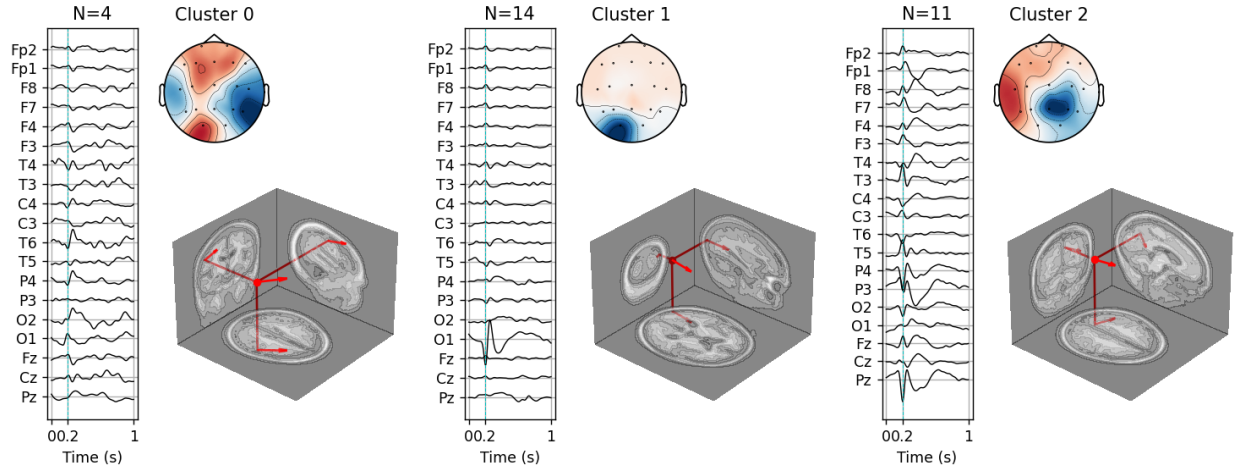

Patient 28

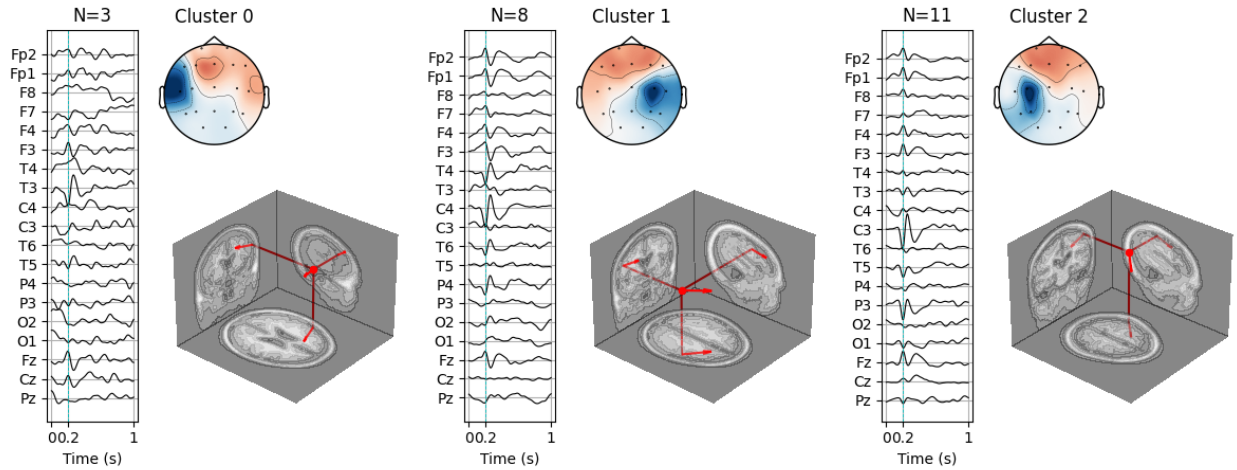

Patient 29

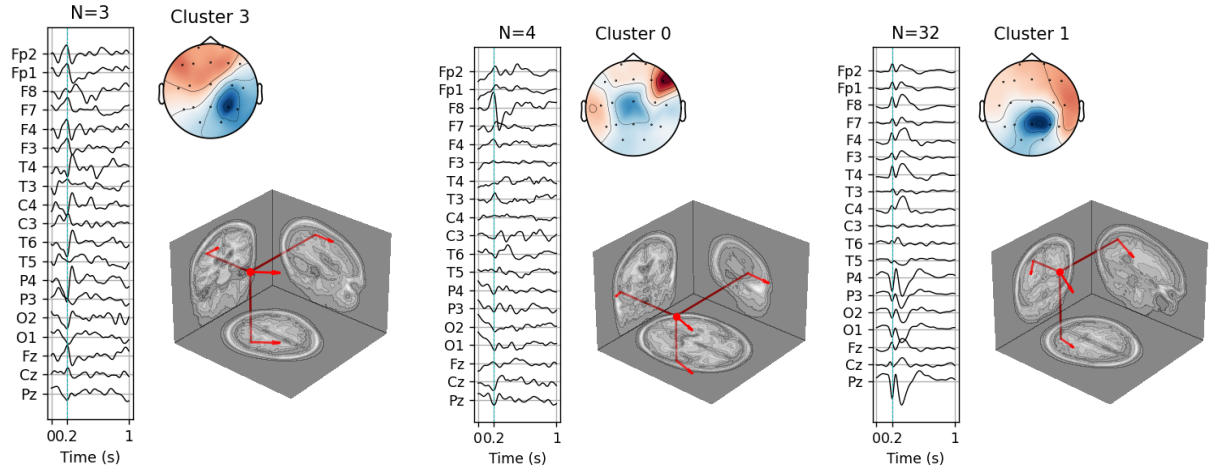

Patient 30

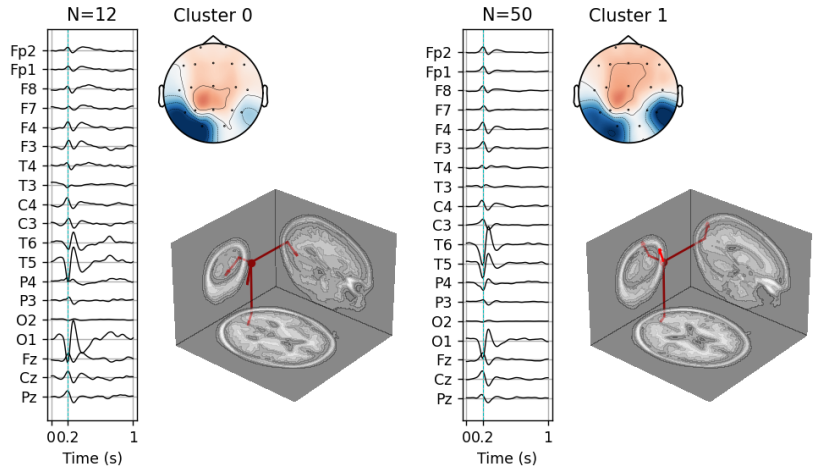

Patient 31

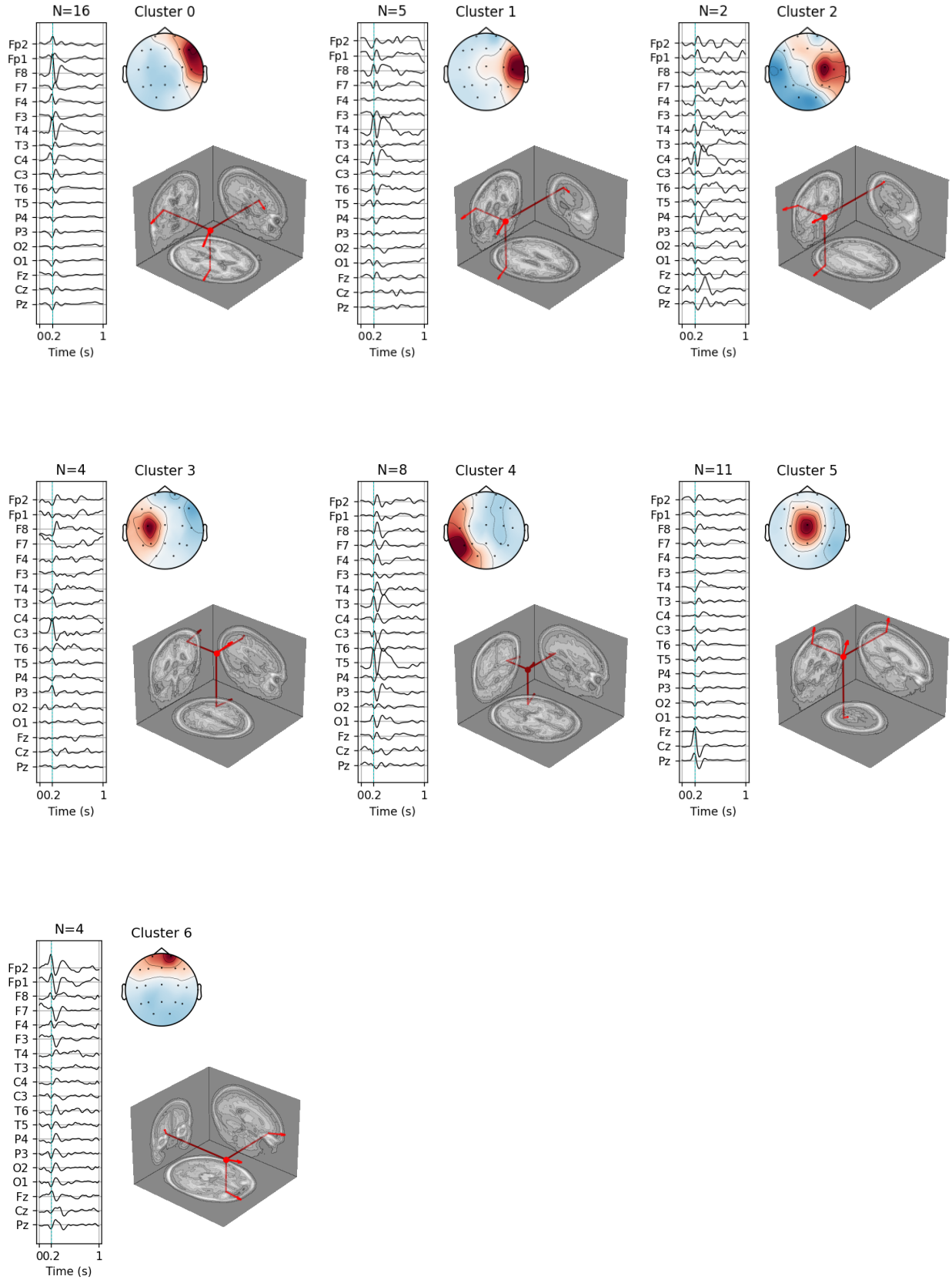
N=16
Cluster 0
N=5
Cluster 1
N=2
Cluster 2
N=4
Cluster 3
N=8
Cluster 4
N=11
Cluster 5
N=4
Cluster 6
Fp2
Fp1
F8
F7
F4
F3
T4
T3
C4
C3
T6
T5
P4
P3
O2
O1
Fz
Cz
Pz
00.2
1
Time (s)

N Influence of VGG sensitivity

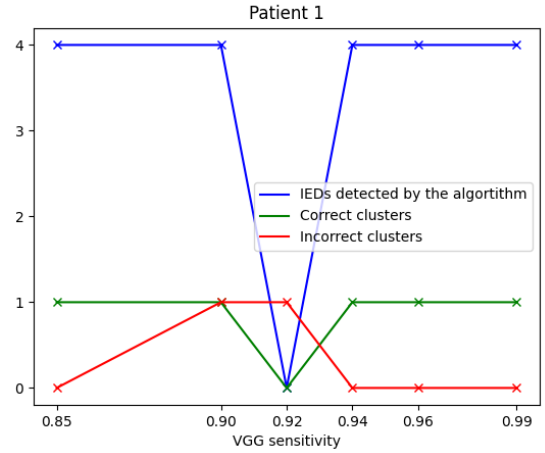

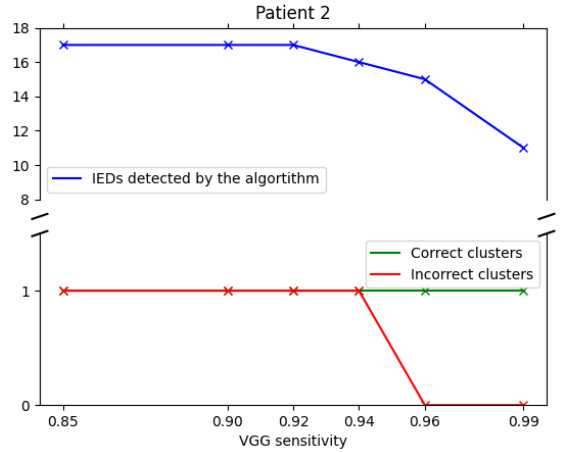

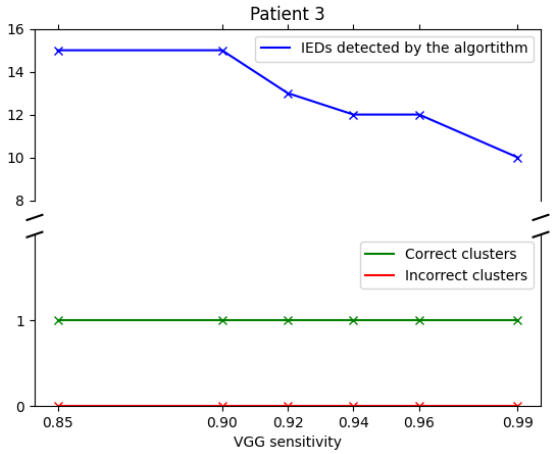

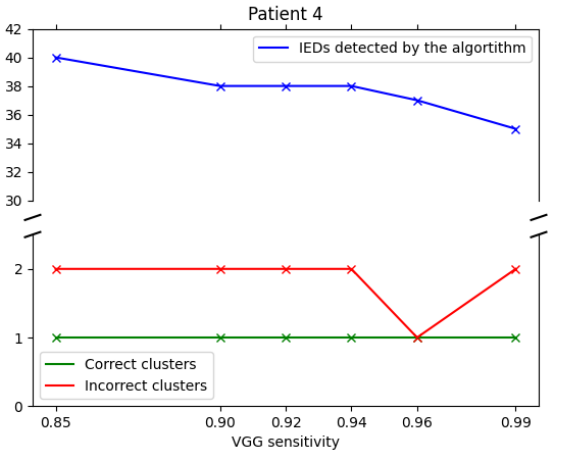

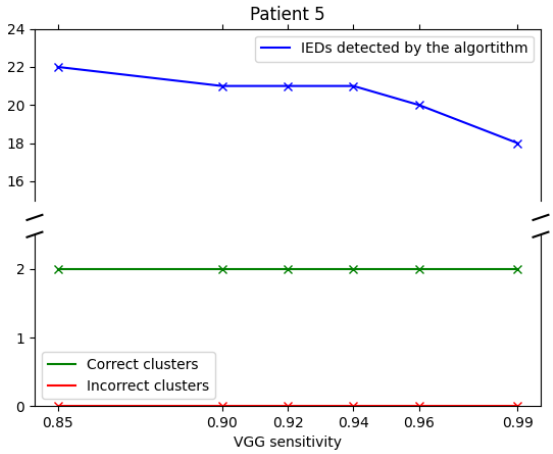

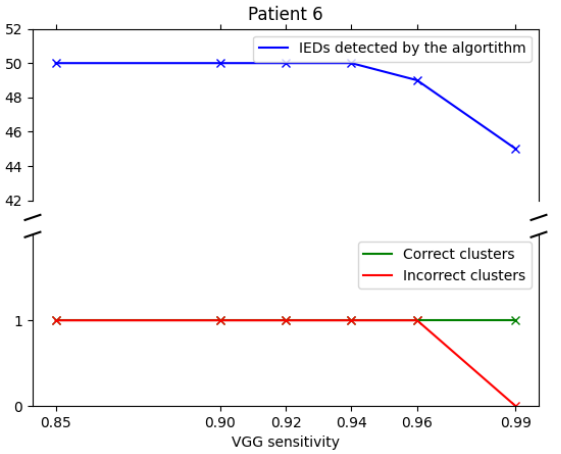

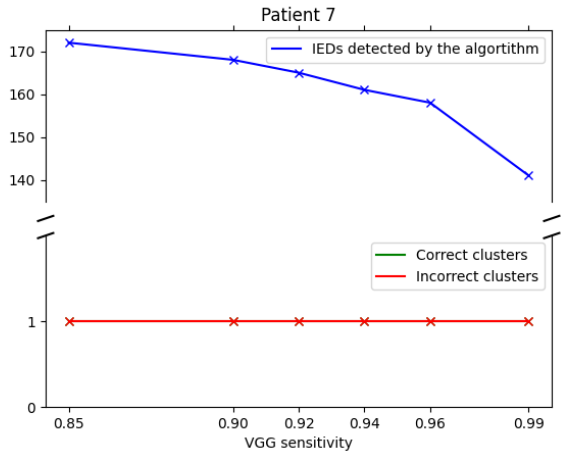
Patient 7
IEDs detected by the algortithm
Correct clusters
Incorrect clusters
VGG sensitivity

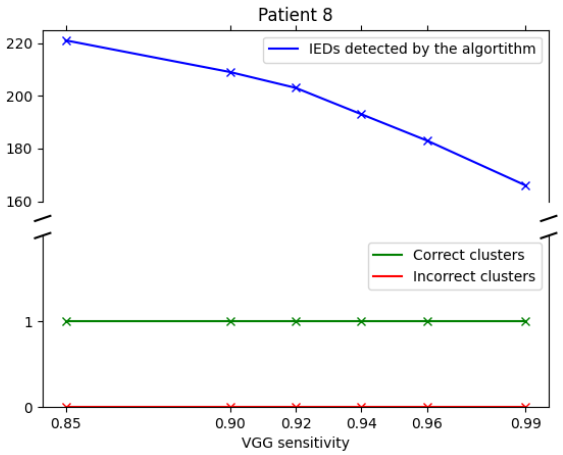
Patient 8
IEDs detected by the algortithm
Correct clusters
Incorrect clusters
VGG sensitivity

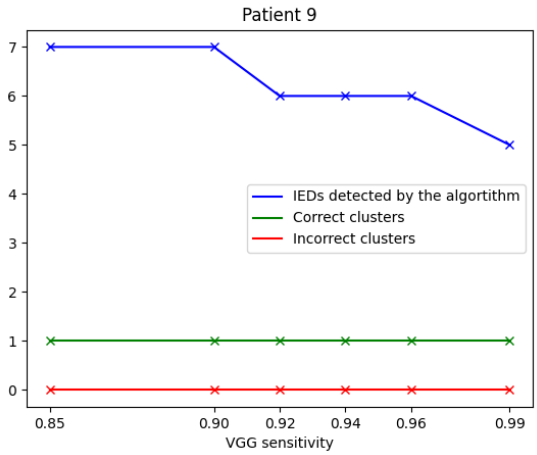
Patient 9
IEDs detected by the algortithm
Correct clusters
Incorrect clusters
VGG sensitivity

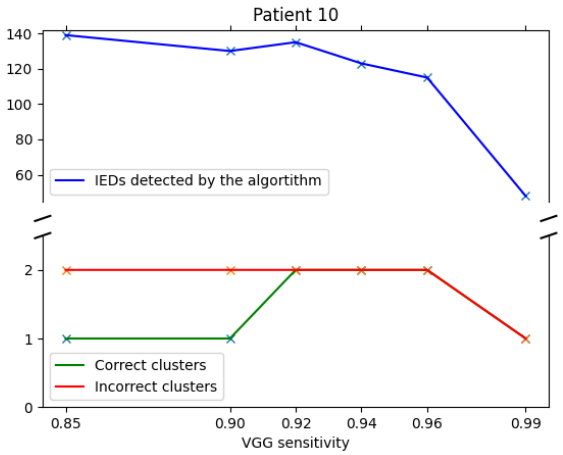
Patient 10
IEDs detected by the algortithm
Correct clusters
Incorrect clusters
VGG sensitivity

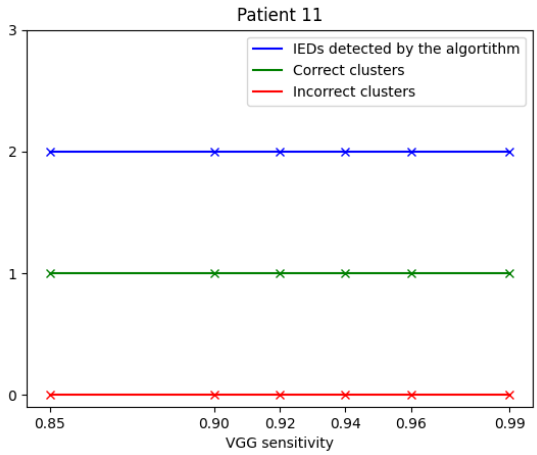
Patient 11
IEDs detected by the algortithm
Correct clusters
Incorrect clusters
VGG sensitivity

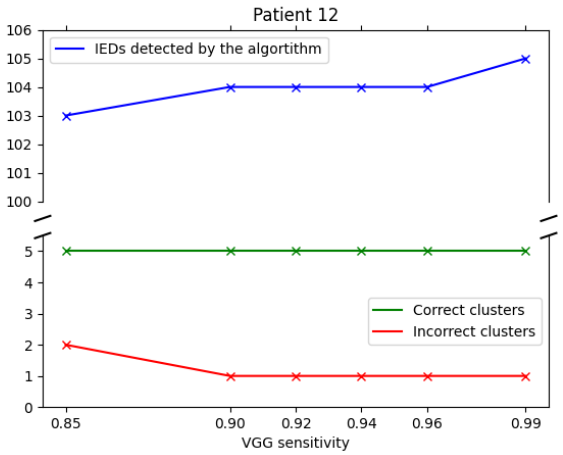
Patient 12
IEDs detected by the algortithm
Correct clusters
Incorrect clusters
VGG sensitivity

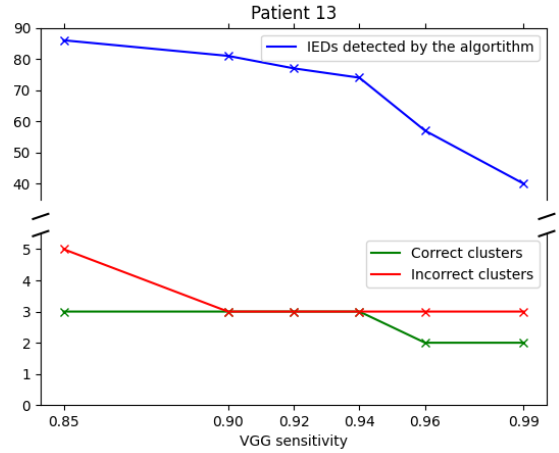
Patient 13
IEDs detected by the algorithm
Correct clusters
Incorrect clusters
VGG sensitivity

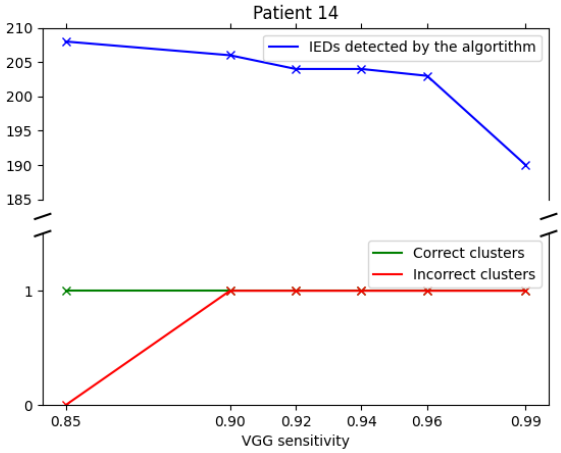
Patient 14
IEDs detected by the algorithm
Correct clusters
Incorrect clusters
VGG sensitivity

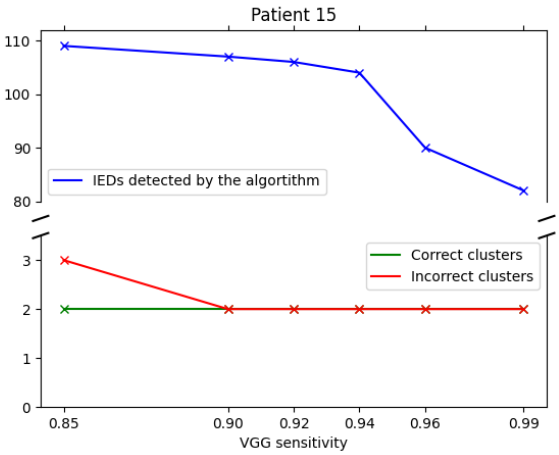
Patient 15
IEDs detected by the algorithm
Correct clusters
Incorrect clusters
VGG sensitivity

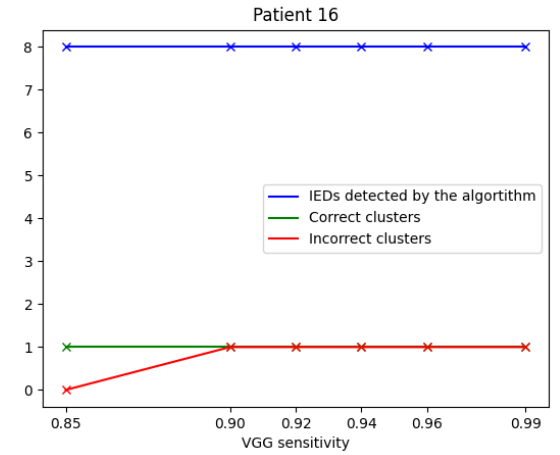
Patient 16
IEDs detected by the algorithm
Correct clusters
Incorrect clusters
VGG sensitivity

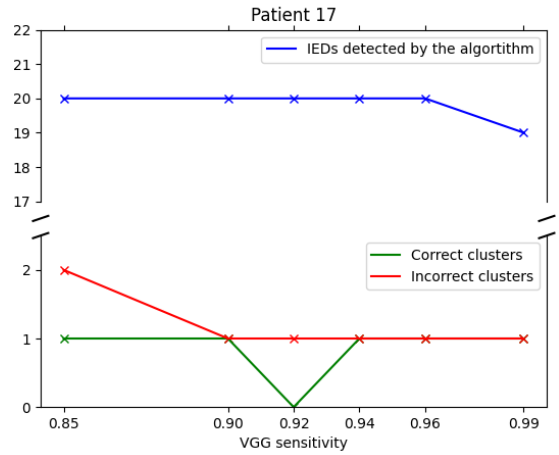
Patient 17
IEDs detected by the algorithm
Correct clusters
Incorrect clusters
VGG sensitivity

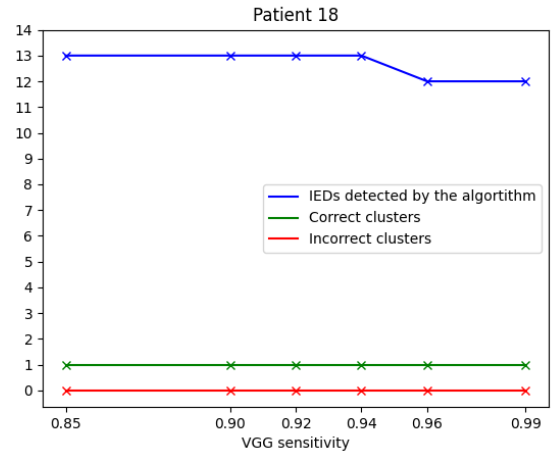
Patient 18
IEDs detected by the algorithm
Correct clusters
Incorrect clusters
VGG sensitivity

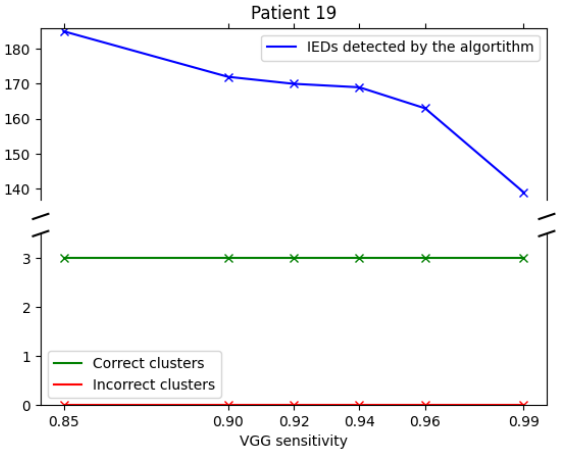
Patient 19
IEDs detected by the algortithm
Correct clusters
Incorrect clusters
VGG sensitivity

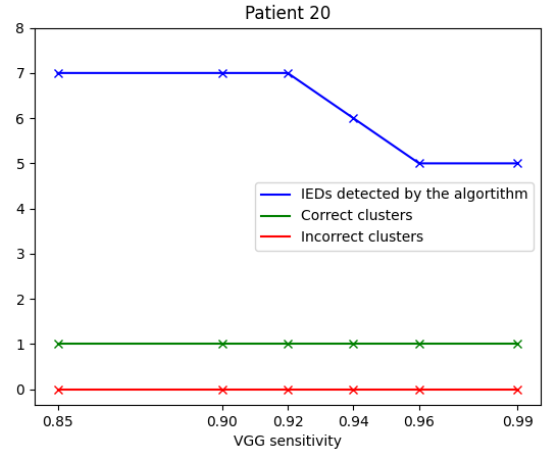
Patient 20
IEDs detected by the algortithm
Correct clusters
Incorrect clusters
VGG sensitivity

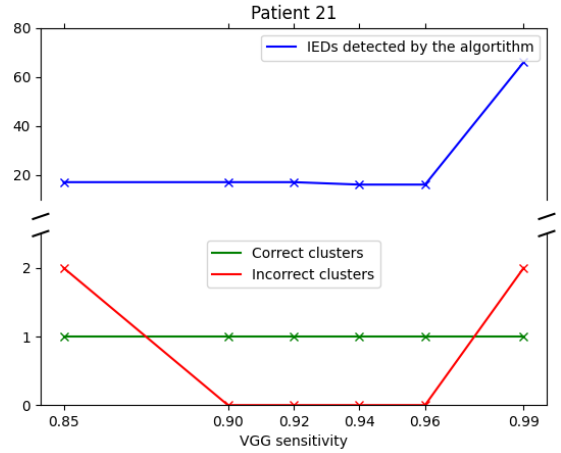
Patient 21
IEDs detected by the algortithm
Correct clusters
Incorrect clusters
VGG sensitivity

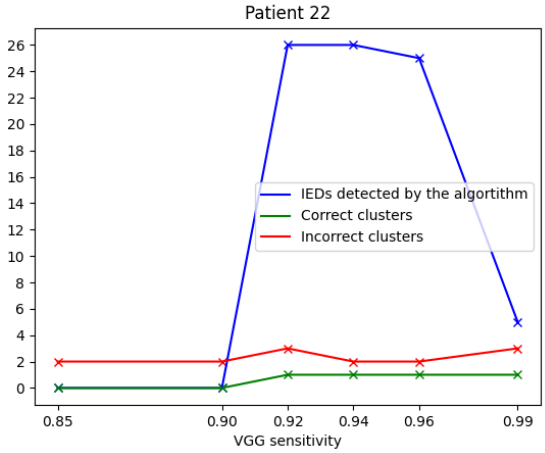
Patient 22
IEDs detected by the algortithm
Correct clusters
Incorrect clusters
VGG sensitivity

O Rolandic dipoles

The average dipoles for 13 patients with Rolandic epilepsy (patient 5 was excluded because of the Double Banana montage) are plotted. The dipoles are plotted onto the MRI of the standard head model. The bottom image is the top of the head, the right is the side and the left is the back. The nose points towards the x-axis. The red dot indicates the dipole position and the arrow shows the orientation. The Goodness of Fit, strength and location of the dipole are included at the top of the figures.

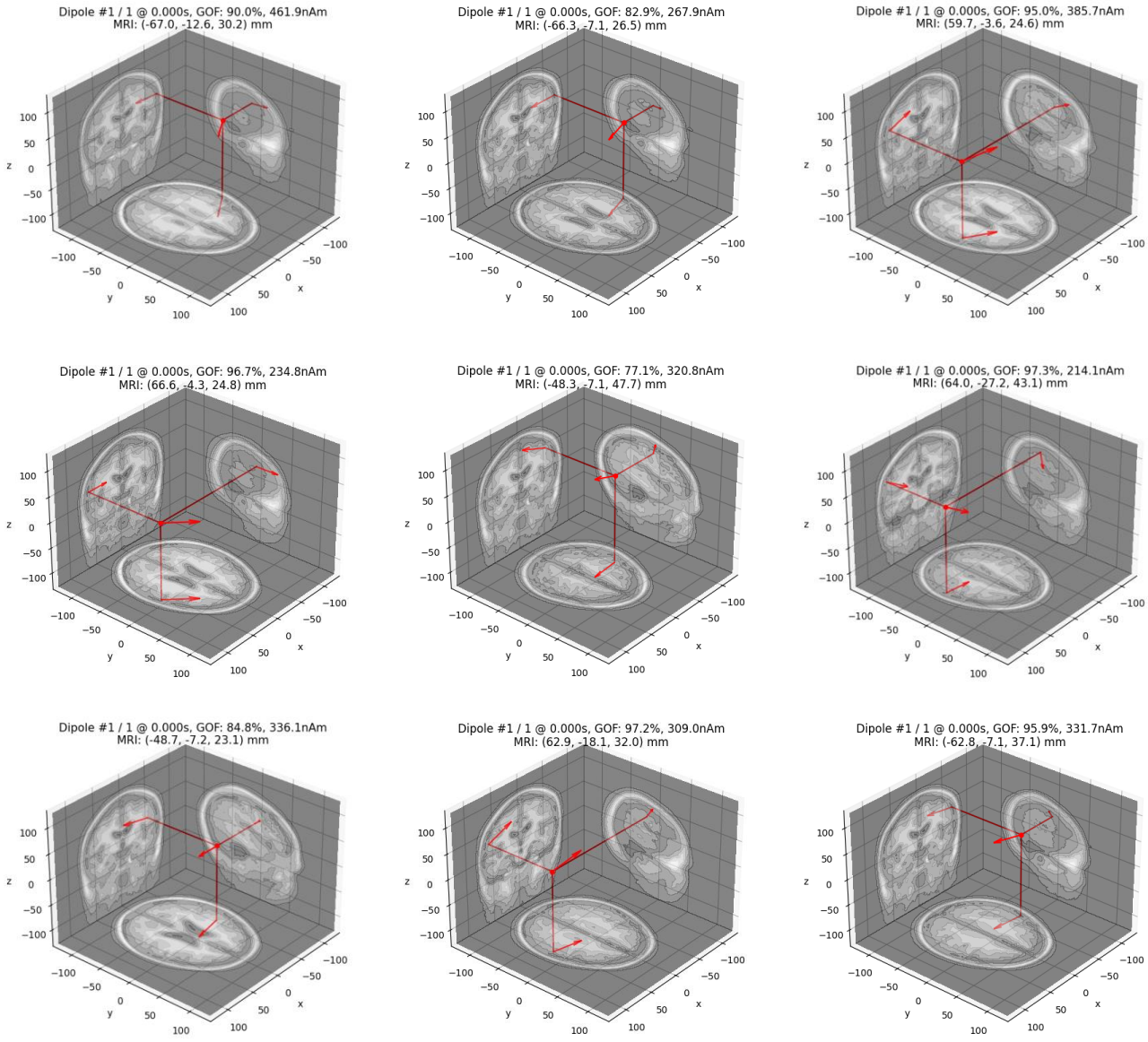

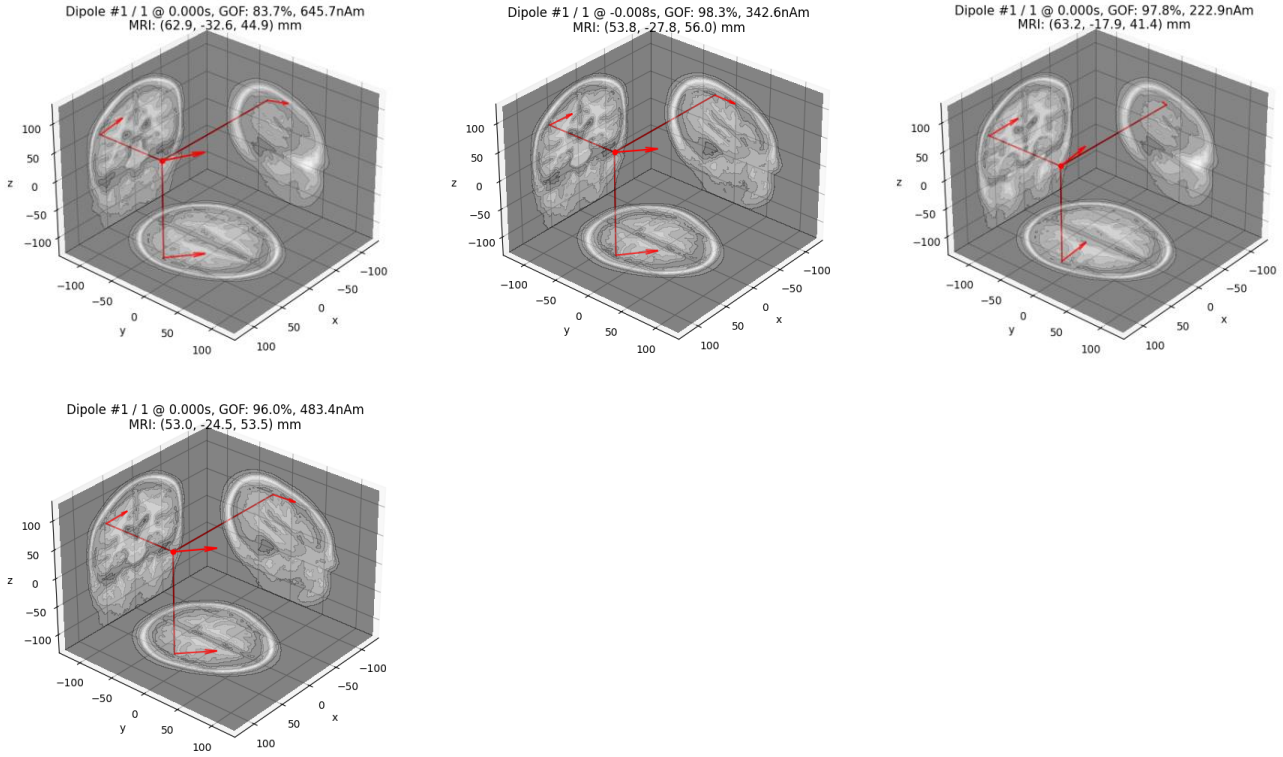

Figure 28: Dipoles of 13 Rolandic patients. The left view shows the back, the right the side and the bottom the top of the head. The dot indicates dipole position and the arrow represents dipole orientation and strength. All patients show a dipole in the centrotemporal area and most have an orientation tangential to the skull.

In an alternative view, the dipoles are plotted onto the MRI of the standard head model. The left image is the back of the head, the middle is the side of the head and the right image is the top of the head. The intersection of lines indicates the dipole position.

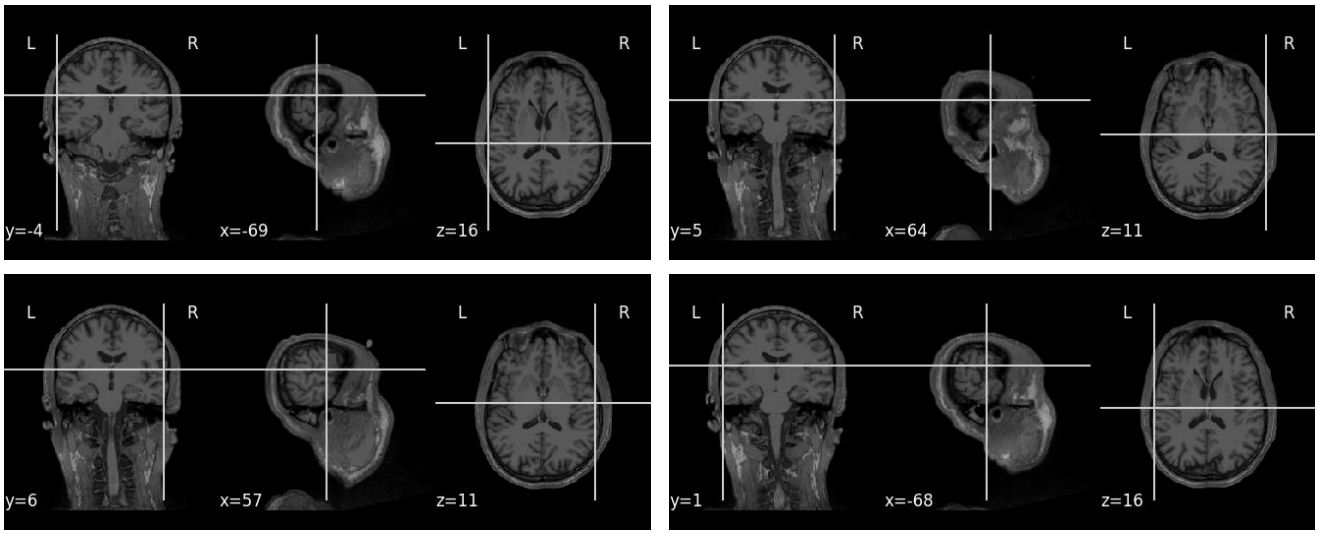

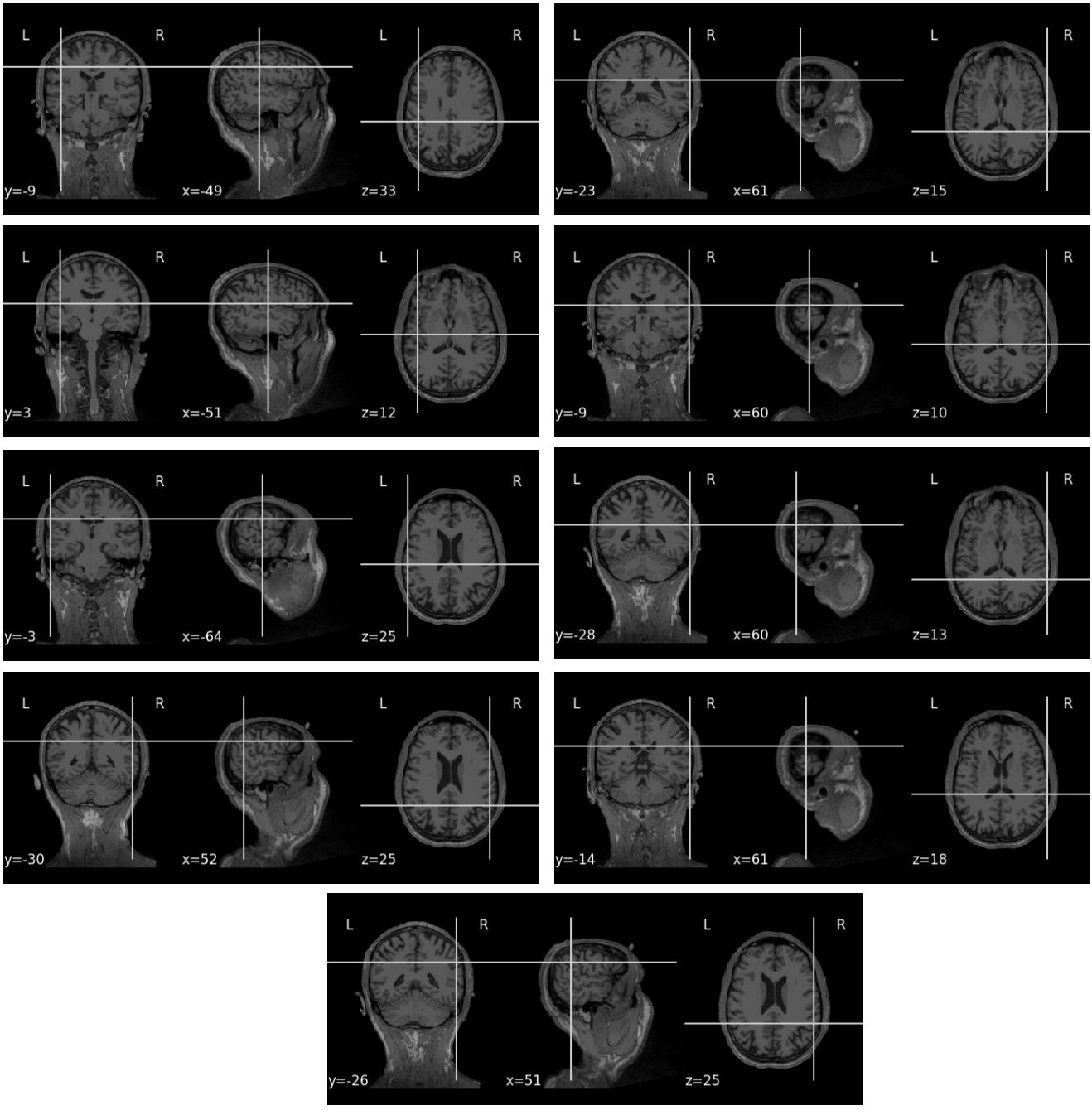

Figure 29: Dipoles of 13 Rolandic patients. The left view shows the back, the middle the side and the right the top of the head. The intersection of lines indicates position of the dipole. All patients show a dipole in the centrotemporal area.

P Dipole characteristics

Table 4: Dipole characteristics (strength and GoF) for all clusters that were correctly identified. Table continues on the next page.

Patient	Epilepsy type	Cluster	Channel	Epochs	Dipole strength (nAm)	Goodness of Fit (%)
1	Rolandic	1	T3	4	461.9	90.0
2	Rolandic	1	T4	11	234.8	96.7
3	Rolanic	1	T4	10	385.7	95.0
4	Rolandic	1	T3	35	267.9	82.9
6	Rolandic	1	C3	45	320.8	77.1
7	Rolandic	2	C4	141	214.1	97.3
8	Rolandic	1	T3	166	336.1	84.8
9	Rolandic	1	T4	5	309.0	97.2
10	Rolandic	1	T3	48	331.7	95.9
11	Rolandic	1	T6	2	645.7	83.7
12	Rolandic	1	T4	3	542.3	88.0
		2	T5	5	497.5	88.7
		3	P3	27	613.3	95.8
		5	C3	17	282.8	97.5
		6	P4	53	342.6	98.3
13	Rolandic	4	C4	34	222.9	97.8
		5	C3	6	154.5	71.9
14	Rolandic	2	C4	190	48.4	96.0
15	Other focal	2	O2	30	95.5	62.6
		4	T6	52	226.2	94.8
16	Other focal	2	C4	8	430.7	93.8
17	Other focal	2	T3	19	264.2	94.9
21	Other focal	3	T4	66	426.9	81.6
22	Other focal	3	O2	5	256.2	95.1
23	Multi-focal	1	Fp1	17	112.	64.4
		2	T4	5	183.9	84.8
24	Multi-focal	1	T3	4	317.3	88.8
		2	C4	4	307.6	88.0
		3	Cz	8	390.5	81.5
25	Multi-focal	1	Fp1	7	358.6	84.1
		2	O2	5	428.4	95.0
		3	O1	2	485.4	90.6
26	Multi-focal	1	F8	15	851.2	76.2
		4	O2	6	161.7	74.4
		6	Fp1	15	862.3	37.6

Patient	Epilepsy type	Cluster	Channel	Epochs	Dipole strength (nAm)	Goodness of Fit (%)
27	Multi-focal	2	O1	14	173.6	92.0
		3	Pz	11	433.9	74.7
28	Multi-focal	2	C4	8	343.7	94.9
		3	C3	11	369.2	91.5
29	Multi-focal	2	P4	32	332.3	92.8
30	Multi-focal	1	O1	12	97.4	23.9
		2	T6	50	164.9	20.1
31	Multi-focal	1	F8	16	517.5	95.8
		2	T4	5	213.1	84.1
		3	C4	2	212.6	82.0
		5	T5	8	267.6	91.4

Table 5: Dipole characteristics (strength and GoF) for all incorrectly identified clusters.

Patient	Epilepsy type	Cluster	Channel	Epochs	Dipole strength (nAm)	Goodness of Fit (%)
4	Rolandic	3	T5	2	92.9	40.2
7	Rolandic	1	Fp1	3	350.8	70.3
10	Rolandic	2	Pz	3	446.6	68.6
12	Rolandic	4	O1	2	231.1	51.4
13	Rolandic	1	Fp1	10	136.9	47.9
		2	F8	11	161.2	60.6
14	Rolandic	1	F8	2	164.8	52.0
15	Other focal	1	T5	3	148.3	56.9
		3	Cz	2	256.1	71.7
16	Other focal	1	O2	2	175.4	52.3
17	Other focal	1	Fp2	3	249.2	48.3
21	Other focal	1	F8	4	213.8	54.9
		2	Pz	2	371.8	52.6
22	Other focal	1	T4	3	226.9	71.9
		2	P3	8	446.8	92.7
		4	Fp1	3	192.9	90.3
26	Multi-focal	3	P3	4	487.7	38.2
		5	Pz	4	856.2	82.1
27	Multi-focal	1	T6	4	107.5	51.6
28	Multi-focal	4	P4	3	439.0	89.7
29	Multi-focal	1	F8	4	200.3	58.5
31	Multi-focal	4	C3	4	313.5	93.7
		6	Cz	11	346.5	94.3
		7	Fp2	4	175.7	62.8

Table 6: Dipole characteristics (strength and GoF) for all clusters. Table continues on the next page.

Patient	Epilepsy type	Cluster	Channel	Epochs	Correct	Dipole strength	Goodness of Fit
1	Rolandic	1	T3	4	yes	461.9 nAm	90.0 %
2	Rolandic	1	T4	11	yes	234.8 nAm	96.7 %
3	Rolanic	1	T4	10	yes	385.7 nAm	95.0 %
4	Rolandic	1	T3	35	yes	267.9 nAm	82.9 %
		2	T6	8	maybe	207.8 nAm	84.7 %
		3	T5	2	no	92.9 nAm	40.2 %
5	Rolandic	1	F4-C4	13	yes	-	-
		2	F3-C3	5	yes	-	-
6	Rolandic	1	C3	45	yes	320.8 nAm	77.1 %
7	Rolandic	1	Fp1	3	no	350.8 nAm	70.3 %
		2	C4	141	yes	214.1 nAm	97.3 %
8	Rolandic	1	T3	166	yes	336.1 nAm	84.8 %
9	Rolandic	1	T4	5	yes	309.0 nAm	97.2 %
10	Rolandic	1	T3	48	yes	331.7 nAm	95.9 %
		2	Pz	3	no	446.6 nAm	68.6 %
11	Rolandic	1	T6	2	yes	645.7 nAm	83.7 %
12	Rolandic	1	T4	3	yes	542.3 nAm	88.0 %
		2	T5	5	yes	497.5 nAm	88.7 %
		3	P3	27	yes	613.3 nAm	95.8 %
		4	O1	2	no	231.1 nAm	51.4 %
		5	C3	17	yes	282.8 nAm	97.5 %
		6	P4	53	yes	342.6 nAm	98.3 %
13	Rolandic	1	Fp1	10	no	136.9 nAm	47.9 %
		2	F8	11	no	161.2 nAm	60.6 %
		3	T3	6	maybe	246.3 nAm	81.9 %
		4	C4	34	yes	222.9 nAm	97.8 %
		5	C3	6	yes	154.5 nAm	71.9 %
14	Rolandic	1	F8	2	no	164.8 nAm	52.0 %
		2	C4	190	yes	48.4 nAm	96.0 %
15	Other focal	1	T5	3	no	148.3 nAm	56.9 %
		2	O2	30	yes	95.5 nAm	62.6 %
		3	Cz	2	no	256.1 nAm	71.7 %
		4	T6	52	yes	226.2 nAm	94.8 %
16	Other focal	1	O2	2	no	175.4 nAm	52.3 %
		2	C4	8	yes	430.7 nAm	93.8 %
17	Other focal	1	Fp2	3	no	249.2 nAm	48.3 %
		2	T3	19	yes	264.2 nAm	94.9 %
18	Other focal	1	T3-T5	12	yes	-	-
19	Other focal	1	T6-O2	12	yes	-	-
		2	T3-T5	13	yes	-	-
		3	Fp2-F8	114	yes	-	-

Patient	Epilepsy type	Cluster	Channel	Epochs	Correct	Dipole strength	Goodness of Fit
20	Other focal	1	Fp2-F8	5	yes	-	-
21	Other focal	1	F8	4	no	213.8 nAm	54.9 %
		2	Pz	2	no	371.8 nAm	52.6 %
		3	T4	66	yes	426.9 nAm	81.6 %
22	Other focal	1	T4	3	no	226.9 nAm	71.9 %
		2	P3	8	no	446.8 nAm	92.7 %
		3	O2	5	yes	256.2 nAm	95.1 %
		4	Fp1	3	no	192.9 nAm	90.3 %
23	Multi-focal	1	Fp1	17	yes	112.1 nAm	64.4 %
		2	T4	5	yes	183.9 nAm	84.8 %
24	Multi-focal	1	T3	4	yes	317.3 nAm	88.8 %
		2	C4	4	yes	307.6 nAm	88.0 %
		3	Cz	8	yes	390.5 nAm	81.5 %
25	Multi-focal	1	Fp1	7	yes	358.6 nAm	84.1 %
		2	O2	5	yes	428.4 nAm	95.0 %
		3	O1	2	yes	485.4 nAm	90.6 %
26	Multi-focal	1	F8	15	yes	851.2 nAm	76.2 %
		2	T6	16	maybe	372.0 nAm	32.5 %
		3	P3	4	no	487.7 nAm	38.2 %
		4	O2	6	yes	161.7 nAm	74.4 %
		5	Pz	4	no	856.2 nAm	82.1 %
		6	Fp1	15	yes	862.3 nAm	37.6 %
27	Multi-focal	1	T6	4	no	107.5 nAm	51.6 %
		2	O1	14	yes	173.6 nAm	92.0 %
		3	Pz	11	yes	433.9 nAm	74.7 %
28	Multi-focal	1	T3	3	maybe	352.1 nAm	86.8 %
		2	C4	8	yes	343.7 nAm	94.9 %
		3	C3	11	yes	369.2 nAm	91.5 %
		4	P4	3	no	439.0 nAm	89.7 %
29	Multi-focal	1	F8	4	no	200.3 nAm	58.5 %
		2	P4	32	yes	332.3 nAm	92.8 %
30	Multi-focal	1	O1	12	yes	97.4 nAm	23.9 %
		2	T6	50	yes	164.9 nAm	20.1 %
31	Multi-focal	1	F8	16	yes	517.5 nAm	95.8 %
		2	T4	5	yes	213.1 nAm	84.1 %
		3	C4	2	yes	212.6 nAm	82.0 %
		4	C3	4	no	313.5 nAm	93.7 %
		5	T5	8	yes	267.6 nAm	91.4 %
		6	Cz	11	no	346.5 nAm	94.3 %
		7	Fp2	4	no	175.7 nAm	62.8 %

Q IED stability

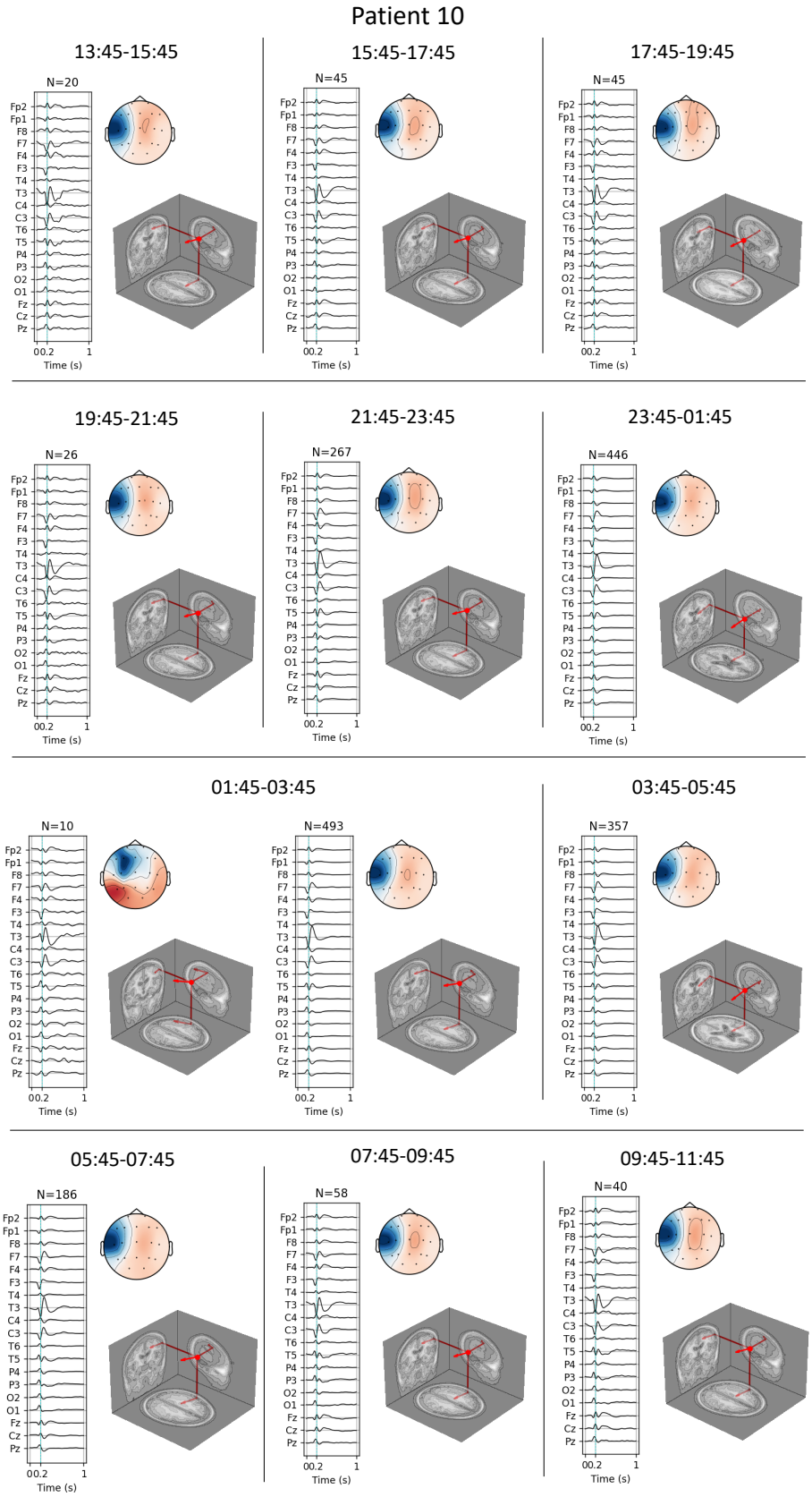

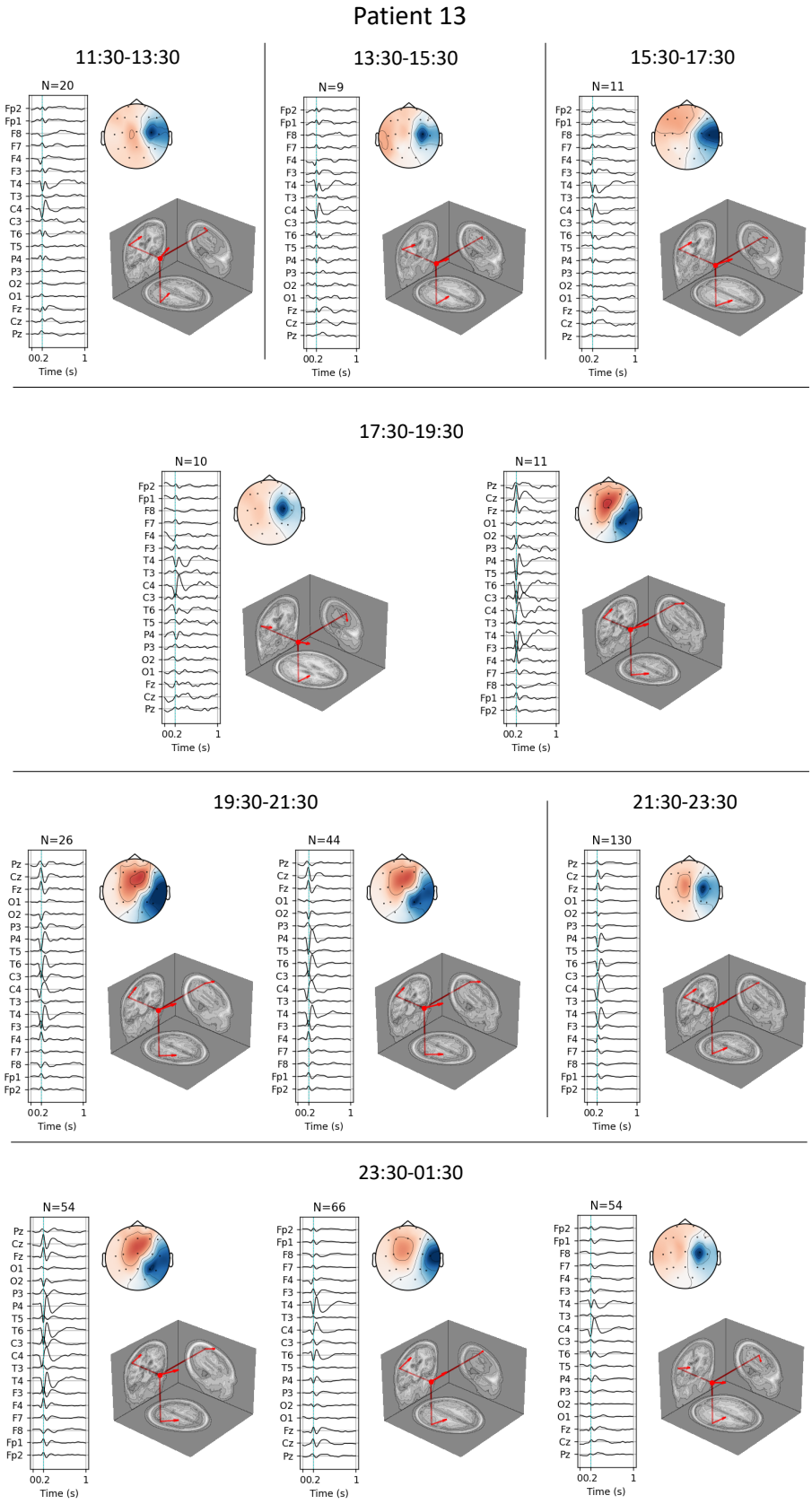
Patient 13
11:30-13:30
N=20
13:30-15:30
N=9
15:30-17:30
N=11
17:30-19:30
N=10
N=11
19:30-21:30
N=26
N=44
21:30-23:30
N=130
23:30-01:30
N=54
N=66
N=54
Time (s)

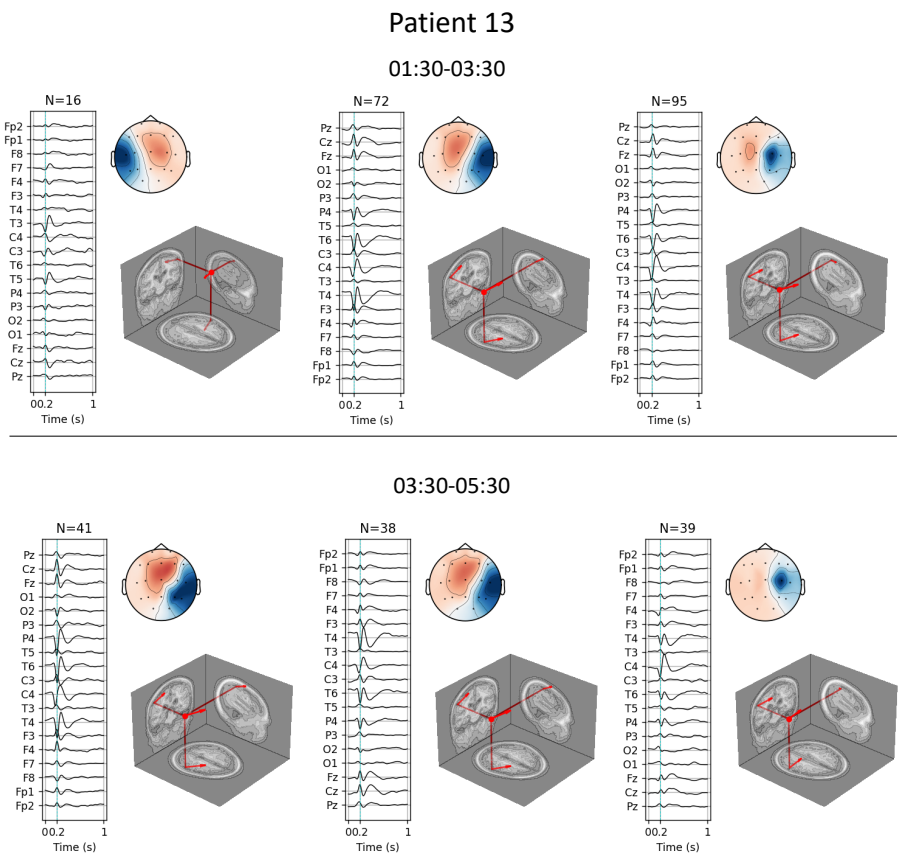
Patient 13
01:30-03:30
N=16
N=72
N=95
Time (s)
03:30-05:30
N=41
N=38
N=39
Time (s)

R Dipole strength over time

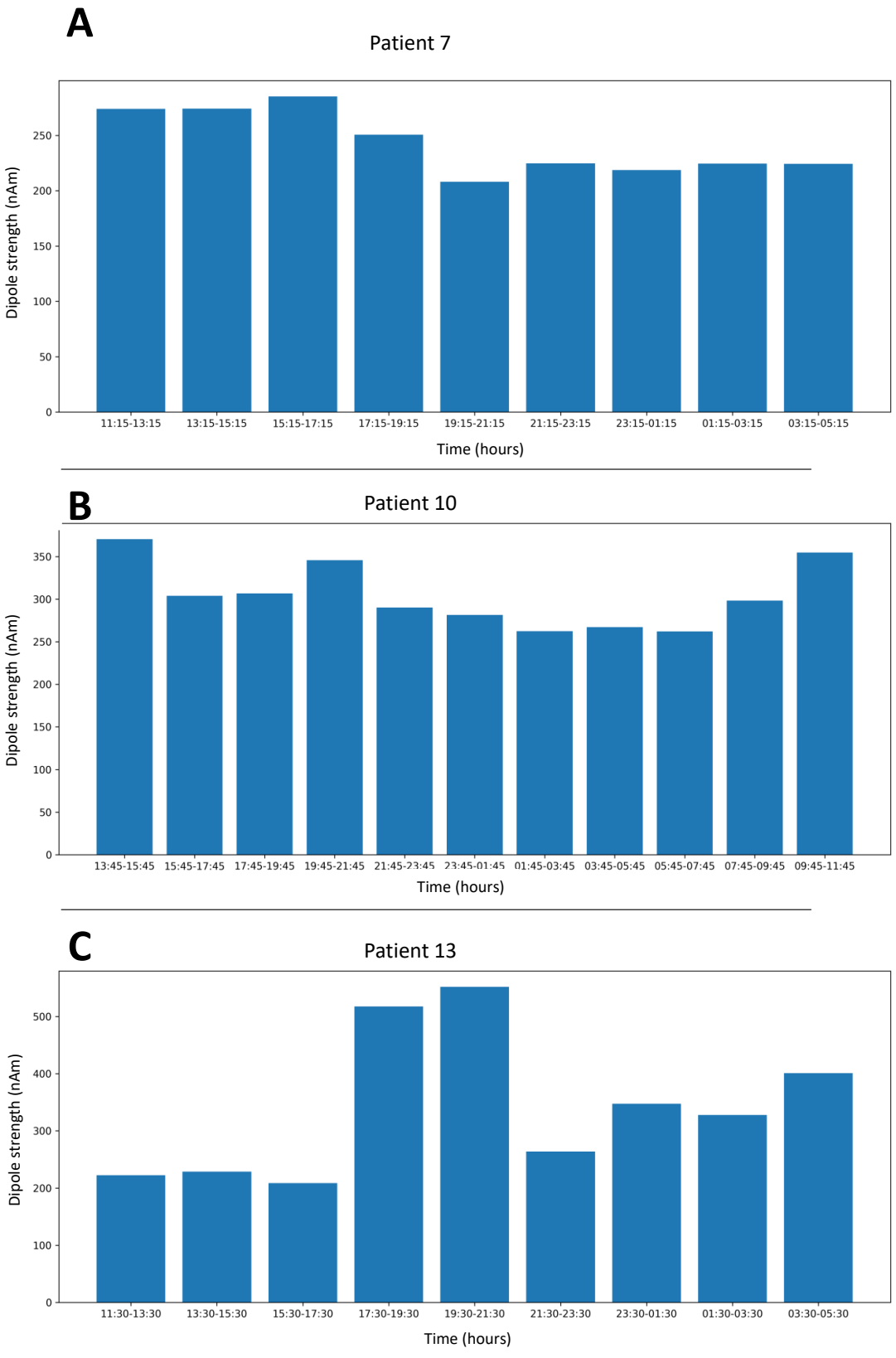

S Interface sketches

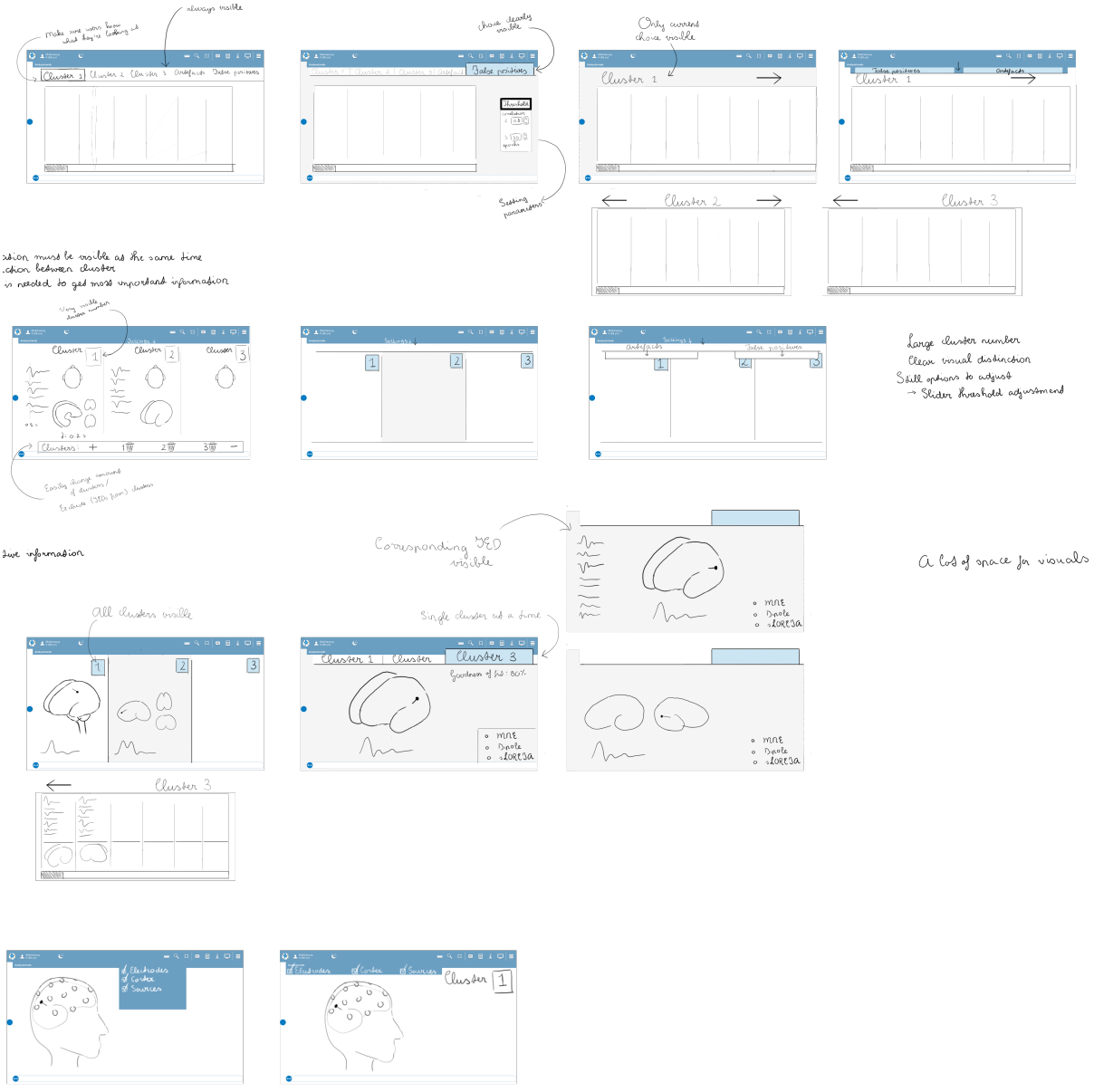

T Concept evaluation

Concept 1

Rule of Thumb	**Is this rule being applied? How so?**
1. Visibility of system status	The current cluster number is visible. The average IED is visible. The other available clusters are indicated
2. Match between system and real world	Trash can to remove epochs/clusters. Longer epochs to mimic EEG recordings.
3. User control and freedom	Undo button when changes have been made. Settings can be adjusted in a separate page.
4. Consistency and standards	Colors consistent with Neurocenter. Consistent phrasing. Trash can as delete icon.
5. Error prevention	Pop-up window before items are deleted. Undo button when changes have been made.
6. Recognition rather than recall	Averages of cluster are displayed in cluster pages.
7. Flexibility and efficiency of use	Settings page is present. Easy way to remove epochs/clusters.
8. Aesthetic and minimalist design	Neutral, light colors. Limited information presented on first access.
9. Help users recognise, diagnose and recover from errors	Pop-up window before items are deleted. Undo button when changes have been made.
10. Help and documentation	Not implemented yet.

Concept 2

Rule of Thumb	**Is this rule being applied? How so?**
1. Visibility of system status	The current cluster number is visible. The average IED is visible. The other available clusters are indicated
2. Match between system and the real world	Trash can to remove epochs/clusters. Longer epochs to mimic EEG recordings. Intuitive expanding and collapsing of clusters.
3. User control and freedom	Undo button when changes have been made. Settings can be adjusted in a separate page. Multiple ways to navigate.
4. Consistency and standards	Colors consistent with Neurocenter. Consistent phrasing. Trash can as delete icon.
5. Error prevention	Pop-up window before items are deleted. Undo button when changes have been made.
6. Recognition rather than recall	Averages of cluster are displayed in cluster pages. Hovering signals possible interaction.
7. Flexibility and efficiency of use	Settings page is present. Easy way to remove epochs/clusters. Multiple ways to navigate.
8. Aesthetic and minimalist design	Neutral, light colors. Limited information presented on first access.
9. Help users recognise, diagnose and recover from errors	Pop-up window before items are deleted. Undo button when changes have been made.
10. Help and documentation	Not implemented yet.

U Usability testing results

Below, the strengths and problems of the concepts found with the usability testing are indicated. For each problem, the number of participants that experienced this problem is indicated. Furthermore, the impact and frequency of all problems are represented by problem number.

Table 7: The strengths of the prototypes as revealed with usability testing. The number of participants that noted the same positive element is indicated.

Nature of strength	**No. of participants**
Intuitive interaction for concept 2	3
Pleasant colors and orderly design	3
Presentation of sources inside cortex is clear and familiar	3
Necessary information is present on the main page	3
The current system state is always clear	3

Table 8: The problems of the prototypes as revealed with usability testing. The number of participants that noted the same problem is indicated.

No.	**Nature of the problem**	**No. of participants**
1	MRI view is ambiguous	3
2	Will not use the sources often	2
3	Will not use individual sources often	3
4	Will not use activation of sources	3
5	Will not use settings	2
6	Setting options may be too specific	3
7	Struggles with horizontal alignment on main page	3
8	Misses the coupling with the raw EEG signal	3
9	Confusion over N=x to indicate the number of epochs	2

High frequency	3	1 8	3 6	3 7	
Lower frequency	2		2 9	4	5
		4	3	2	1
		High impact		Low impact	